

University of Southern Queensland
Faculty of Engineering and Surveying

The Effect of DC Current on Power Transformers

A dissertation submitted by

Ashley Karl Zeimer

in fulfilment of the requirements of
Courses ENG4111 and 4112 Research Project

towards the degree of

Bachelor of Electrical/Electronic Engineering

Submitted: October, 2000

Abstract

Power transformers are an integral part of almost all electrical transmission and distribution networks. Their reliable service is of the utmost importance in modern society which is dependent on a constant electricity supply. There are a range of factors that can hinder the operation of a power transformer. This dissertation presents the results of investigations into one of these factors through an analysis of the effect that direct current has on the operational characteristics of a power transformer.

There are a host of adverse effects that can accompany the presence of a direct current in a transformer's windings. The predominant effect that is witnessed is half cycle saturation. This leads to increased harmonic distortion, increased reactive power losses, overheating and elevated acoustic noise emissions.

Direct current can be found in a transformer's windings as a result of imperfections in connected equipment and also due to magnetic disturbances of the earth's field. Tests conducted indicate that personal computers are a potentially significant source of DC when a large number of units are connected to a common point of coupling. Similarly the possibility exists for AC and DC induction motor drives to contribute sizeable quantities of DC Bias.

University of Southern Queensland
Faculty of Engineering and Surveying

ENG4111 & ENG4112 *Research Project*

Limitations of Use

The Council of the University of Southern Queensland, its Faculty of Engineering and Surveying, and the staff of the University of Southern Queensland, do not accept any responsibility for the truth, accuracy or completeness of material contained within or associated with this dissertation.

Persons using all or any part of this material do so at their own risk, and not at the risk of the Council of the University of Southern Queensland, its Faculty of Engineering and Surveying or the staff of the University of Southern Queensland.

This dissertation reports an educational exercise and has no purpose or validity beyond this exercise. The sole purpose of the course pair entitled 'Research Project' is to contribute to the overall education within the student's chosen degree program. This document, the associated hardware, software, drawings, and other material set out in the associated appendices should not be used for any other purpose: if they are so used, it is entirely at the risk of the user.

Prof G Baker
Dean
Faculty of Engineering and Surveying

Certification

I certify that the ideas, designs and experimental work, results, analyses and conclusions set out in this dissertation are entirely my own effort, except where otherwise indicated and acknowledged.

I further certify that the work is original and has not been previously submitted for assessment in any other course or institution, except where specifically stated.

Ashley Karl Zeimer

Student Number: 0019922370

Signature

Date

Acknowledgements

I would like to thank the following people for their invaluable assistance and contributions which have aided the success of this project:

Mr. Ron Sharma (Supervisor) whose willing assistance and wealth of information could be relied upon throughout the entire project process.

Dr. Anthony Ahfok whose technical guidance was essential to the success of this project.

Mr. Don Gelhaar for the many long hours spent in the laboratory and the invaluable assistance provided along the way.

Contents

Abstract	i
Acknowledgements	iv
List of Figures	xi
List of Tables	xvii
Chapter 1 Introduction	1
1.1 Project Objectives.....	2
1.2 Dissertation Layout.....	3
Chapter 2 Transformer Theory Background	5
2.1 Basic Operation.....	5
2.1.1 No-Load Operation.....	7
2.1.2 Loaded Operation.....	7

2.2	Core Saturation.....	10
2.3	Hysteresis.....	10
Chapter 3	Transformer Operation with DC Bias	12
3.1	Theory of Affect.....	12
3.2	Specific Affects.....	15
3.2.1	Saturation and Generation of Harmonics.....	15
3.2.2	Power Considerations.....	16
3.2.3	Overheating.....	16
3.2.4	Acoustic Noise Emissions.....	17
3.2.5	Corrosive Effects.....	18
3.2.6	Residual Magnetism.....	18
3.2.7	External Considerations.....	18
3.3	Sources of DC Bias.....	18
3.3.1	Geomagnetically Induced Currents.....	19
3.3.2	Photovoltaic Systems.....	19
3.3.3	AC and DC Drives.....	20
3.4	Mitigation of the Effects of DC Injection.....	20
3.4.1	Transformer Related Measures.....	21
3.4.2	Equipment Related Measures.....	22
Chapter 4	Methodology	23
4.1	Overview.....	23

4.2	Outline of Chapter Purpose and Methodology.....	24
4.2.1	Chapter 5 – Sources of DC Bias.....	24
4.2.2	Chapter 6 – Single Phase Analysis – Magnetising Characteristics.....	25
4.2.3	Chapter 7 – Single Phase Analysis – Harmonic Characteristics.....	26
4.2.4	Chapter 8 – Single Phase Analysis – Hysteresis Characteristics.....	27
4.2.5	Chapter 9 – Three Phase Analysis – Magnetising Characteristics.....	27
Chapter 5	Sources of Direct Current	29
5.1	Overview.....	29
5.2	Computers.....	29
5.2.1	Test Theory and Method.....	30
5.2.2	Test Results and Analysis.....	30
5.3	AC and DC Drives.....	32
5.3.1	Test Theory and Method.....	32
5.3.2	Test Results and Analysis.....	33
Chapter 6	Single Phase Analysis – Magnetising Characteristics	35
6.1	Zero AC Load Test.....	35
6.1.1	Test Theory and Method.....	36

6.1.2	Test Results and Analysis.....	37
6.2	Magnetising Characteristics at Rated Load.....	43
6.2.1	Test Theory and Method.....	44
6.2.2	Test Results and Analysis.....	45
Chapter 7	Single Phase Analysis – Harmonic Effects	49
7.1	Primary and Secondary Harmonic Distortion.....	49
7.2	Harmonic Analysis – Half-Wave Rectified DC.....	52
7.2.1	Test Theory and Method.....	52
7.2.2	Test Results and Analysis.....	53
7.3	Harmonic Analysis – Smoothed Half-Wave Rectified DC.....	57
7.3.1	Test Theory and Method.....	57
7.3.2	Test Results and Analysis.....	58
Chapter 8	Flux and Magnetising Current Prediction	62
8.1	Theory Overview.....	62
8.2	Practical Hysteresis Measurements.....	65
8.2.1	Test Theory and Method.....	65
8.2.2	Test Results and Analysis.....	67
8.3	Software Simulation of Magnetising Characteristics.....	70
8.3.1	Program Methodology, Assumptions and Limitations.....	70
8.3.2	Discussion of Results.....	72

Chapter 9	Three Phase Analysis	77
9.1	Magnetising Characteristics – Phase to Neutral DC Injection.....	78
9.1.1	Test Theory and Method.....	78
9.1.2	Test Results and Analysis.....	79
9.2	Magnetising Characteristics – Phase to Phase DC Injection.....	82
9.2.1	Test Theory and Method.....	82
9.2.2	Test Results and Analysis.....	83
Chapter 10	Conclusions and Recommendations for Future Work	85
10.1	Achievement of Objectives.....	85
10.2	Future Work.....	87
10.2.1	Sources of DC.....	87
10.2.2	Single Phase Analysis.....	88
10.2.3	Three Phase Analysis.....	89
References		91
Appendix A	Project Specification	95
Appendix B	Single Phase Analysis – Magnetising Characteristic Results	97
Appendix C	Single Phase Analysis – Harmonic Effects Results	107

Appendix D	Experimental Hysteresis Results	116
Appendix E	MATLAB CODE –Magnetising_Current_Prediction.m	120
Appendix F	Three Phase Analysis Results	124

List of Figures

2.1	Two Winding, Core-Type Single Phase Transformer, Open Circuit Secondary	6
2.2	Two Winding, Core-Type Single-Phase Transformer-Loaded Secondary.....	8
2.3	Transformer Equivalent Circuit.....	9
2.4	Simplified Equivalent Circuit Referred to the Primary.....	10
2.5	The Hysteresis Loop.....	11
3.1	Single Phase Transformer Operating Under Asymmetrical Load Current Conditions	12
3.2	Transformer Equivalent Circuit Showing Secondary DC Current Path.....	13
3.3	Flux Waveform Offset Resulting from Biased Current Waveform.....	14
3.4 (a)	Horizontal Cross-Section for an Asymmetric Transformer.....	21
3.4 (b)	Horizontal Cross-Section for a Symmetric Transformer.....	21
6.1	Voltage Cancellation Circuit Utilised for No-Load Test.....	36

6.2	Plot of Core Loss Current and Magnetising Current Against a Secondary DC Bias.....	38
6.3	Variation in Real, Reactive and Apparent Power with a Secondary DC Bias.....	40
6.4	Variation in Displacement Power Factor with DC Bias.....	40
6.5	Flux Paths Established due to the Secondary DC and Magnetising Current.....	41
6.6 (a)	No-Load Current Waveform for Zero DC Injection.....	42
6.6 (b)	No-Load Current Waveform for 80 mA DC Injection.....	42
6.7	Circuit Used to Determine Transformer Magnetising Characteristics at Rated Load.....	44
6.8	Plot of Core Loss Current and Magnetising Current against DC Bias.....	46
6.9	Variation in Real, Reactive and Apparent Power with a Secondary DC Bias.....	46
6.10	Variation in Displacement Power Factor with a Secondary DC Bias.....	47
7.1	Circuit Configuration for DC Injection via Half-Wave Rectifier.....	52
7.2	CRO Screen Shot of Half-Wave Rectified Direct Current.....	53
7.3	Secondary Current Harmonic Distortion with a Secondary DC Current.....	54
7.4	Secondary Voltage Harmonic Distortion with a Secondary DC Current.....	55
7.5	Primary Current Harmonic Distortion with a Secondary DC Current.....	56

7.6	Primary Voltage Harmonic Distortion with a Secondary DC Current.....	56
7.7	Circuit Configuration for Capacitor Smoothed DC Injection via Half-Wave Rectifier.....	57
7.8	CRO Screen Shot of Smoothed Rectified DC Current.....	58
7.9 (a)	Secondary Voltage Waveform for Zero DC Secondary Component	61
7.9 (b)	Secondary Voltage Waveform for 300 mA DC Secondary Component.....	61
8.1	Transformer Flux-Magnetising Current Hysteresis Characteristic.....	63
8.2	Circuit Utilised to Conduct Hysteresis Experiment.....	66
8.3	Hysteresis Characteristic with 240 V Supply and Open Circuit Secondary.....	67
8.4	Hysteresis Characteristic with 270 V Supply and Open Circuit Secondary.....	68
8.5	Hysteresis Characteristic with a 100 mA Secondary DC Component.....	69
8.6	Hysteresis Plot with Piecewise Linearly Approximated Mid Point Locus.....	71
8.7	Plot of Flux-Magnetising Current Relationship with Zero Flux Bias.....	73
8.8	Plot of Biased Magnetising Current with Zero Flux Bias.....	73
8.9	Plot of Primary Magnetising Current with Zero Flux Bias.....	74
8.10	Plot of Flux-Magnetising Current Relationship with 20% Flux Bias.....	75
8.11	Plot of Biased Magnetising Current with 20% Flux Bias.....	75
8.12	Plot of Primary Magnetising Current with 20% Flux Bias.....	76

9.1	Secondary Phase to Neutral DC Injection.....	78
9.2	Plot of Primary Phase Currents with ‘A’ Phase to Neutral DC Injection.....	79
9.3	Plot of Primary Phase Currents with ‘B’ Phase to Neutral DC Injection.....	80
9.4	Plot of Primary Phase Currents with ‘C’ Phase to Neutral DC Injection.....	80
9.5	‘A’ Phase Primary Current Waveform with Zero Secondary DC Injection.....	81
9.6	‘A’ Phase Primary Current Waveform with 200 mA Secondary DC Injection.....	81
9.7	Secondary Phase to Phase DC Injection.....	82
9.8	Plot of Primary Phase Currents with ‘A’ Phase to ‘B’ Phase DC Injection.....	83
9.9	Plot of Primary Phase Currents with ‘C’ Phase to ‘B’ Phase DC Injection.....	84
9.10	Plot of Primary Phase Currents with ‘C’ Phase to ‘A’ Phase DC Injection.....	84
B.1	Primary Current Waveform with Zero AC Load and Zero Secondary DC Current.....	100
B.2	Primary Current Waveform with Zero AC Load and 10 mA Secondary DC Current.....	100

B.3	Primary Current Waveform with Zero AC Load and 20 mA	
	Secondary DC Current.....	101
B.4	Primary Current Waveform with Zero AC Load and 30 mA	
	Secondary DC Current.....	101
B.5	Primary Current Waveform with Zero AC Load and 40 mA	
	Secondary DC Current.....	102
B.6	Primary Current Waveform with Zero AC Load and 50 mA	
	Secondary DC Current.....	102
B.7	Primary Current Waveform with Zero AC Load and 60 mA	
	Secondary DC Current.....	103
B.8	Primary Current Waveform with Zero AC Load and 70 mA	
	Secondary DC Current.....	103
B.9	Primary Current Waveform with Zero AC Load and 80 mA	
	Secondary DC Current.....	104
B.10	Primary Current Waveform with Zero AC Load and 90 mA	
	Secondary DC Current.....	104
B.11	Primary Current Waveform with Zero AC Load and 100 mA	
	Secondary DC Current.....	105
B.12	Primary Current Waveform with Zero AC Load and 200 mA	
	Secondary DC Current.....	105
B.13	Primary Current Waveform with Zero AC Load and 300 mA	
	Secondary DC Current.....	106
B.14	Primary Current Waveform with Zero AC Load and 400 mA	
	Secondary DC Current.....	106

C.1	Variation in Primary Voltage Harmonic Distortion for Secondary Smoothed Half-Wave Rectified Current.....	112
C.2	Variation in Primary Current Harmonic Distortion for Secondary Smoothed Half-Wave Rectified Current.....	113
C.3	Variation in Secondary Voltage Harmonic Distortion for Secondary Smoothed Half-Wave Rectified Current.....	114
C.4	Variation in Secondary Current Harmonic Distortion for Secondary Smoothed Half-Wave Rectified Current.....	115
D.1	Hysteresis Characteristic with 240 V Supply and Open Circuit Secondary.....	117
D.2	Hysteresis Characteristic with 270 V Supply and Open Circuit Secondary.....	117
D.3	Hysteresis Characteristic with 240 V Supply and 25 mA Secondary DC Component.....	118
D.4	Hysteresis Characteristic with 240 V Supply and 50 mA Secondary DC Component.....	118
D.5	Hysteresis Characteristic with 240 V Supply and 75 mA Secondary DC Component.....	119
D.6	Hysteresis Characteristic with 240 V Supply and 100 mA Secondary DC Component.....	119

List of Tables

5.1	Results for Measurement of DC Load Current Component for Computers.....	31
5.2	Results for Measurement of DC Load Current Component for AC Drives.....	33
5.3	Results for Measurement of DC Load Current Component for DC Drives.....	33
7.1	Current Distortion Limits for General Distribution Limits as Defined by Standard IEEE 519 – 1992.....	50
7.2	Low-Voltage System Classification and Distortion Limits as Defined by Standard IEEE 519 – 1992.....	51
B.1	Results of Zero AC Load DC Injection Tests.....	98
B.2	Results of Rated AC Load DC Injection Tests.....	99
C.1	Primary Side Harmonic Effects with Half-Wave Rectified Secondary DC Component.....	108

C.2	Secondary Side Harmonic Effects with Half-Wave Rectified Secondary DC Component.....	109
C.3	Primary Side Harmonic Effects with Smoothed Half-Wave Rectified Secondary DC Component.....	110
C.4	Secondary Side Harmonic Effects with Smoothed Half-Wave Rectified Secondary DC Component.....	111
F.1	Results of 'A' Phase to Neutral DC Injection.....	125
F.2	Results of 'B' Phase to Neutral DC Injection.....	126
F.3	Results of 'C' Phase to Neutral DC Injection.....	127
F.4	Results of DC Injection between 'A' and 'B' Phases.....	128
F.5	Results of DC Injection between 'C' and 'B' Phases.....	129
F.6	Results of DC Injection between 'A' and 'C' Phases.....	130

Chapter 1

Introduction

Power transformers are an integral part of almost all electrical transmission and distribution networks. Their reliable service is of the utmost importance in modern society which is dependent on a constant electricity supply. There are a range of factors that can hinder the operation of a power transformer. This project aims to investigate one of these factors through an analysis of the effect that direct current has on the operational characteristics of a power transformer.

Direct current can be found in a transformer's windings as a result of imperfections in connected equipment and also due to magnetic disturbances of the earth's field. There are a host of adverse effects that can potentially accompany the presence of a direct current in a transformer's windings. These include increased harmonic distortion, increased reactive power losses, overheating, elevated acoustic noise emissions and corrosion.

This project aims to validate, clarify and expand upon the theoretical concepts that have been documented through past research. Available literature does not provide an in depth analysis of precisely how a transformer's operational characteristics are affected when a DC bias is present. This project aims to bridge this void in the topic knowledge base.

1.1 Project Objectives

Provided in the following list is an outline of the project objectives which are primarily as defined by the project specifications. It should be noted that a number of additions have been made to these objectives to cater for broadening of the project scope which occurred midway through the research process.

1. Research existing theory pertaining to the affect of DC current on power transformers as well as review transformer theory.
2. Investigate saturation with respect to transformers and detail how DC injection induces this phenomenon.
3. Analyse the variation in transformer magnetising characteristics which occurs as a result of biased load currents.
4. Determine the harmonic distortion that can be attributed to the presence of asymmetrical currents in a transformer's secondary winding.
5. Explore potential sources of DC biasing and look into the severity of these sources.
6. Examine factors that exacerbate and potentially accelerate the adverse affects of DC injection.
7. Investigate the variation in affect due to DC biasing across the variety of transformer construction styles that exist and conduct tests to simulate this.
8. Examine variation in affects for DC injection common across all three phases and localized to one or two of the three phases.
9. Research methods for the alleviation or elimination of the adverse effects of DC biasing.
10. Investigate the creation of software that could model this phenomenon.

In addressing the objectives as defined above a decision was made to initially focus upon single phase concepts. It is believed that this is a necessary stepping stone that must be tackled prior to the progression to the more complex three phase system.

1.2 Dissertation Layout

In compiling the research material for this project the objectives as defined in section 1.1 served as the primary source of direction. The following chapters are arranged such that each objective is addressed in a logical format. This section provides a brief overview of the content covered by each chapter and how this content strives to fulfil the project goals.

Provided in Chapter 2 is a brief overview of what a transformer is and how it is intended to operate in the ideal sense. Chapter 3 presents a summary of literature pertaining to the affect that direct current has on power transformers. This includes details of how a transformer's operational characteristics are altered through the presence of a DC bias. Also, an outline is provided of potential sources of DC and methods that can be employed to mitigate the adverse effects of direct current. Chapters 2 and 3 address each of the first five objectives and also the 9th objective.

Chapter 4 details the methodology employed throughout this project. This includes what each chapter aims to achieve and why these goals are important and necessary. It provides a description of how the goals will be met and in some instances a prediction of what results are expected.

Chapter 5 looks into sources of direct current bias, a requirement of objective 5. This is achieved through investigating two potential sources in the form of computers and AC and DC motor drives. Computers are prevalent in domestic and commercial installations whilst motor drives primarily exist in industrial applications. This chapter aims to asses the significance of any potential contribution.

Chapter 6 assesses the variation in single phase transformer magnetising characteristics when a DC bias is present. This chapter addresses specifications 2, 3, 6 and 7. It provides an insight into magnetising characteristics with DC injection when the transformer is operating under no-load and load conditions.

Chapter 7 provides the results of tests undertaken to determine harmonic distortion characteristics when a secondary direct current component is introduced into a transformer operating at rated load. The level of distortion witnessed is compared to relevant standards to determine whether it is within limit. This series of testing is in accordance with objective 4.

Presented in Chapter 8 is a comprehensive analysis of hysteresis characteristics in a single phase transformer. Included in this chapter is a software simulation that can be utilised to predict magnetising currents for a transformer exhibiting biased core flux behaviour. This addresses the objectives 2, 3, 6 and 10.

Chapter 9 presents the results of preliminary tests conducted to determine the magnetising characteristics of a three phase transformer exposed to load bias. The content contained in this chapter fulfils the 5th and 6th specifications. Chapter 10 presents conclusions and recommendations for future work.

Chapter 2

Transformer Theory Background

2.1 Basic Operation

The transformer is a static machine that utilises the principle of electromagnetic mutual induction to alter voltage and current levels in an AC circuit without affecting frequency. It is comprised of two or more coils situated in such a manner that they will be linked by the same magnetic flux when an alternating supply is connected to one of the coils. Often these coils are referred to as the primary and secondary windings. Several coils may be connected in series or parallel to form a winding.

The coils of a power transformer are positioned on a high permeability iron core in an endeavour to ensure that the magnetic flux created links all turns and that there is minimal leakage flux (Grainger & Stevenson 1994). The windings of a transformer are generally either of the core type or shell type construction. Figure 2.1 depicts two windings arranged in a core type construction to form a single-phase transformer. It can be seen from this figure that the flux is common to both coils.

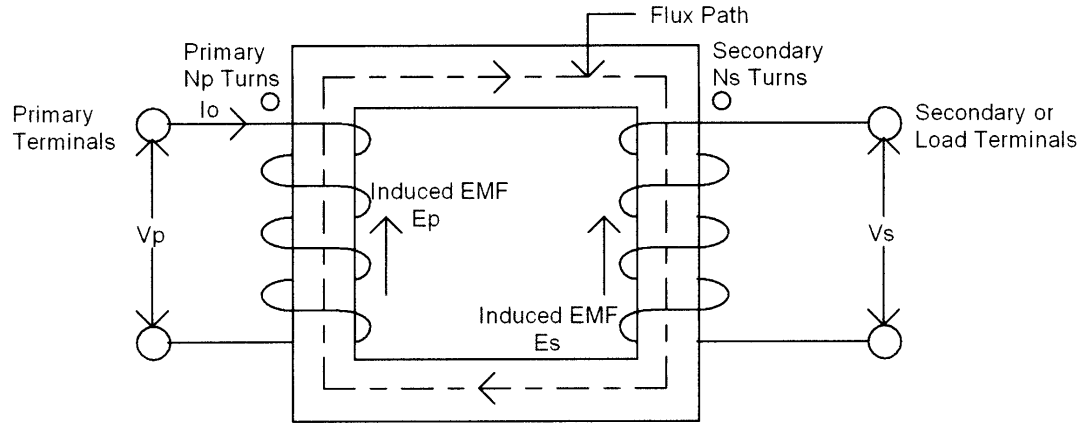


Figure 2.1: Two Winding, Core-Type Single Phase Transformer, Open Circuit Secondary

Figure 2.1 illustrates the ideal transformer condition. That is the core is considered to have infinite permeability which in turn results in zero leakage flux. If this assumption is upheld and core losses and winding resistance are considered negligible, then it can be seen that the terminal voltages V_p and V_s will be equal to the voltages E_p and E_s which are induced by the changing flux. Then, through application of Faraday's Law (Grainger & Stevenson 1994) the following relationships are found to exist:

$$V_p = E_p = N_p \frac{d\phi}{dt} \quad (2.1)$$

$$V_s = E_s = N_s \frac{d\phi}{dt} \quad (2.2)$$

N_p and N_s represent the number of turns on the primary and secondary coils whilst ϕ represents the instantaneous value of flux. If a sinusoidal supply is assumed then the flux will also vary in a sinusoidal manner. Division of the two equations above will yield the following ratios:

$$\frac{V_p}{V_s} = \frac{E_p}{E_s} = \frac{N_p}{N_s} \quad (2.3)$$

2.1.1 No-Load Operation

The transformer shown in Figure 2.1 is operating under no-load conditions. In this state, a small current defined as the no-load current (I_o) flows. This current is comprised of two components and is represented by Equation 2.4 as follows:

$$I_o = I_m + I_c \quad (2.4)$$

When operating under no-load conditions current I_o lags the supply voltage by an angle Φ_o . Component I_m lags V_p by 90° and represents the magnetisation current that creates the magnetic field within the iron core. Component I_c is in phase with V_p and represents the hysteresis and eddy current losses (Jenneson 1999). The two no-load components can be represented as follows:

$$I_m = |I_o| \sin \Phi_o \quad (2.5)$$

$$I_c = |I_o| \cos \Phi_o \quad (2.6)$$

2.1.2 Loaded Operation

When a load is applied to the secondary of a transformer a secondary current (I_s) will flow. This is shown in Figure 2.2. As a result of I_s the secondary winding will produce a flux (often referred to as the demagnetising flux) which will oppose the flux generated by the additional component of primary current (Jenneson 1999). This will ensure that the mutual flux remains relatively unchanged. This should be the case provided the supply voltage is held constant.

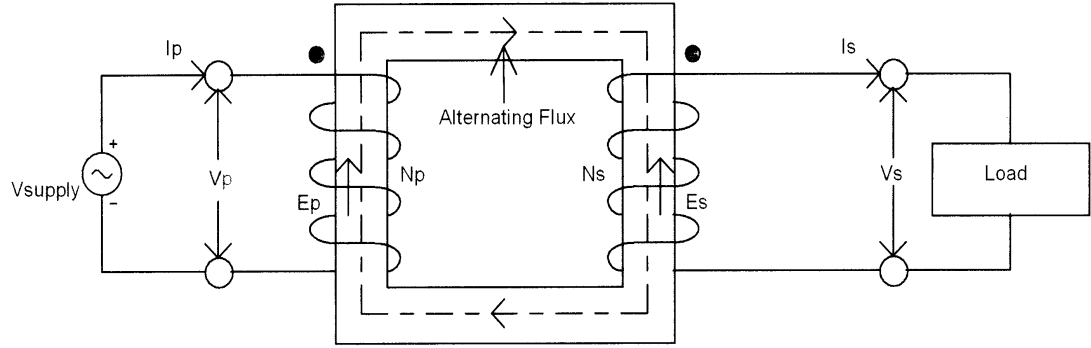


Figure 2.2: Two Winding, Core-Type Single-Phase Transformer-Loaded Secondary

Assuming ideal conditions with a symmetric load current, the ratio of primary current to secondary current is inversely proportional to the corresponding voltage and turns ratios. This relationship is shown in Equation 2.7.

$$\frac{V_P}{V_S} = \frac{N_P}{N_S} = \frac{I_S}{I_P} \quad (2.7)$$

Transformer impedances can be referred to either the primary or the secondary. The supply side impedance is:

$$Z_{in} = \frac{V_P}{I_P} \quad (2.8)$$

The load side impedance is:

$$Z_L = \frac{V_S}{I_S} \quad (2.9)$$

It can then be seen that the supply side impedance is related to the load side impedance in terms of the turn's ratio ($a = \frac{N_P}{N_S}$) as shown by Equation 2.10.

$$Z_{in} = a^2 Z_L \quad (2.10)$$

The transformer configuration depicted in Figure 2.2 can be represented by an equivalent circuit as shown in Figure 2.3. This equivalent circuit includes the ideal transformer. In the diagram below R_P and X_P represent the resistance and reactance of the primary winding while R_S and X_S represent the resistance and reactance of the secondary winding.

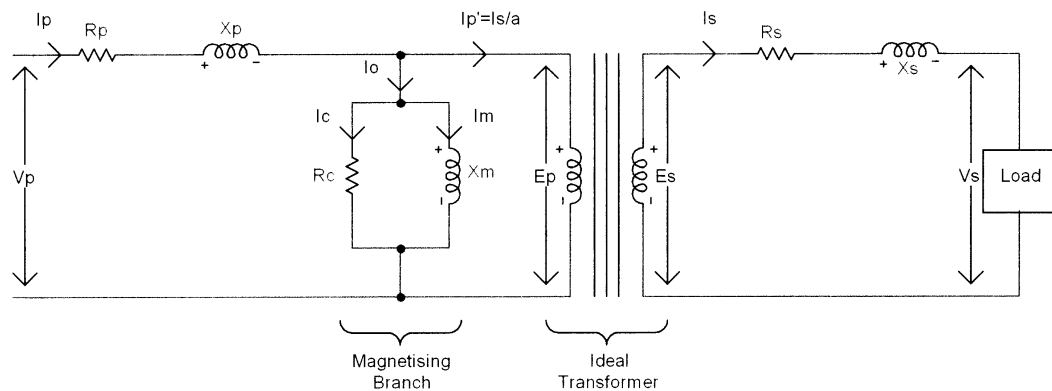


Figure 2.3: Transformer Equivalent Circuit

Further simplification can be achieved through referring impedances to the primary or secondary and collecting like terms. Figure 2.4 illustrates this with the impedances referred to the primary side. In this circuit the effect of the shunt impedance has been neglected and the resistance and reactance have been represented as follows:

$$R_{ep} = R_P + a^2 R_S \quad (2.11)$$

$$X_{ep} = X_P + a^2 X_S \quad (2.12)$$

The primary current is:

$$I_P = I'_S = \frac{I_S}{a} \quad (2.13)$$

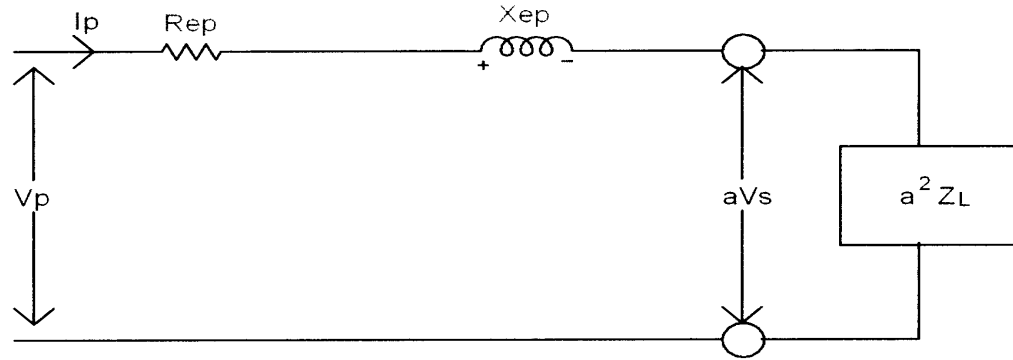


Figure 2.4: Simplified Equivalent Circuit Referred to the Primary

2.2 Core Saturation

Core saturation is one of the primary factors limiting the performance of a transformer. The transformer core cannot support an infinite magnetic flux density and exhibits the tendency of saturation at a certain level of magnetomotive force. Increases in magnetomotive force beyond this level do not yield a proportional increase in magnetic field flux. The level at which a transformer will enter saturation is generally dependent upon the material that has been utilised in the core as well as core construction and dimensions. Some potential causes of core saturation are over voltage on the primary winding, operation below rated frequency and/or an offset load current (Kuphaldt 2003).

2.3 Hysteresis

The flux “flow” within a transformer core changes direction at a rate set by the supply frequency. During this change in flux direction the magnetomotive force will reach zero. At this same point the magnetisation of the core will not have reduced to zero. The magnetisation remaining when the magnetic field has been returned to zero is known as the remanence. In order to obtain zero magnetisation a force known as the coercive force must be applied in the form of a reverse magnetic field. If an

alternating magnetic field is applied to a magnetic material such as a transformer core then the magnetisation will trace out a path known as the hysteresis loop. This phenomenon is illustrated in Figure 2.5 (Nave 2000).

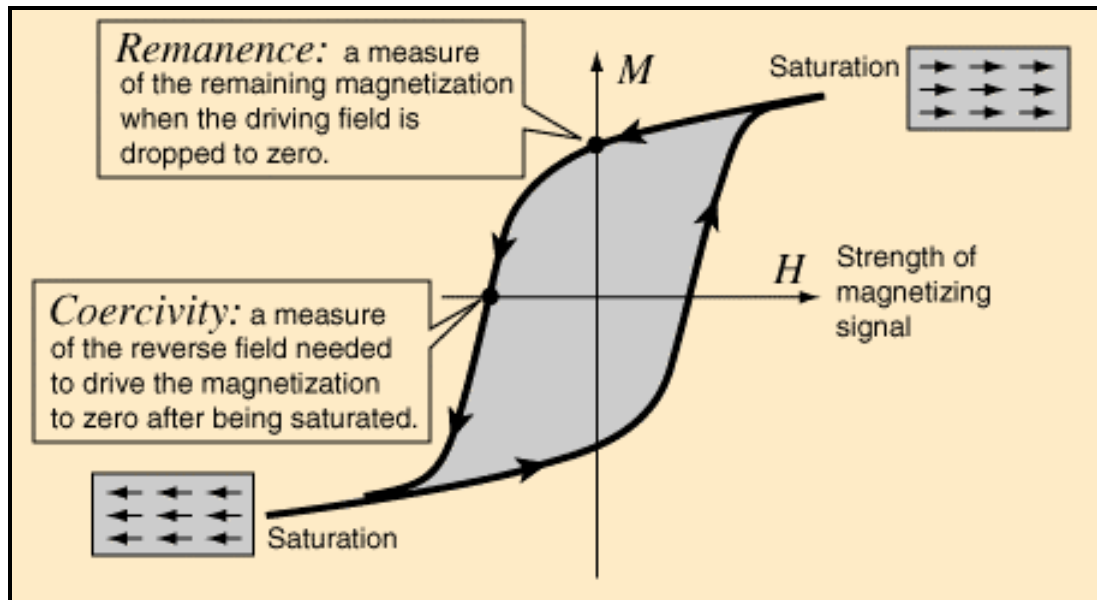


Figure 2.5: The Hysteresis Loop
(Nave 2000)

The alternating flux within the transformer core causes corresponding changes in the alignment of molecules. The forces causing this change consume energy and thus cause a loss in the form of heat. This loss is commonly referred to as the hysteresis loss. The hysteresis characteristics of a transformer are very much dependent on the type of material used in the core (Jenneson 1999).

Chapter 3

Transformer Operation with DC Bias

3.1 Theory of Effect

When a transformer supplies a secondary current containing a DC component, a unipolar flux is established in the core. This flux accompanies the bipolar flux that is created as a result of the alternating component of current. This is illustrated below in Figure 3.1. The direction of this DC flux is dependent on the sign of the DC offset.

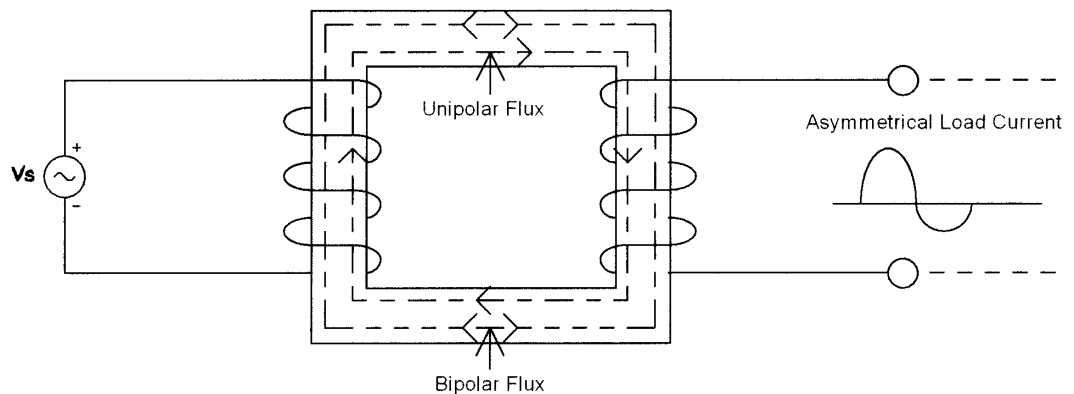


Figure 3.1: Single Phase Transformer Operating Under Asymmetrical Load Current Conditions

Under pure symmetric load current operating conditions a flux is produced in the secondary which opposes the flux created by the additional component of primary

current. Hence the mutual flux remains relatively unchanged. It can be shown that the flux created in the secondary as a result of the DC current component will not be reflected to the primary.

Through analysis of the equivalent circuit for a transformer shown in Figure 3.2 it can be seen that the DC current in the secondary will not be reflected to the primary as a result of the magnetising reactance. The magnetising reactance will appear as a dead short to the DC component of current due to the fact that DC has a frequency equal to zero. The inductive reactance can be modelled using Equation 3.1.

$$X_L = 2\pi FL \quad (3.1)$$

With DC current $F = 0 \therefore X_L = 0$

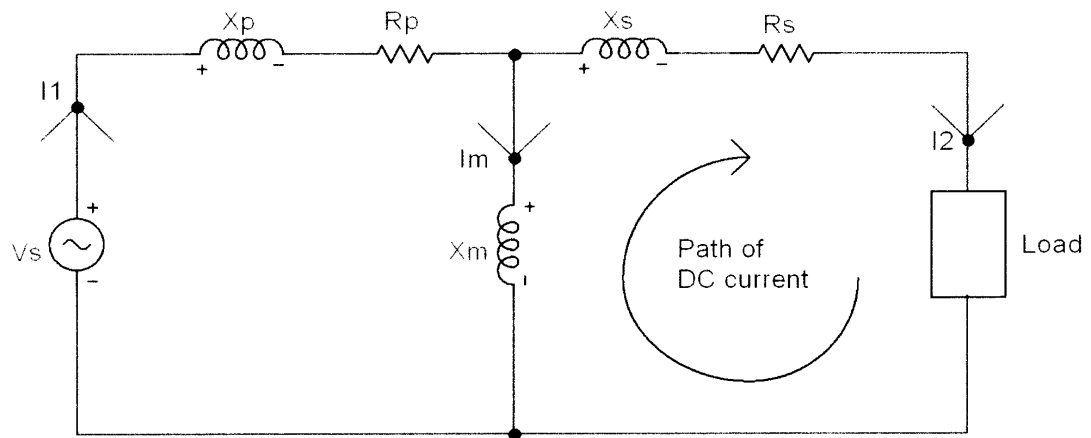


Figure 3.2: Transformer Equivalent Circuit Showing Secondary DC Current Path

With the magnetising reactance appearing as a dead short, the DC component of secondary current will take the path as shown in Figure 3.2. As a result of this there will be an excess component of flux present in the secondary that is not being cancelled by a corresponding component in the primary. If the transformer is operating close to the knee point on the saturation curve or in other words close to its limits, it could be pushed into saturation by the additional component of flux. This trend is shown in Figure 3.3 where the flux offset is evident.

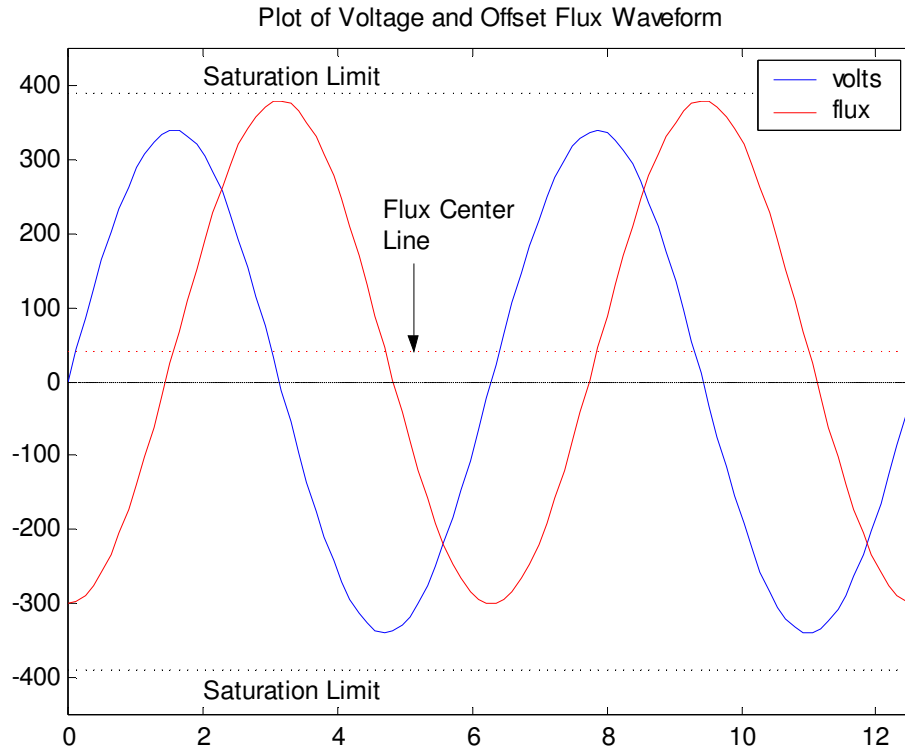


Figure 3.3: Flux Waveform Offset Resulting from Biased Current Waveform

Often the supply to a transformer can be considered as an infinite bus and thus the following relationship exists:

$$V \propto \phi \quad (3.2)$$

Thus it can be assumed that the flux remains constant.

The relationship between flux, magnetising reactance and magnetising current can be defined as follows:

$$\phi \propto X_m I_m \quad (3.3)$$

If the transformer enters saturation as a result of the presence of DC current in the secondary then an increase in magnetising current must occur to maintain the constant flux. Hence if magnetising current increases a corresponding decrease in magnetising reactance will occur in accordance with the relationship described above. Another point that must be noted is that Equation 2.7 will not hold since the extra secondary DC component of current will not be reflected to the primary.

3.2 Specific Affects

The presence of a DC current component in the load current of a power transformer can result in a range of adverse affects. Studies conducted, have shown that there is a variation in these affects across the range of transformer construction styles (Fujiwara et al. 1994). Following is an overview of the effects, however no differentiation is made between varying construction styles.

3.2.1 Saturation and Generation of Harmonics

It has been established that one of the major effects on a transformer operating under a biased load current is the tendency towards half cycle saturation (Bolduc et al. 1997). During the saturated half cycle interval an increase in magnetising current will be experienced. This will result in a non-linear current waveform containing an assortment of odd and even harmonics (Price 2002). This is a particularly undesirable condition, one which is recognised in the standard ANSI/IEEE C57.12.00-1987, IEEE Standard General Requirements for Liquid Immersed Distribution, Power and Regulating Transformers, which states that power transformers should not be expected to carry load currents with a harmonic factor greater than 5 percent of rating (Baranowski et al. 1996).

With a DC bias present, transformers become a significant source of harmonics (De La Ree, Liu & Lu 1993). This harmonic distortion adversely affects the network

through degradation of the power quality experienced by other equipment connected to the affected transformer.

3.2.2 Power Considerations

An effect which can also stem from core saturation is increased VAR absorption (Price 2002). This can be explained by realising that core saturation results in an increase in magnetising current which is basically an inductive current. Increases in this inductive current will result in greater reactive power loss across the magnetising reactance (Ahfock, A 2004, pers. comm., 18 August). Thus if the existing load current through the transformer is inductive rather than capacitive (which is often the case) then the overall reactive power (VAR absorption) will increase as a result of the increased magnetising current. If saturation is severe the VAR absorption will become noticeable, along with an associated decrease in displacement power factor. This is a particularly undesirable feature as it indicates increased losses.

3.2.3 Overheating

Another effect that can be attributed to biased transformer load currents is overheating. Overheating can initially be seen to be manifested in the windings of a transformer as a result of the increased harmonic distortion and the skin effect.

When a transformer enters the saturated region of operation as a result of DC bias extra harmonics are generated. These harmonics at their elevated frequency levels encounter greater resistance as a result of the skin effect. This in turn exacerbates heating effects through increased I^2R losses (Sharma, R 2004, pers. comm., 25 August).

Another heating effect that has been pinpointed as the cause of transformer failure is severe eddy current heating of a winding. This effect is particularly evident in transformers with high current windings such as generator transformers. It has been

surmised that this effect occurs due to the variation in magnitude and direction of leakage flux during the half cycle saturation interval. This is said to cause an increased component of flux perpendicular to the major dimension of the winding strands (Fujiwara et al. 1994).

When a transformer enters saturation the flux is forced to seek paths exterior to the core (De La Ree, Liu & Lu 1993). This often has the affect of overheating of components within the transformer such as brackets and bolts and even the transformer tank itself (Jewell & Warner 1999). Studies have shown that the tie plate within a transformer is particularly susceptible to DC induced saturation, experiencing rapid temperature rise as a result (Bolduc et al 1997).

For oil immersed transformers DC saturation induced overheating also has the effect of increasing levels of CO and CO² gases (Fujiwara et al. 1994). Accumulation of these gases can cause operation of Buckholtz protection, thus removing the transformer from service (Cardoso et al. 1998).

3.2.4 Acoustic Noise Emissions

A transformer driven into the saturated operating region as the result of DC bias will produce greater levels of acoustical noise. Studies have shown that relatively small levels of DC voltage on a transformer's lines can cause the device to emit greater levels of noise.

There are a number of mechanisms that produce this noise. Firstly the Lorentz Force Acoustic Signal (LFAS) causes mechanical forces between core laminations hence inducing rattling and thus noise. This particular form of noise production is largely dependent on construction style.

The next form of noise stems from the rotation of magnetic domains. This form of noise becomes a concern when the transformer enters saturation and the

magnetostriction becomes large and movement is experienced within core laminations (De Leon et al. 2000).

3.2.5 Corrosive Effects

A particularly adverse impact arising from biased transformer load currents is that corrosive affects are accelerated. The injection of DC can create ground currents which can rapidly corrode equipment (Ledwich & Masoud 1999).

3.2.6 Residual Magnetism

The magnetic history of a transformer operating under asymmetric load conditions cannot be discounted. With a DC bias present transformers can exhibit residual magnetism. This is particularly evident in those which have a tank. If the gap between the tank and the transformer core is small, any residual magnetism is likely to impact significantly upon the magnetising currents and hysteresis characteristic (Fuchs, Roesler & You 1999).

3.2.7 External Considerations

The effect of asymmetric currents on power transformers will be dependent on a number of external factors. If a transformer is operating at or above rated voltage the effects of DC offset are likely to be accelerated. Ambient temperatures will govern the severity of heating effects as well as transformer loading.

3.3 Sources of DC Bias

A DC bias is experienced by a transformer when the load current through that transformer is not perfectly symmetrical. Such a bias can originate from a number of sources, some of which are listed below.

- Geomagnetically induced currents (GIC)
- Photovoltaic (PV) systems grid connected without mains frequency transformers
- AC and DC drives

3.3.1 Geomagnetically Induced Currents

Geomagnetically induced currents flow on the surface of the earth as a result of solar magnetic disturbances (Al-Haj & El-Amin 2000). An example of such a disturbance occurred on March 13, 1989 in the form of an intense magnetic storm which impacted upon the Northern Hemisphere. This storm was attributed with the general failure of the Hydro-Quebec power system (Dutil et al. 1992). These currents can flow in power system transmission lines and transformers through entering and exiting the earthed neutrals of star connected equipment.

This form of DC bias is characterised by very low frequencies of the range 0.01-0.001 Hz and as such is often referred to as quasi DC. GIC magnitudes of the order of several hundred amperes in neutrals have been observed in Finland and Sweden. More typical values of 10-15A were reported in the National Grid Company transmission system in England and Wales (Price 2002).

3.3.2 Photovoltaic Systems

Another source of DC bias that can adversely affect transformers stems from the use of photovoltaic systems that are directly grid connected without a mains frequency transformer. In Queensland the power distribution authority Energex has created a policy allowing the direct connection for renewable energy generation up to 30 kVA (3-phase) or 10 kVA (1-phase) (Khouzam 1999). Photovoltaic systems that are connected via an inverter to the grid can cause a DC bias due to the following mechanisms (Ledwich & Masoud 1999):

- Imbalance in on state impedances of switches
- Different switching times for switches
- Imperfection in implementing timing of drivers

It must be noted that the Australian Standard AS4777.2-2002 (Grid connection of energy systems via inverters) does impose strict limits on the level of direct current injection. The standard states that the level of DC output current of an inverter shall not exceed 0.5% of rated output current or 5 mA, whichever is greater. This however is not a worldwide standard. If a large number of inverter interfaced systems are grid connect the DC effect may be cumulative.

3.3.3 AC and DC Drives

AC and DC drives are a significant source of DC injection in industry. Studies have shown variable frequency drives to have asymmetrical input current waveforms when operated at maximum output (Swamy & Rossiter 1998). The severity of this DC injection will be dependent upon the type of conduction devices utilised (e.g. diodes and thyristors) and the quality of device matching.

With respect to DC drives there a number of drive topologies that can inject significant components of DC. The half-wave rectifier is notorious for injection of DC however it's practical use is limited. The three phase half controlled rectifier can also be a source of DC injection (Swamy & Rossiter 1998).

3.4 Mitigation of the Effects of DC Injection

Mitigation of the effects of DC can generally be approached from two angles. Firstly there are those measures that can be implemented to alleviate effects at the transformer. Secondly there are those measures that can be undertaken on equipment connected to a transformer to prevent DC injection.

3.4.1 Transformer Related Measures

From a transformer construction viewpoint there are a range of measures that can be implemented. At the initial design phase allowance can be built into core parameters to cater for any DC injection. Where it is known that a load is likely to contain a large DC component, use of a Zig-Zag transformer may be advantageous. The main benefit of the zigzag connection is that the currents in the two halves of the windings on each leg of the transformer flow in opposite directions. Thus any DC component is cancelled. The drawback of this method is that it is generally more expensive to construct (Sankaran 2000).

Another method that has been proposed to negate the effects of DC bias is to utilize a symmetric transformer construction style. Shown below in Figures 3.4 (a) and (b) are the horizontal cross sections of the asymmetric and symmetric models.

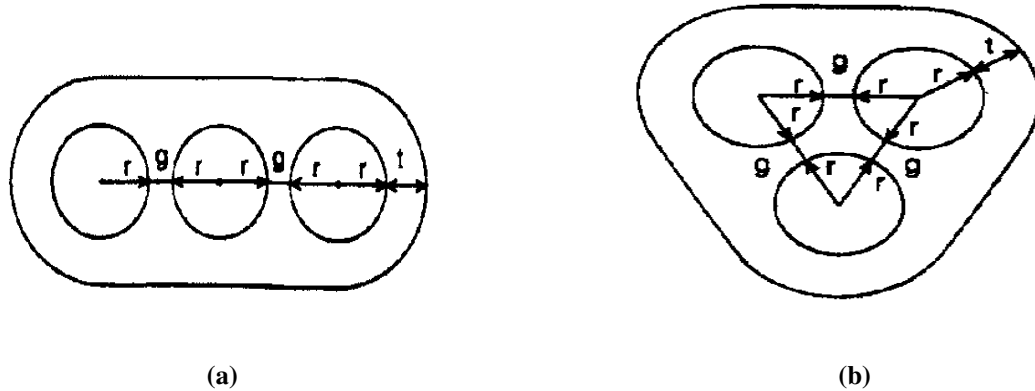


Figure 3.4: (a) Horizontal Cross-Section for an Asymmetric Transformer; (b) Horizontal Cross-Section for a Symmetric Transformer (Fuchs, Roesler & You 1999)

Studies conducted by Fuchs, You and Roesler (1999) at the University of Colorado, Boulder suggested that the magnetising currents of a transformer arranged in a symmetric style would generate no triplen harmonics and the effects of any DC bias currents would be suppressed.

GIC currents find their way into power systems by way of the directly earthed neutrals of certain three phase equipment. A method proposed to eliminate the effects of this form of DC bias is the installation of a Neutral Blocking Device (NBD). An NBD (usually a capacitor) is inserted between the earth point and the neutral star point of the effected equipment. The capacitor does not allow the path of DC current thus negating the effects of GIC currents (Dutil et al. 1992).

The residual magnetism of a transformer's core and tank can impact significantly upon magnetising current characteristics (Fuchs, Roesler & You 1999). Certain studies have shown that non-magnetic steel plate utilised in transformer construction does not experience significant temperature rise as a result of DC bias (Bolduc et al 1997). Hence use of non-magnetic materials during transformer construction can be beneficial in not only reducing residual magnetism but also in alleviating heating effects.

3.4.2 Equipment Related Measures

The most successful measure that can be implemented to combat the adverse effects of DC injection from an equipment perspective is the creation of standards to govern the allowable level of DC injection. There has been some progress along this path with standards such as the Australian Standard AS4777.2-2002 (Grid connection of energy systems via inverters) stipulating maximum levels of DC injection (Khouzam 1999). This standard states that the level of DC output current of an inverter shall not exceed 0.5% of rated output current or 5 mA, whichever is greater. Also the IEEE 519 standard proposes limits for voltage and current harmonic distortion as will be seen in Chapter 7.

From a technical viewpoint and with respect to directly grid connected photovoltaic inverters a number of schemes have been investigated in an attempt to prevent DC injection. Examples of these schemes include closed loop control and voltage feedback control (Ledwich & Masoud 1999).

Chapter 4

Methodology

4.1 Overview

Chapter 2 presented a brief overview of transformer operation based on ideal conditions. Chapter 3 provides the results of a literature review which outlines the theoretical variation in transformer operation when exposed to a biased secondary current. The ideal model for a transformer is shown to be invalidated through the presence of a secondary bias current. Specific adverse effects are presented and potential sources of DC bias are established. Methods for the mitigation of the adverse effects of offset transformer load currents are also explored.

The proceeding chapters aim to validate, clarify and expand upon the theoretical concepts that have been documented. This chapter aims to detail the process that shall be undertaken to achieve this. The reasoning behind chosen courses of action will be detailed and where possible predictions shall be made to pre-empt results.

4.2 Outline of Chapter Purpose and Methodology

This section provides an overview of the purpose and methodology employed in each of the proceeding chapters.

4.2.1 Chapter 5 – Sources of DC Bias

Section 3.3 listed a number of potential sources of DC bias. That there exists a realistic source of DC bias is critical to the relevance of this project. Without a credible source of direct current there is little point in pursuing investigations into the adverse effects that DC current can have on power transformers. Chapter 3 established Geomagnetically Induced Currents as a significant source of direct current. There have been numerous studies conducted into this phenomenon. As such further investigations are unlikely to yield any new contributions. Also equipment and time limitations present themselves as considerable obstacles to further analysis of the GIC problem. Hence alternate sources of bias will be researched.

Chapter 5 investigates sources of DC that are likely to occur in domestic, commercial and industrial applications. Namely the direct current contributions of personal computers (PC's) and AC and DC drives are analysed.

The personal computer can be found in great numbers in commercial establishments such as libraries and office buildings and many domestic dwellings have a PC. In general, PC's interface to the 230 V mains via a switch mode power supply. It is hypothesised that this interface could potentially act as a source of DC bias.

AC and DC motor drives exist in large numbers in industry and they often represent a large portion of the load connected to an establishments supply transformer. As such their contributions if significant could potentially represent a serious source of direct current bias.

The analysis of the DC bias created by AC and DC drives will entail recording a minimum and maximum value for DC injection across each unit's three line side phases. Measurement will be achieved through use of a DC current clamp utilising hall-effect technology. A range of drives will be tested including both AC and DC topologies with a variety of different manufacturers and ratings. The aim is to gain a representative cross section of the drives that are in use in industry today. The results obtained will be evaluated to determine whether the direct current component present (if any) follows a consistent pattern across the test sample. This will provide an indication as to whether the combined DC currents of a number of units exhibit a cumulative or cancelling affect.

The analysis of the DC offset created by personal computers will be achieved through use of an ammeter connected in series with the line side of the PC supply. This is possible due to the single phase nature of computers and their relatively low current requirements. With the meter in circuit measurement of the direct current average, minimum and maximum will be possible. An analysis of the results achieved once again will aim to identify whether or not a consistent injection pattern exists. That is, is there always a positive offset or does the sign of the offset vary from one unit to the next? This will assist in determining whether the effects of multiple computers DC injection are cumulative or whether cancellation occurs.

4.2.2 Chapter 6 – Single Phase Analysis – Magnetising Characteristics

The next step undertaken in the fulfilment of the project specifications was to determine the effect that a biased secondary current has on a transformer's magnetising characteristics. This initial analysis was conducted on the basic single phase case. A solid understanding of single phase concepts should be gained before the progression to three phase applications is undertaken. Many of the adverse effects that stem from the presence of a direct current in a transformer's secondary winding can be attributed to the variation in the unit's magnetising characteristics.

To begin this analysis, tests will be conducted on a 1.2 kVA single phase transformer operating under zero AC load conditions. The only load connected to the unit secondary will be via a diode thus creating a half-wave rectifier. The secondary load will be variable thus allowing for a variable secondary direct current. For each level of secondary bias a number of primary parameters will be recorded. This will allow calculation of the magnitude of core loss current and magnetising current.

Existing literature indicates that a biased transformer load current will lead to an increase in magnetising current, increased VAR absorption and decreased power factor. An evaluation of the test results will be aimed at determining whether the effects outlined above actually occur in practice and to what extent.

With the zero AC load magnetising characteristics determined a new series of tests will be undertaken where by the magnetising currents will be monitored when the transformer is supplying rated AC load in parallel with the half-wave rectified DC component. The purpose of this procedure is to ascertain whether there are any variations in the transformer magnetising characteristics when operating at full load when compared with the zero AC load case. The difficulty with this procedure will lie in extracting the magnetising current component from the primary current.

4.2.3 Chapter 7 – Single Phase Analysis – Harmonic Characteristics

It has been established from existing literature that one of the adverse effects that can result from biased transformer load currents is increased harmonic distortion. This chapter aims to establish the level of harmonic distortion that is generated when a transformer's load current contains a DC component. Prior to presenting the results of the harmonic tests, relevant standards pertaining to harmonic distortion limits will be researched. An analysis of the factors governing the severity of primary and secondary voltage and current harmonic distortion will also be made.

Two series of tests will be conducted to determine the harmonic performance of a 1.2 kVA single phase transformer. Firstly the primary and secondary voltage and current harmonic characteristics will be noted, (up to the 9th harmonic and including THD) when the transformer is loaded with rated AC current in parallel with a variable half-wave rectified current. The relevant trends will be plotted and adherence to standards determined.

The next test undertaken is almost identical in arrangement to the first test. The only difference is that a capacitor will be placed across the variable DC load. This capacitor will serve to smooth the rectified DC voltage. The purpose of this test is to determine whether variation will occur in harmonic distortion when the direct current waveform shape is altered. Once again the magnitude of the distortion levels will be compared to relevant standards to assess compliance.

4.2.4 Chapter 8 – Single Phase Analysis – Hysteresis Characteristics

Chapter 8 will firstly present plots for the 1.2 kVA single phase transformer hysteresis curve for a number of secondary DC levels. The hysteresis curve provides a suitable method for the graphical depiction of transformer saturation. This chapter will also provide the results of a MATLAB program which given a transformer's B-H characteristic and value of flux bias will be able to predict the magnetising current waveform and RMS value. The B-H characteristic will be obtained from the experimental hysteresis plot that was obtained.

4.2.5 Chapter 9 – Three Phase Analysis – Magnetising Characteristics

Chapter 9 provides the results of preliminary tests conducted on a 7.5 kVA three phase transformer to determine magnetising characteristics. In a similar fashion to the single phase case, zero AC load tests will be conducted. Each secondary phase to neutral combination will be biased with a half-wave rectified component. For each

bias test the three phase primary parameters will be monitored. Injection phase to phase will then be conducted with similar measurements recorded.

Chapter 5

Sources of Direct Current

5.1 Overview

There are numerous potential sources of direct current which can bias a transformer's load current. Section 3.3 outlines three significant sources of DC bias, namely Geomagnetically Induced Currents, Photovoltaic systems and AC and DC Drives. There are however numerous other sources of DC bias. One other potentially serious source of direct current stems from non-linear loads such as computers. This chapter aims to investigate the level of DC injection caused by computers and AC and DC Drives. The results of tests undertaken will be presented.

5.2 Computers

Within computers a potential source of DC bias can be seen to originate from the switch mode power supply (SMPS). The switch mode power supply serves as the interface between the required computer supply voltages and the 230 V mains supply. The primary purpose of the SMPS is to act as a DC to DC converter. It initially rectifies the alternating supply voltage then it converts the resulting DC into

the voltages as required by the PC through use of a “chopper”. Switch mode power supplies are not only restricted to computers as they can also be found in Television, Video and Audio equipment.

The ideal switch mode power supply draws a symmetrical current with zero DC offset. However, imperfections in conduction devices can lead to asymmetry and hence the creation of a DC bias. This section aims to determine the level of DC bias (if any) that computers are responsible for.

5.2.1 Test Theory and Method

A total of ten desktop computers were tested to determine if a measurable line side DC component actually existed. The aim was to gain a representative sample of the PC's that are in use today. As such the sample tested consisted of a range of different manufacturers, ratings and styles (laptop/Desktop). The sample also contained a wide range of different aged PC's. One of the PC's tested had an INTEL 486 processor.

The test was conducted with a multimeter set to the DC milliamp range inserted in series with the line side active supply. The meter utilised, had the capability of monitoring the minimum, maximum and average signal values. To gain an accurate picture of these time varying quantities the test was conducted over a ten minute period after which the necessary values were recorded. Whilst the test was conducted a Windows Media application was run on each PC to simulate normal operating conditions.

5.2.2 Test Results and Analysis

The results of the tests are provided in Table 5.1. An initial analysis of these results indicates that the level of DC noted was by no means constant. The overall trend does however exhibit consistency in that every computer tested displayed a positive

DC offset in its line side current. In fact for the ten units tested an average DC component of 11.3 mA was recorded.

DC Injection Tests for Computers			
<i>Style and Power Supply Size</i>	<i>Minimum Value (mA)</i>	<i>Maximum Value (mA)</i>	<i>Average Value (mA)</i>
Desktop (400 W)	-57	56	17
Desktop (250 W)	-44	43	12
Desktop (200 W)	-38	30	6
Desktop (350 W)	-44	43	11
Desktop (350 W)	-41	51	13
Desktop (250 W)	-44	44	13
Desktop (300 W)	-33	34	10
Desktop (350 W)	-42	49	11
Desktop (400 W)	-57	74	16
Laptop (90 W)	-15	26	4
Average Minimum Value = -41.5 mA			
Average Maximum Value = 45 mA			
PC Average = 11.3 mA			

Table 5.1: Results for Measurement of DC Load Current Component for Computers

There are a number of implications that accompany these findings. Firstly, a computer does represent a source of DC bias even though the level is relatively small. Secondly, if there are a number of computers connected to a common bus there may be a cumulative effect in which the DC bias of each unit is of the same sign and hence adds. One must however be cautious in stating this second implication. The sample size utilised was only ten. To confidently state that there is a consistent cumulative effect would require a test be conducted with a much larger sample size with supporting results. Also, increasing the test duration would allow greater confidence to be attributed to findings.

These findings are however important. This is particularly the case in commercial establishments, such as universities and offices, where it is possible that hundreds of

computers will be connected to a common bus and hence a common transformer. If a cumulative DC effect does occur the resulting DC bias could be of a considerable magnitude.

5.3 AC and DC Drives

AC and DC drives are one of the most serious potential sources of DC bias in industry. Drives are used in applications where it is necessary to control the speed of a motor. This form of control is prevalent throughout industry. There are a variety of conduction topologies that can be utilised to achieve either an AC or DC adjustable speed drive arrangement. Some of these arrangements are more likely to create DC offset than others. This section will present the results of experimental work conducted on a range of drives with the aim of quantifying the level of DC that can potentially be created.

5.3.1 Test Theory and Method

A range of AC and DC drives were chosen for the test sample at Tully Sugar Mill in Far North Queensland. The drives chosen covered a broad range of ratings with a number of different manufacturers. Also the applications they were utilised in varied considerably from a simple conveyor belt to a mud pump drive.

The measurement of direct current was achieved through use of a DC current clamp utilising hall-effect technology. The point of measurement was on the line side of each unit. The procedure undertaken to determine the DC bias component entailed measuring each phase's contribution for a five minute period. During each period a minimum and maximum value for bias was recorded.

5.3.2 Test Results and Analysis

The results of the tests conducted are presented in Table 5.2 and Table 5.3. The level of DC figure displayed represents the minimum and maximum value that was recorded for all three phases.

AC Drives			
<i>Manufacturer</i>	<i>Model</i>	<i>Rating (kW)</i>	<i>Level of DC(mA)</i>
Allen-Bradley	Powerflex 70	7.5	2-20
Control Techniques	Unidrive VTC	5.5	8-14
	Commander CDV	7.5	10-30
	Commander CDE	22	13-55
	Unidrive VTC	22	400-1100
	Unidrive VTC	30	-500-2300
	Unidrive VTC	55	500-1900
	Unidrive VTC	160	600-1600
Toshiba	VF-A3	3.7	-10-30
	VF-A3	7.5	30-200
	Tosvert-130G2	4	10-50
Zener	Zener	11	6-10

Table 5.2: Results for Measurement of DC Load Current Component for AC Drives

DC Drives			
<i>Manufacturer</i>	<i>Model</i>	<i>Rating</i>	<i>Level of DC (A)</i>
Control Techniques (Slat Conveyor)	Mentor II	75 kW	2.3-4.8
Control Techniques (Rubber Belt)	Mentor II	75 kW	0.2-1.6
Control Techniques (Bosco Fugal)	Mentor II	75 kW	0.3-1.2
Control Techniques (High Grade Fugal)	Mentor II	410 A	0.6-1.7

Table 5.3: Results for Measurement of DC Load Current Component for DC Drives

The results displayed in the Tables on the previous page indicate that in some instances the level of DC injected by a unit can be considerable however a large amount of variation is also noted. The level of bias does seem to have a loose relationship with the size of the drive.

Over the entire sample the sign of the direct current was most often positive; however there were isolated cases where the variation in bias extended into the negative region. The measurement equipment utilised did not have the capability of recording an average value as with the PC test case. As such caution is once again taken regarding whether a cumulative effect is likely to occur. Further tests need to be conducted with a larger sample size and with equipment that provides an average value for direct current.

There however is an indication that AC and DC drives are indeed a significant source of DC bias. Assuming a cumulative effect and with magnitudes as depicted in the results, the severity of this form of DC source could potentially be substantial. When the drive controlled loads represent a large portion of a supply transformer's connected load (as at Tully Sugar Mill) the effect could be magnified.

Chapter 6

Single Phase Analysis – Magnetising Characteristics

The initial step in understanding the effect of DC current on power transformers is to gain a solid understanding of the effects of direct current on single phase transformers. This chapter will present the results and analysis of experimental procedures conducted on a single phase transformer under a variety of DC bias conditions. To begin with the zero AC load case is analysed. That is, the magnetising characteristics for a single phase transformer are analysed when the secondary current is purely DC. Next the magnetising characteristics are again analysed however this time the secondary is loaded such that rated secondary current flows as well as a DC component.

6.1 Zero AC Load Test

The primary aim of this series of tests was to determine the magnetising characteristics of a single transformer when exposed to DC biased load current conditions. The most accurate way to achieve this is to arrange the transformer such that there is no secondary alternating current component. The secondary should only have direct current flowing in it. Hence any variations in magnetising characteristics are attributed to deviations in the secondary DC component.

6.1.1 Test Theory and Method

The test circuit utilised to complete this phase of testing is illustrated below in Figure 6.1. This circuit illustrates two identical 1.2 kVA single phase transformers connected in such a manner that their secondary voltages oppose and as such cancel. This technique is utilised so as to ensure that there is no secondary AC current present and hence no secondary alternating flux.

The secondary DC component is injected through use of a 12 volt battery and a variable resistive load. Diode D1 is in place to ensure that any small amount of alternating current is half wave rectified. The presence of a small alternating secondary component could potentially occur due to small output voltage mismatches between transformers 1 and 2.

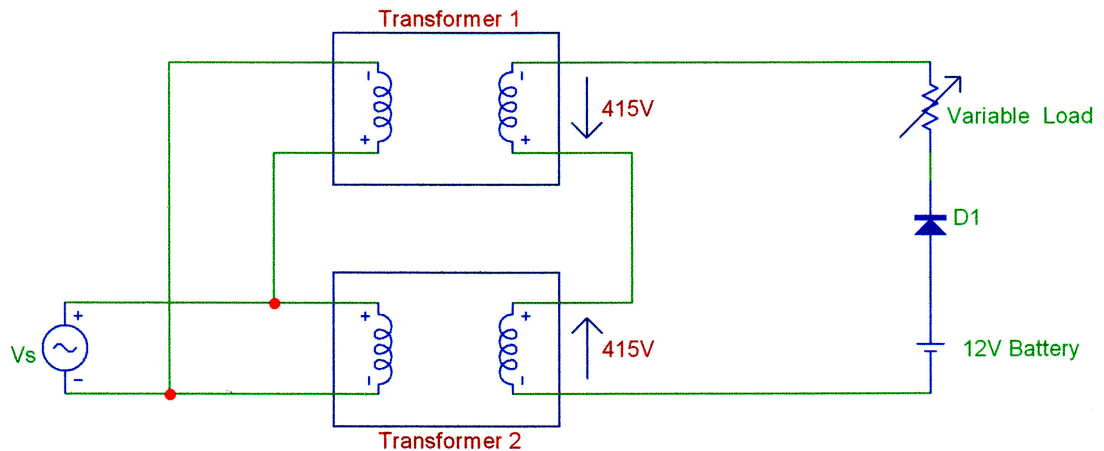


Figure 6.1: Voltage Cancellation Circuit Utilised for No-Load Test

With the circuit arranged as shown in Figure 6.1 the level of DC injected into the secondary can be altered through changing the resistance of the variable load. To gain an accurate picture of the effects of DC the secondary current was varied from 0 to 100 mA in increments of 10 mA. Levels of 200, 300 and 400 mA were also tested. The primary side parameters of Transformer 1 were monitored through use of a Fluke Power Quality Analyser.

6.1.2 Test Results and Analysis

The results of the zero AC load tests are provided in Table B.1 of Appendix B. In order to be able to determine the transformer magnetising characteristics under zero AC load conditions the magnetising current had to be extracted from the no-load current. To solve this problem an expression had to be derived for the primary side power loss.

Prior to formulating this expression it must be realised that the secondary circuit will have negligible effect on primary power loss as there is no secondary AC component (due to dual transformer voltage cancelling) and the secondary DC component will not reflect to the primary side. However it should also be mentioned that it is the secondary DC component that leads to half cycle saturation and thus increased magnetising current. The factors contributing to the primary side power loss will be the loss associated with the primary winding resistance and the loss associated with the core loss current. Hence an expression for the primary side power loss is as follows:

$$P = I_{RMS}^2 R_W + I_C V_S \quad (6.1)$$

where,

- P = Primary Side Power Loss
- I_{RMS} = Primary RMS current
- R_W = Primary Winding Resistance
- I_C = Core Loss Current
- V_S = Supply Voltage

The unknown factor in Equation 6.1 is the core loss current. The other factors were either obtained from the power quality analyser or measured separately using a multimeter. Hence the core loss current is determined as follows:

$$I_C = \frac{P - I_{RMS}^2 R_W}{V} \quad (6.2)$$

With the core loss current calculated the transformer magnetising current can now be found. To do this the assumption is made that the primary RMS current is comprised totally of the core loss current and the magnetising current. This is true provided there is no alternating component present in the secondary. The magnetising current can be found using:

$$I_M = \sqrt{I_{RMS}^2 - I_C^2} \quad (6.3)$$

Figure 6.2 illustrates the effect that a secondary DC bias has on core loss current and magnetising current.

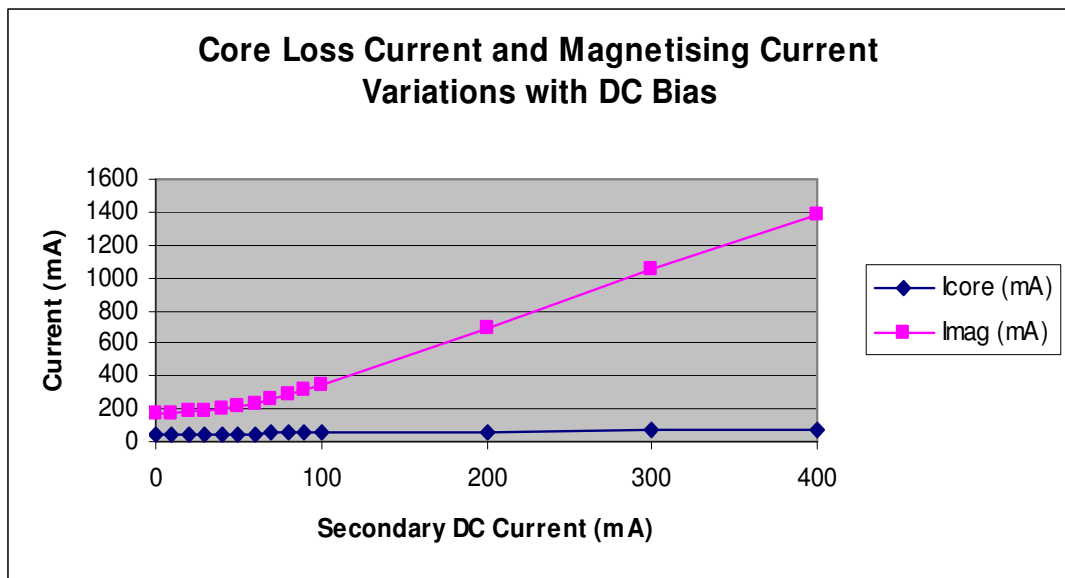


Figure 6.2: Plot of Core Loss Current and Magnetising Current against a Secondary DC Bias

It is evident that the magnetising current rises significantly as the secondary DC component is increased. This effect however is relatively subdued until

approximately 30 mA of direct current is injected. That is equivalent to approximately 23 % of the transformers magnetising current.

The increases in magnetising current are indicative of the effects explained in section 3.1. That is, the transformer is entering half cycle saturation as a result of the secondary DC component. The excess flux in the secondary is not cancelled by a corresponding component in the primary and thus to maintain a constant flux the magnetising current increases.

An analysis of the Figure 6.2 indicates that there is very little variation in the core loss current. The core loss current is comprised of two primary components; the hysteresis losses and the eddy current losses. These losses are functions of frequency and maximum flux density, neither of which has changed during this test. Hence it is expected that there will be very little variation in the core loss current. The small rise that does occur can be attributed to a slight mismatch between the secondary voltages of the two transformers connected in an opposing manner.

Shown in Figure 6.3 is a plot of real, reactive and apparent power for an increasing secondary direct current. This plot verifies the claim that a transformer operating under biased load current conditions will exhibit increased levels of VAR absorption. The volt amp reactive trend can be seen to resemble the same behaviour as the magnetising current from Figure 6.2. This is in line with expectations as the magnetising current is a purely inductive current and hence accounts for all reactive losses (assuming negligible primary winding leakage reactance).

The trend exhibited for real power absorption is similar to that displayed by the core loss current from Figure 6.2. This is also expected as the core loss current is a major factor contributing to real power losses. The level of increase is however slightly greater and can be attributed to the I^2R losses across the primary winding. With little increase in real power it is evident that the apparent power trend will mimic the behaviour of reactive power. This is in evidence in Figure 6.3.

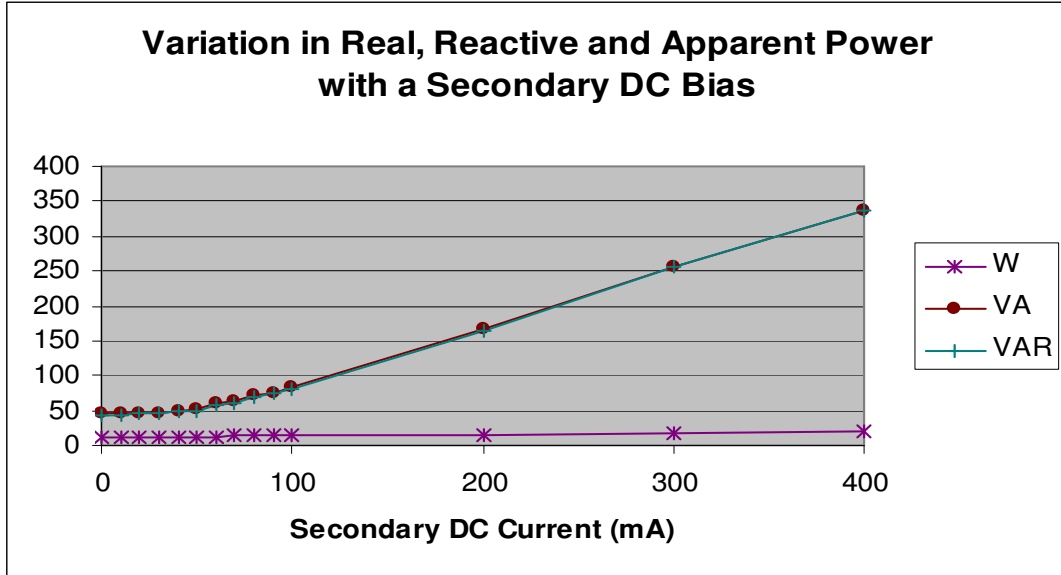


Figure 6.3: Variation in Real, Reactive and Apparent Power with a Secondary DC Bias

Figure 6.4 depicts the relationship between displacement power factor and secondary DC current. With the large increase in reactive power illustrated in Figure 6.3 it is no surprise that the displacement power factor exhibits a downward trend. Once again it is evident that there is little variation in the displacement power factor for the first 30 mA. An interesting observation that can be made is that the gradient of the displacement power factor plot reduces towards the end of the scale tested.

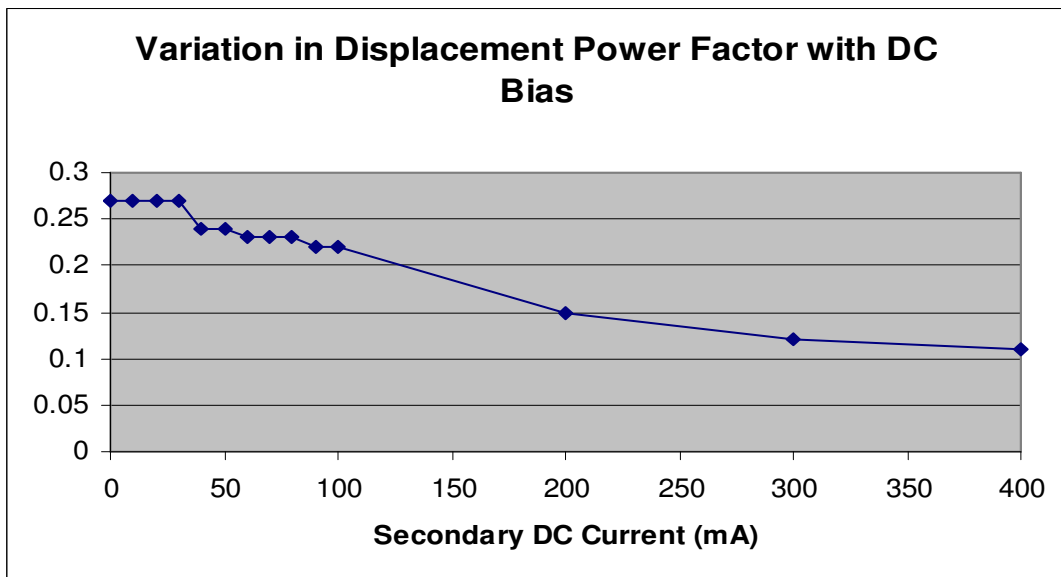


Figure 6.4: Variation in Displacement Power Factor with DC Bias

The next step in the analysis of the results is to inspect the plots of the no-load current waveforms. Before completing this however a better understanding should be obtained of the flux paths in the transformer core when the arrangement depicted in Figure 6.1 is utilised. The direction of the flux created by the secondary DC component can be found through simple application of the right hand thumb rule for a solenoid. The direction of the flux in the positive and negative cycles as created by the transformer magnetising current can be defined in a similar manner. The flux paths are illustrated below in Figure 6.5. On analysis of these paths it is evident that the flux established by the secondary DC current will reinforce the flux created during the positive cycle of the transformer magnetising current. The secondary DC flux will have the opposite effect on the flux created during the negative cycle of magnetising current. Hence a flux offset will occur as depicted in Figure 3.3.

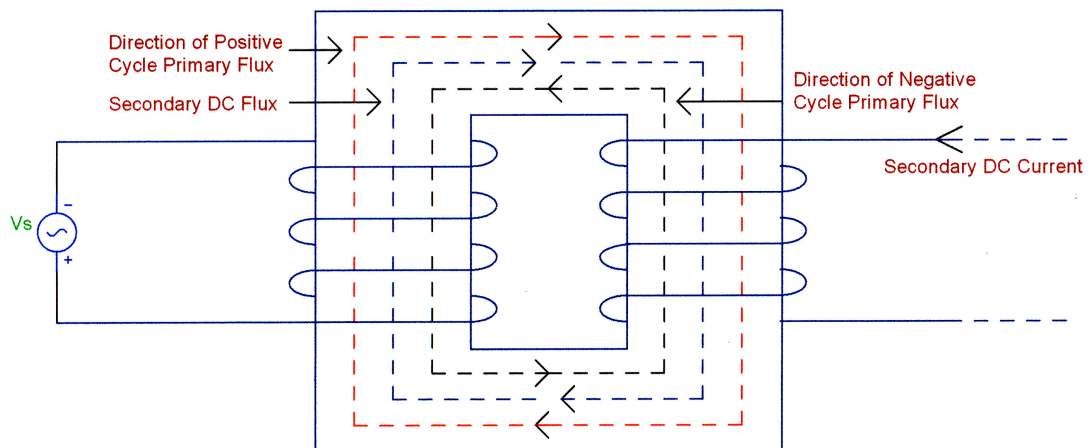
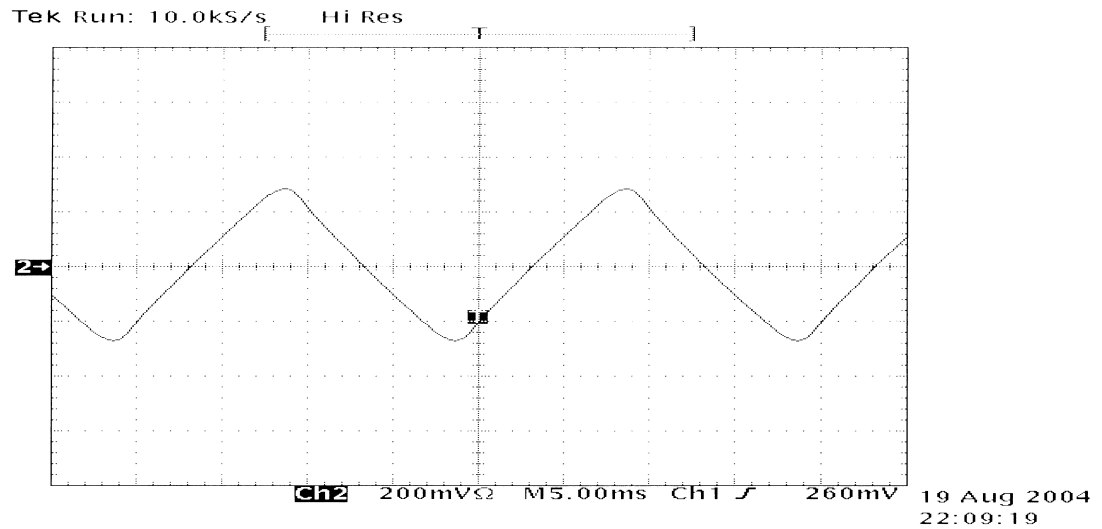


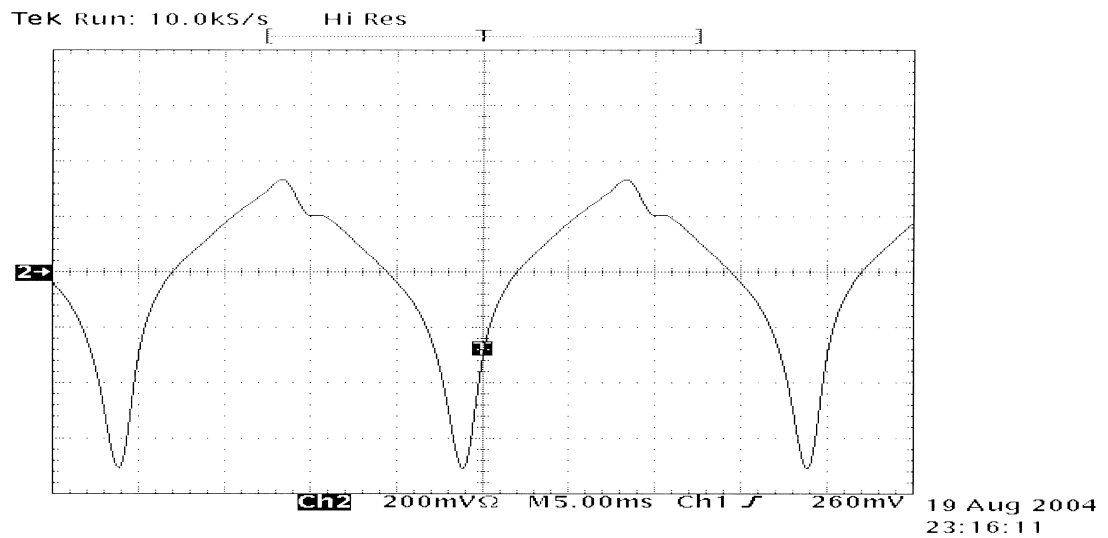
Figure 6.5: Flux Paths Established due to the Secondary DC and Magnetising Current

With the flux paths defined the transformer no-load current waveforms can be analysed. Shown in Figure 6.6 (a) and (b) are the plots for the transformer no-load current for zero DC injection and for 80 mA DC injection respectively. The most evident variation between the two plots is the duration of the negative cycle. The negative cycle duration for zero DC injection is 10 milliseconds as one would expect with a 50 Hz supply. However with 80 mA DC injected the negative cycle duration is reduced to approximately 7.5 milliseconds. This trend can be seen to be

manifested in the other no-load current plots in Appendix B. For 400 mA DC the negative cycle duration has further decreased to 4 milliseconds.



(a)



(b)

Figure 6.6: (a) No-Load Current Waveform for Zero DC Injection; (b) No-Load Current Waveform for 80 mA DC Injection

The decrease in no-load current negative cycle duration is not at all unexpected when the characteristics exhibited in Figure 6.5 are considered. As the DC component is increased the negative cycle flux is further reduced whilst the positive cycle flux is

reinforced. The result is that the net core flux becomes increasingly positive biased. This bias reduces the duration of the negative cycle for the flux waveform and as a result the duration of the no-load current negative cycle is diminished.

Another very interesting point that is noticed in Figure 6.6 (b) is the relatively large magnitude of the negative peak of the no-load current when 80 ma of direct current is injected. An analysis of the no-load current waveforms for larger levels of DC injection (provided in Appendix B) shows that the value of this peak becomes progressively larger.

Prior to explaining this it must be remembered that the secondary DC component is not reflected to the primary. This can be verified by placing a DC ammeter in series in the primary circuit. Even when a very large DC component is injected in the secondary there will be zero direct current present in the primary. Thus no-load current remains symmetrical.

When a positive bias exists in a transformer's secondary load current the flux waveform itself becomes biased. As a result of this the duration of the negative cycle of magnetising current is reduced. The waveform of this current must however maintain symmetry or in other words the area encompassed by the positive half cycle must equal the area encompassed by the negative half cycle. Hence to maintain symmetry the peak value of the negative cycle progressively increases to compensate for a reduction in negative cycle duration. The converse occurs when a negative flux bias is induced.

6.2 Magnetising Characteristics at Rated Load

The purpose of this series of tests was to determine the single phase transformer's magnetising characteristics with a secondary DC component and rated AC load current in the secondary. It is suggested that the presence of rated load current will have little effect on the magnetising characteristics which are flux dependent.

6.2.1 Test Theory and Method

The primary difficulty that was encountered in this test was extracting the no-load current from the load current. A means had to be found from which the effect of the load current could be cancelled out. This was achieved through utilisation of the circuit depicted in Figure 6.7. To cancel out the effects of the resistive load current the primary and secondary load current components had to appear equal but opposite to the Power Quality Analyser (PQA) current clamp. To achieve this, the leads to the transformer primary and secondary positive inputs must be coiled in such a manner that they reflect the transformer voltage ratio (TVR) which is:

$$TVR = V_P : V_S = 240 : 415 = 0.578 \quad (6.4)$$

The optimum combination to achieve the ratio shown Equation 6.4 is to create a coil of 7 turns on the primary input and 12 turns on the secondary input. This yielded the following measurement ratio (MR):

$$MR = 7_{TURNS} : 12_{TURNS} = 0.583 \quad (6.5)$$

This results in ratio which is approximately 0.87% greater than the ideal ratio.

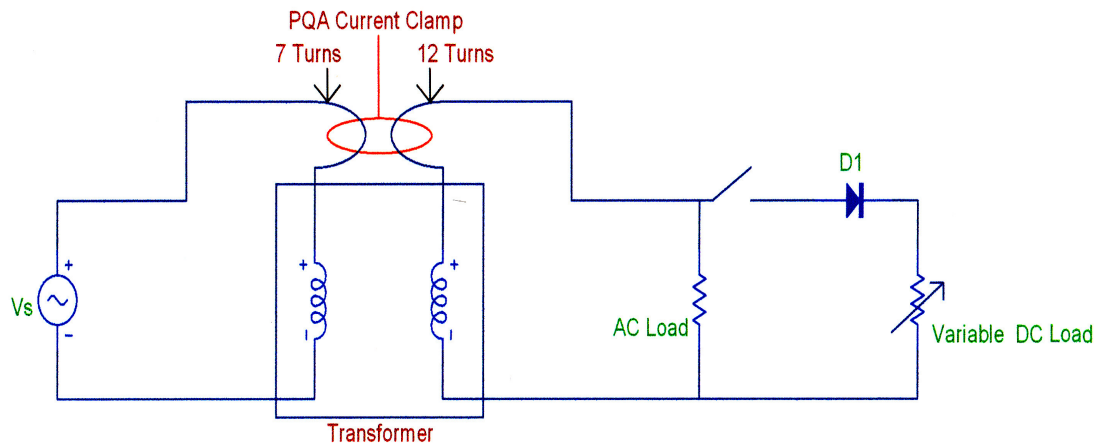


Figure 6.7: Circuit Used to Determine Transformer Magnetising Characteristics at Rated Load

With the primary and secondary measurement coils created the PQA current clamp is clamped over both coils. The two coils have to be arranged such that the flux created by each in the current clamp flows in opposite directions hence cancelling out. With this method utilised the resistive current due to the AC load cancels out and the PQA only measures the no-load current. The DC current in the secondary is not a problem as the current clamp cannot measure DC. There will be a slight error in the current measured due to the slight mismatch between the ideal ratio and measurement ratio.

6.2.2 Test Results and Analysis

The results of this series of tests are provided in Table B.2 of Appendix B. The method used to calculate the core loss current and magnetising current differs to that which was used in Section 6.2. The method employed in Section 6.2 takes into account the contribution to primary power loss made by the primary winding resistance losses. This is not necessary using the technique shown in Figure 6.7 as these losses have been cancelled. Thus the core loss current can be calculated as follows:

$$I_C = I_{1RMS} \times DPF \quad (6.6)$$

The values for I_{1RMS} and DPF were measured and are provided in Table X of Appendix X. With the core loss current calculated the magnetising current can be computed as follows:

$$I_M = \sqrt{I_{RMS}^2 - I_C^2} \quad (6.7)$$

Shown in Figure 6.8 is a plot of the core loss current and magnetising current for a secondary DC range of 0 to 400 mA. The trend exhibited in this plot is very similar to the trend exhibited Figure 6.2 which depicted the zero AC load case. This indicates that the presence of an AC load has little effect on the magnetising

characteristics and the presence of a secondary DC component causes a large increase in magnetising current which can potentially lead to half cycle saturation.

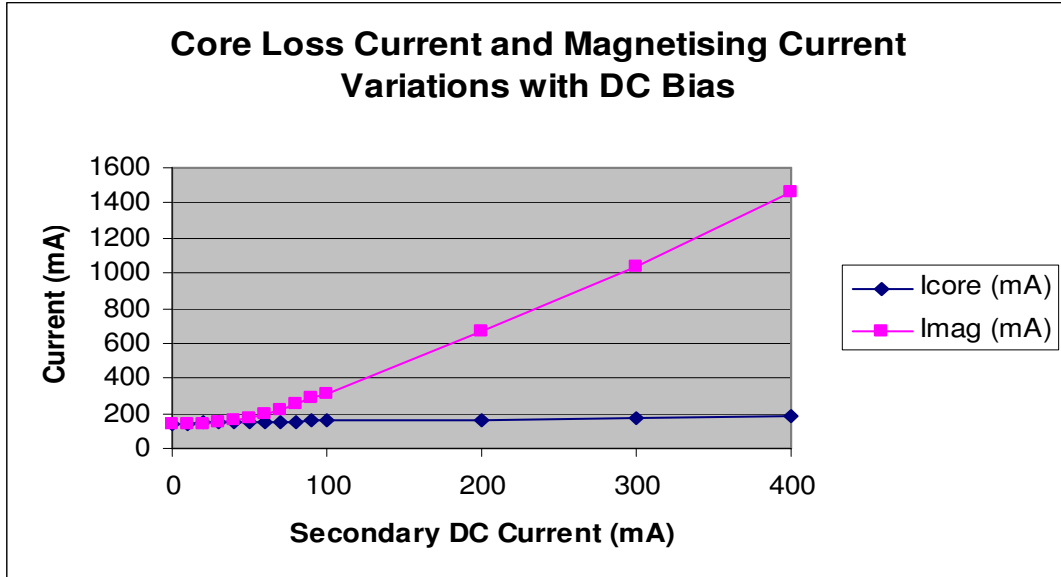


Figure 6.8: Plot of Core Loss Current and Magnetising Current against DC Bias

It is noted that the core loss current shown in Figure 6.8 is slightly enlarged on the results shown in Figure 6.2. This is attributed to ratio mismatch.

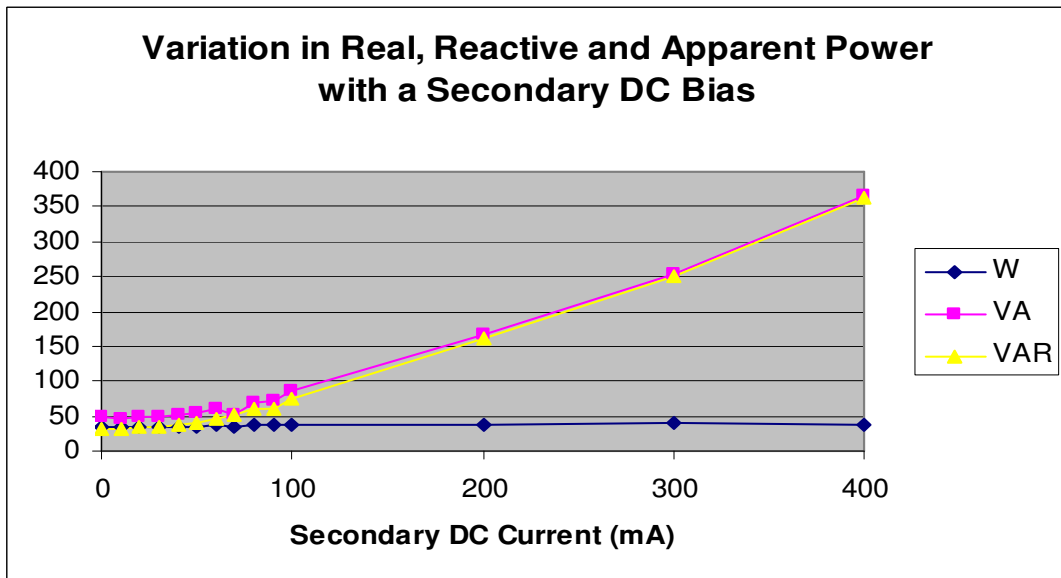


Figure 6.9: Variation in Real, Reactive and Apparent Power with a Secondary DC Bias

Shown in Figure 6.9 is the plot of real, reactive and apparent power with a secondary DC Bias. This plot emulates the results shown in Figure 6.3. The absorption of volt amperes reactive with a secondary DC bias present and rated AC load can be seen to rise in a fashion almost identical to that which occurred with the zero AC load case.

Figure 6.10 depicts the relationship between displacement power factor and a secondary DC component. This trend differs considerably from that which was illustrated in Figure 6.4 for the zero AC load case. With a zero DC component the displacement power factor is much larger in this instance at a value of 0.72 as opposed to the zero AC load case where the zero DC displacement power factor was 0.27. This large variation can be attributed to the increased core loss current which is shown due to the error in measurement ratios.

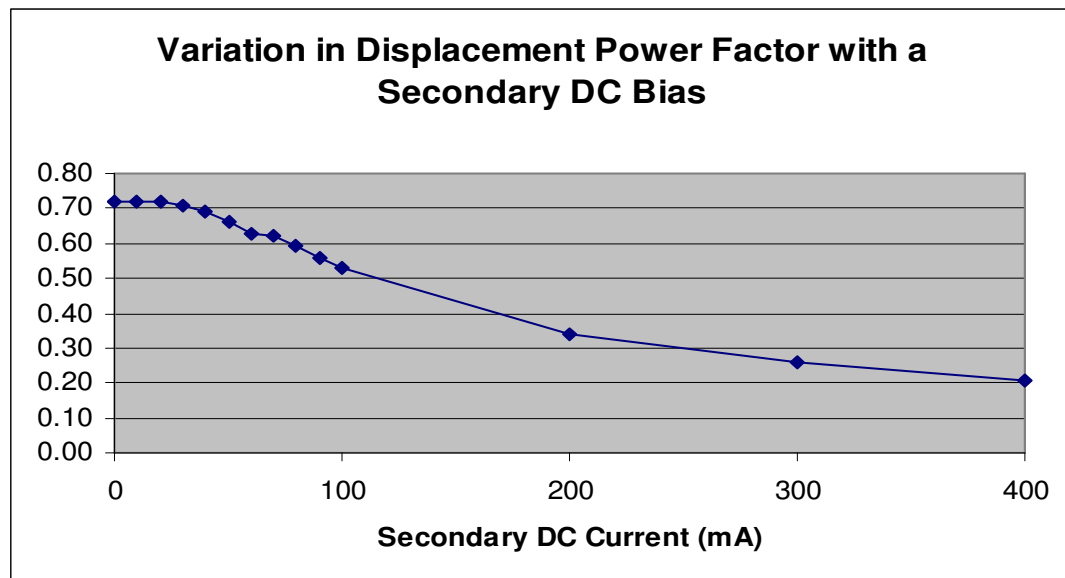


Figure 6.10: Variation in Displacement Power Factor with a Secondary DC Bias

It can be concluded that the presence of a secondary DC component does have a significant affect on a transformer’s magnetising current. This has the potential to induce half cycle saturation. The level of load on the transformer has little effect on this characteristic. As a result of increased magnetising current, increases in VAR

absorption are evident and this also has the effect of decreasing displacement power factor.

Chapter 7

Single Phase Analysis – Harmonic Effects

Chapter 3 established that a transformer operating under biased load current conditions will generate greater levels of harmonic distortion. This chapter aims to analyse the level of primary and secondary voltage and current harmonic distortion created in a single phase transformer when exposed to a DC bias. The level of harmonic distortion created will be analysed and compared to relevant standards. The harmonic spectrum will be investigated to determine which harmonic orders dominate and why.

7.1 Primaries and Secondary Harmonic Distortion

Increased harmonic distortion of a transformer's secondary load current is created through load asymmetry and non-linearity. When a transformer's secondary current contains a DC component asymmetry is induced and hence harmonics are created. The presence of a secondary DC bias results in asymmetrical $i-v$ characteristics which in turn results in elevated levels of even harmonics and in particular the second harmonic (Emanuel & Orr 2000).

Current Distortion limits have been established within the IEEE 519 – 1992 as a guide to restricting the level of distortion created by electrical apparatus. These limits

are illustrated in Table 7.1. The maximum allowable current harmonic distortion is taken in percent of I_L . I_L represents the maximum demand load current at the point of common coupling (PCC). The allowable level of current distortion is dependent on the short circuit ratio of the system. The short circuit ratio can be defined as the ratio of short circuit current at the PCC to the customer's maximum demand current (Colosino, Hoevenaars & LeDoux 2003).

Table 10.3, p78
Current Distortion Limits for General Distribution Systems
(120 V Through 69,000 V)

Maximum Harmonic Current Distortion in Percent of I_L						
Individual Harmonic Order (Odd Harmonics)						
I_{sc}/I_L	<11	$11 \leq h < 17$	$17 \leq h < 23$	$23 \leq h < 35$	$35 \leq h$	TDD
<20*	4.0	2.0	1.5	0.6	0.3	5.0
20<50	7.0	3.5	2.5	1.0	0.5	8.0
50<100	10.0	4.5	4.0	1.5	0.7	12.0
100<1000	12.0	5.5	5.0	2.0	1.0	15.0
>1000	15.0	7.0	6.0	2.5	1.4	20.0

Where:

I_{sc} = maximum short-circuit current at PCC.

I_L = maximum demand load current (fundamental frequency component) at PCC.

Table 7.1: Current Distortion Limits for General Distribution Limits as Defined by Standard IEEE 519 – 1992 (Colosino, Hoevenaars & LeDoux 2003).

The level of voltage harmonic distortion that can be attributed to a particular piece of equipment is a function of the harmonic currents drawn by that piece of equipment and the impedance of the system at the various harmonic frequencies (Colosino, Hoevenaars & LeDoux 2003). The level of voltage harmonic distortion on the secondary of a transformer is particularly important as the secondary is often the point of common coupling for a range of equipment. If a piece of equipment draws a biased load current a certain degree of voltage harmonic distortion is likely to be created. Hence the voltage quality experienced by other devices will be compromised. Certain computing equipment has been found to be particularly sensitive to the level of voltage harmonic distortion. Erratic behaviour has in some instances been found to occur when the voltage total harmonic distortion (THD) has exceeded 5% (Colosino, Hoevenaars & LeDoux 2003).

The standard IEEE 519 – 1992 proposes limits for voltage THD. These limits are illustrated below in Table 7.2. The allowable range of distortion is dependent upon application. At the high end of the scale a voltage THD of 10% is allowable for dedicated systems. The dedicated system includes those arrangements that are comprised only of converter loads. At the low end of the scale there are special applications (hospitals, airports) which require a voltage waveform which is not more than 3% distorted. General systems, which encompass the majority of applications, should be supplied with a voltage with THD not greater than 5% and no individual harmonic greater than 3% (Colosino, Hoevenaars & LeDoux 2003).

Table 10.2, p77
Low-Voltage System Classification and Distortion Limits

	Special Applications¹	General System	Dedicated System ²
Notch Depth	10%	20%	50%
THD (voltage)	3%	5%	10%
Notch Area (A_N) ³	16 400	22 800	36 500

NOTE: The Value A_N for other than 480 V systems should be multiplied by $V/480$

¹ **Special applications include hospitals and airports**

² A dedicated system is exclusively dedicated to the converter load

³ In volt-microseconds at rated voltage and current

Table 7.2: Low-Voltage System Classification and Distortion Limits as Defined by Standard IEEE 519 – 1992 (Colosino, Hoevenaars & LeDoux 2003).

The current harmonic distortion on the primary side is important as it will impact on those devices that are connected upstream in the power system. The distortion of the primary current reflects not only the distortion in the secondary current but also distortion in the transformer magnetising currents when operating in the saturated region of the B-H curve.

The severity of the effect of primary side voltage harmonic distortion is dependent on the system short circuit ratio. If the system which the transformer is connected to is relatively large, infinite bus conditions can be assumed. In this instance the effect of primary voltage harmonic distortion will be negligible.

7.2 Harmonic Analysis – Half-Wave Rectified DC

The aim of this series of tests was to determine the primary and secondary voltage and harmonic characteristics when the transformer was loaded with rated AC load in parallel with a half-wave rectified DC component. Harmonic trends are illustrated and the harmonic levels are analysed to determine if standards have been exceeded.

7.2.1 Test Theory and Method

As stated above the injection of DC was achieved through use of a half-wave rectifier. The circuit utilised for the test is illustrated in Figure 7.1. The single phase transformer utilised in this test was rated at 1.2 kVA.

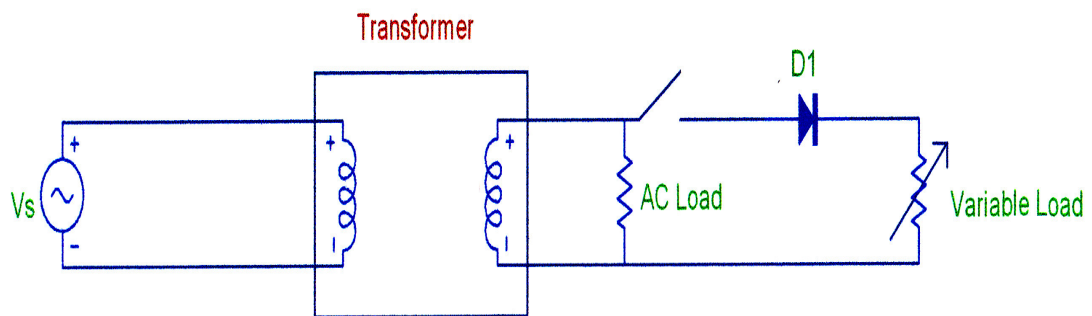


Figure 7.1: Circuit Configuration for DC Injection via Half-Wave Rectifier

The arrangement of this circuit is such that diode D1 only conducts for half the AC cycle. Hence the direct current waveform will be as shown in Figure 7.2. The voltage and current harmonic characteristics of both the primary and secondary were analysed with a FLUKE Power Quality Analyser.

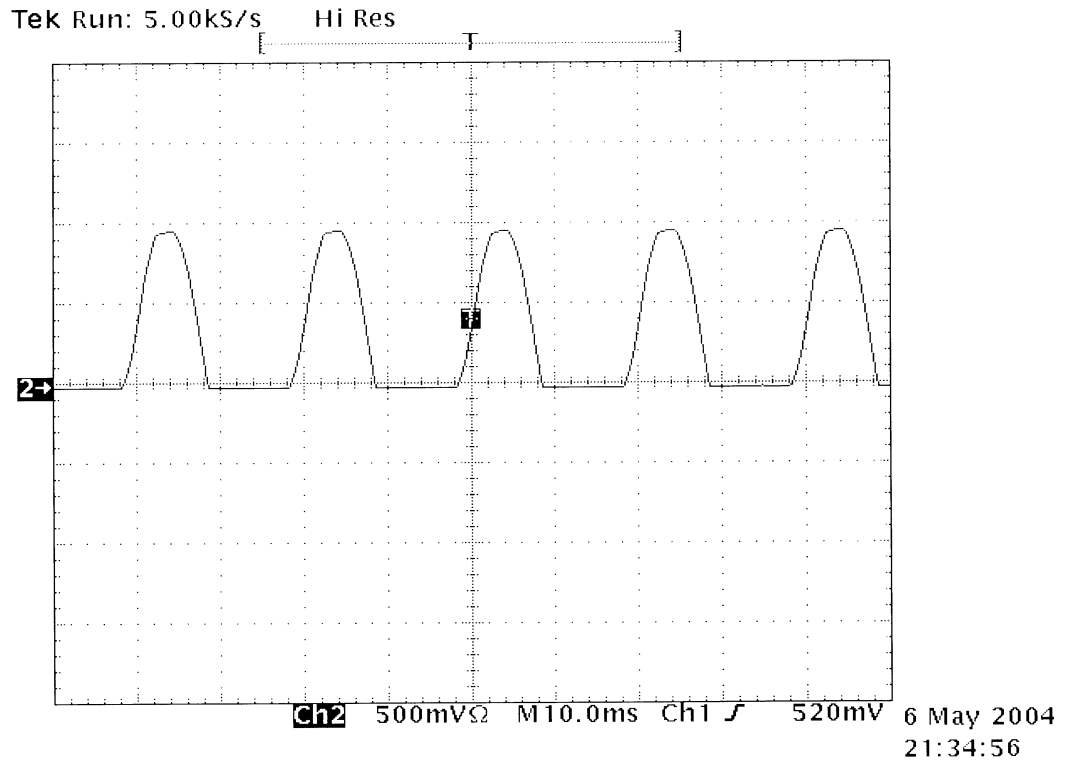


Figure 7.2: CRO Screen Shot of Half-Wave Rectified Direct Current

7.2.2 Test Results and Analysis

The results of the tests conducted on the circuit depicted in Figure 7.1 are provided in Appendix C. Table C.1 contains the primary voltage and current harmonic results whilst Table C.2 contains the secondary voltage and current harmonic results. In recording the results it was decided to truncate the harmonic series at the 9th order. This was due in part to time limitations and also the fact that the value of harmonics above this were in most instances negligible.

Shown in Figure 7.3 is a graph depicting harmonics of 2nd order through to 6th order as well as the total harmonic distortion. Whilst the 7th, 8th and 9th orders were measured, little variation occurred over the range of secondary DC currents injected.

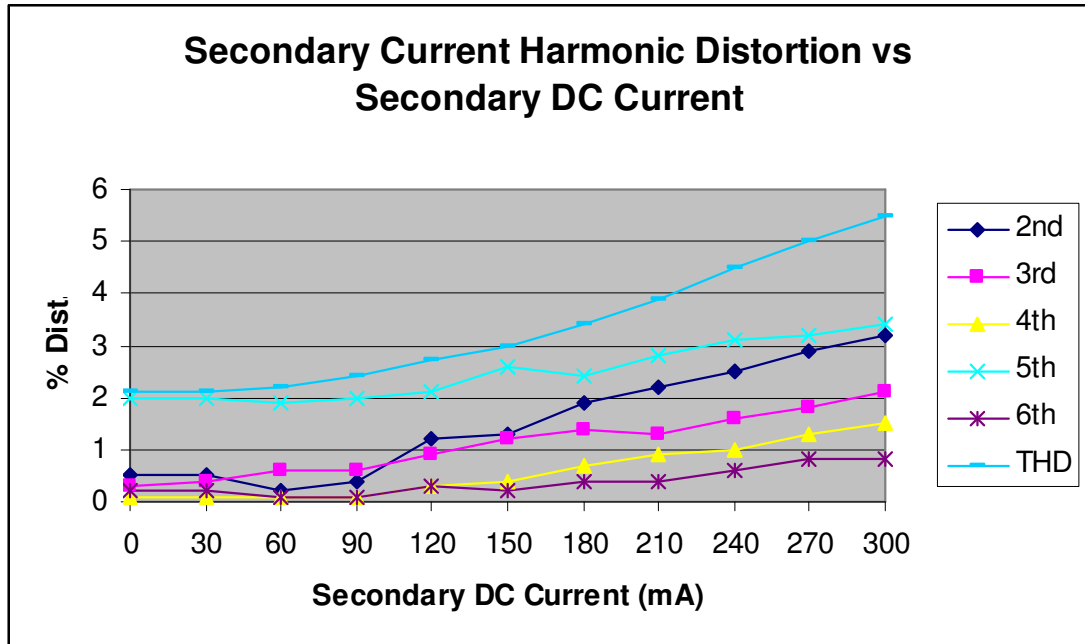


Figure 7.3: Secondary Current Harmonic Distortion with a Secondary DC Current

The distortion patterns displayed in Figure 7.3 are a result of the waveform asymmetry induced by the secondary DC bias. This asymmetry has caused a significant percentage increase in the 2nd and 4th even harmonics. The 3rd order zero sequence harmonic has also experienced a significant percentage increase. The 5th order harmonic, whilst of a relatively high magnitude, has not experienced a significant percentage increase for the range of secondary DC covered. Its high magnitude can be attributed to the existing distortion of the Engineering Block supply voltage waveform.

The distortion levels of the harmonics recorded do not exceed even the strictest current distortion limits as defined by Table 7.1 for the range tested. For an infinite bus supply the level of current distortion would have to be considerably greater to be of any real concern.

Figure 7.4 depicts the secondary voltage harmonic distortion that has resulted due to the injection of a secondary DC component. Once again the 7th through to 9th order components have been omitted due to lack of significant effect.

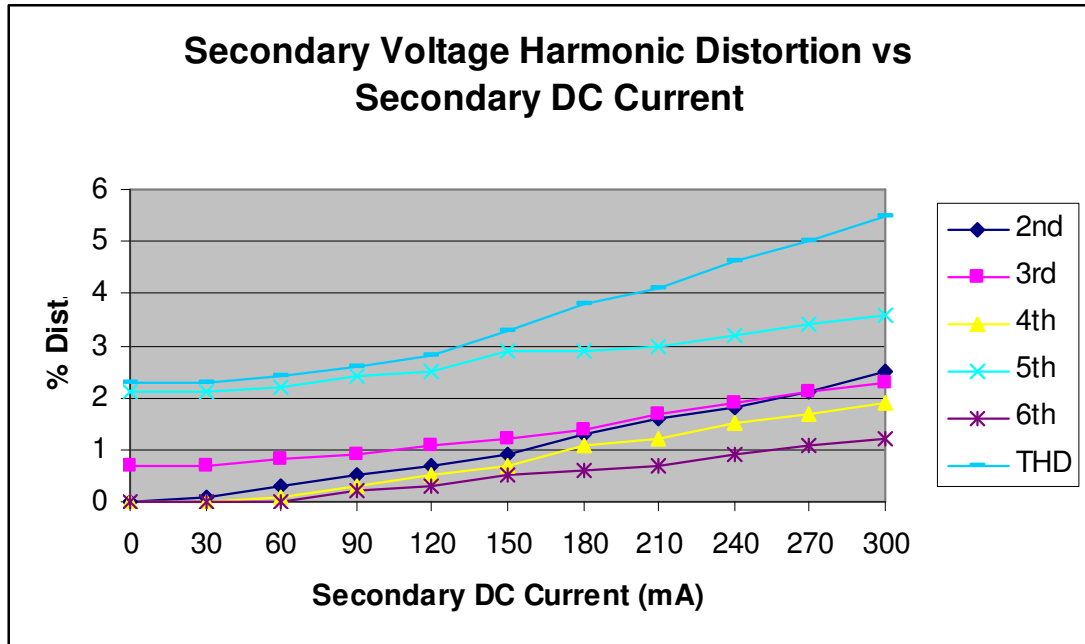


Figure 7.4: Secondary Voltage Harmonic Distortion with a Secondary DC Current

With respect to the voltage distortion limits as established by the IEEE 519-1992 standard a number of violations are noted in Figure 7.4. The standard states that the value for voltage total harmonic distortion for a general system (which we are assumed to be working with) should not exceed 5% nor should it exceed 3% for any individual harmonic component. The 5% limit for total harmonic distortion is exceeded after approximately 270 mA of secondary direct current is injected. The 5th order harmonic can be seen to exceed the 3% limit after approximately 210 mA of secondary DC is injected. Hence it can be seen that a certain degree of unacceptable voltage harmonic distortion has been created. However the level of DC required to exceed the limits is large and of the order of 7% to 9% of the transformer's rated current.

Quite large levels of primary current harmonic distortion are noticed on analysis of Figure 7.5. The distortion depicted is a combination of the distortion resulting from the distorted secondary current waveform and the distortion of the magnetising current due to the transformer entering the saturated region of operation.

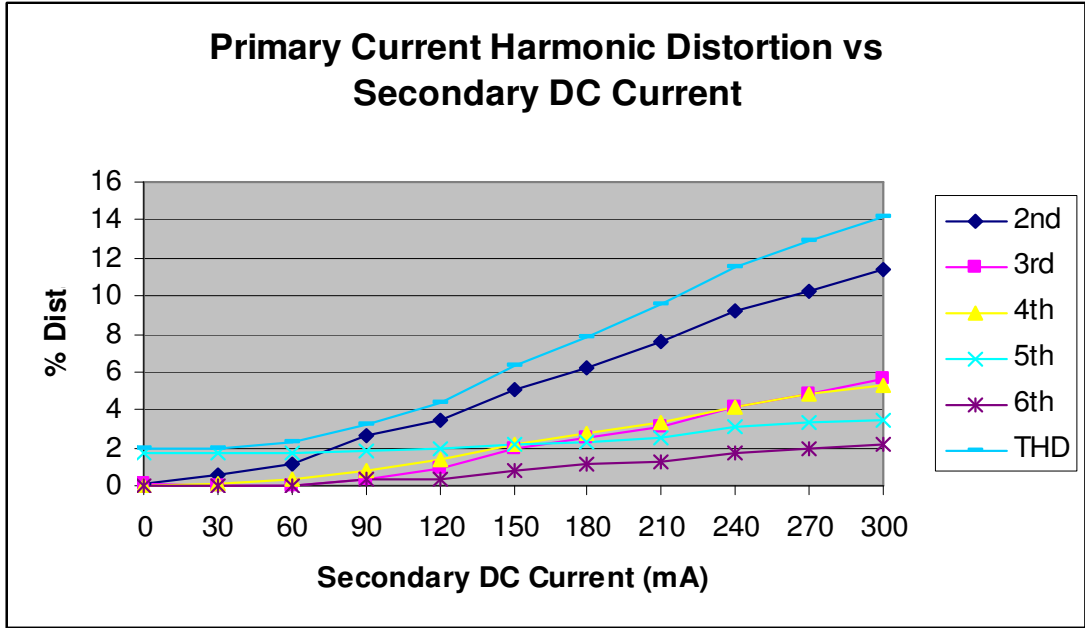


Figure 7.5: Primary Current Harmonic Distortion with a Secondary DC Current

The primary current will not contain a DC component since the transformer cannot reflect its secondary DC bias. Therefore equipment on the line side of the DC biased transformer will not be exposed to a zero order harmonic; however the level of other harmonics as depicted in figure 7.5 will certainly be elevated.

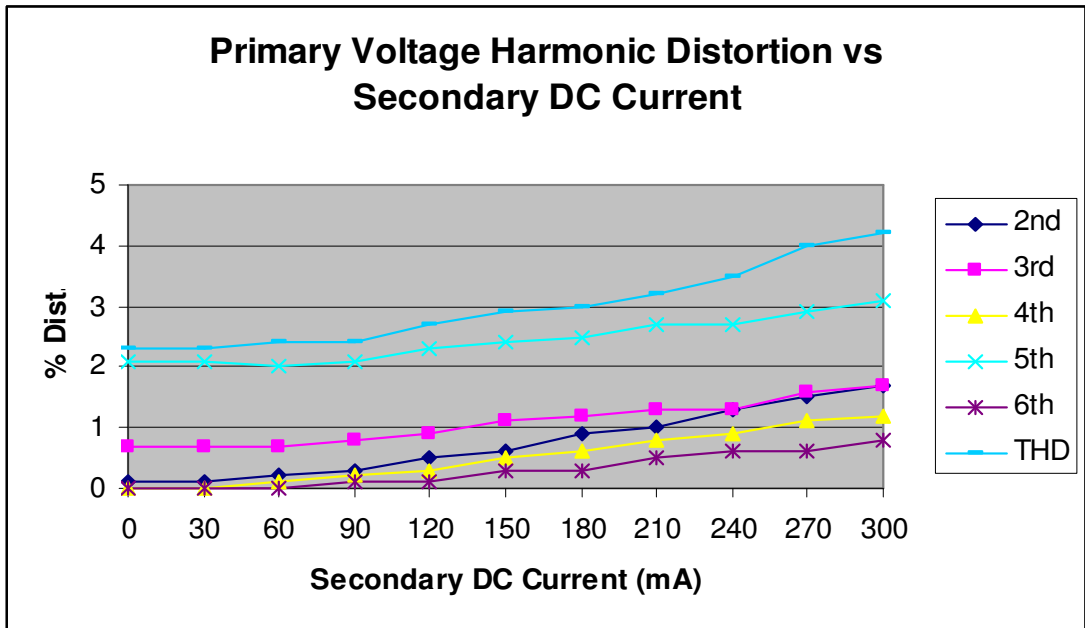


Figure 7.6: Primary Voltage Harmonic Distortion with a Secondary DC Current

The significance of primary voltage harmonic distortion is dependent on the system short circuit ratio. The system for which these tests were conducted on is part of a very large distribution system. As such it is safe to assume the system is relatively “stiff”. As such the effects of this distortion will be negligible. The results for primary voltage harmonic distortion are shown in Figure 7.6.

7.3 Harmonic Analysis – Smoothed Half-Wave Rectified DC

The purpose of this test was similar to that of the previous test with the exception that the half-wave rectified secondary DC component was smoothed through use of a capacitor in parallel with the DC load. The aim was to determine if there was any significant variation in the harmonic distortion with the altered DC component.

7.3.1 Test Theory and Method

Shown below in Figure 7.7 is the schematic of the circuit utilised to achieve DC injection. This circuit differs from that shown in Figure 7.1 in that it has a capacitor in parallel with the variable DC load. This capacitor serves to smooth the half-wave rectified DC voltage waveform. When the AC cycle reaches its positive peak the capacitor will be fully charged. It will then dispense its charge for the remainder of the positive cycle and all of the negative cycle. This will increase the average value of the DC voltage waveform and hence the direct current waveform.

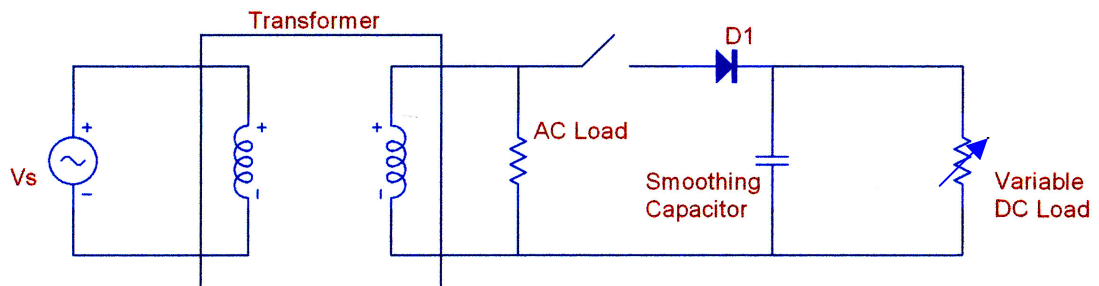


Figure 7.7: Circuit for Capacitor Smoothed DC Injection via Half-Wave Rectifier

Shown below in Figure 7.8 is a CRO screen shot of the smoothed half-wave rectified direct current waveform. The value of the smoothing capacitor used in this test was 10 μF . A larger value of capacitance could have been utilised to improve the smoothing effect, however the value used was considered adequate for this test as it significantly smoothes the waveform compared to the half-wave rectifier.

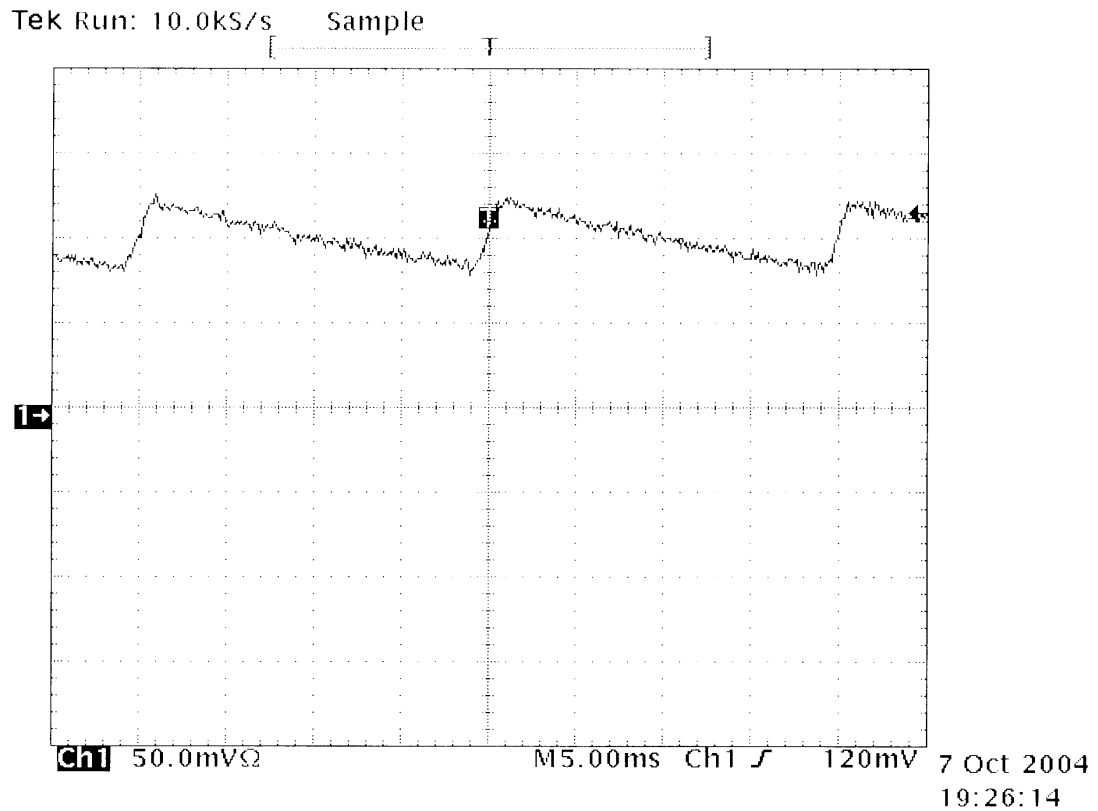


Figure 7.8: CRO Screen Shot of Smoothed Rectified DC Current

7.3.2 Test Results and Analysis

Both the primary and secondary voltage and current harmonic parameters were monitored through use of the FLUKE Power Quality Analyser. The primary and secondary results are provided in Appendix C, Tables C.3 and C.4 respectively. Also provided in Figures C.1 through to C.4 are the plots of the harmonic components that were measured for primary and secondary, voltage and current harmonic distortion.

A number of interesting trends were noted. Firstly the level of secondary current distortion could be seen to be significantly increased using the injection arrangement depicted in Figure 7.7 as opposed to the arrangement utilised in Figure 7.1. The direct current waveform created through use of capacitor smoothing induces a greater level of harmonics when introduced into the secondary AC current compared to the simple half-wave rectified version.

Another interesting affect that was noted using the arrangement depicted in Figure 7.7 was that the majority of secondary current harmonics measured tended to peak at around 120-180 mA after which they either levelled off or decreased. The exception to this was the secondary harmonic which continued to display a positive gradient over the entire range recorded. This continued increase in the secondary harmonic is representative of the increased asymmetry that accompanies the increasing secondary component.

The flattening off trend exhibited by the remaining harmonics can be attributed to the fact that a constant capacitance was utilised in the DC voltage smoothing procedure. The effect that this capacitor had on smoothing the secondary direct current component decreased as the level of direct current was increased. The harmonic content induced by a smooth DC component is greater than that created by a half-wave rectified component. Hence it is of little surprise that the harmonics associated with the capacitor smoothed secondary DC component level off and in some instances even reduce as the effect of the capacitor diminishes.

The increased secondary current distortion does not appear to have appreciably affected the level of secondary voltage harmonic distortion. The level of secondary voltage distortion with the capacitor smoothed DC component is comparable to the half-wave rectified version. The level of voltage harmonic distortion appears to be a function of the average level of DC. Little correlation can be found to say that currents of the same magnitude but with differing harmonic distortion levels will have differing impacts on voltage distortion. In terms of adherence to voltage

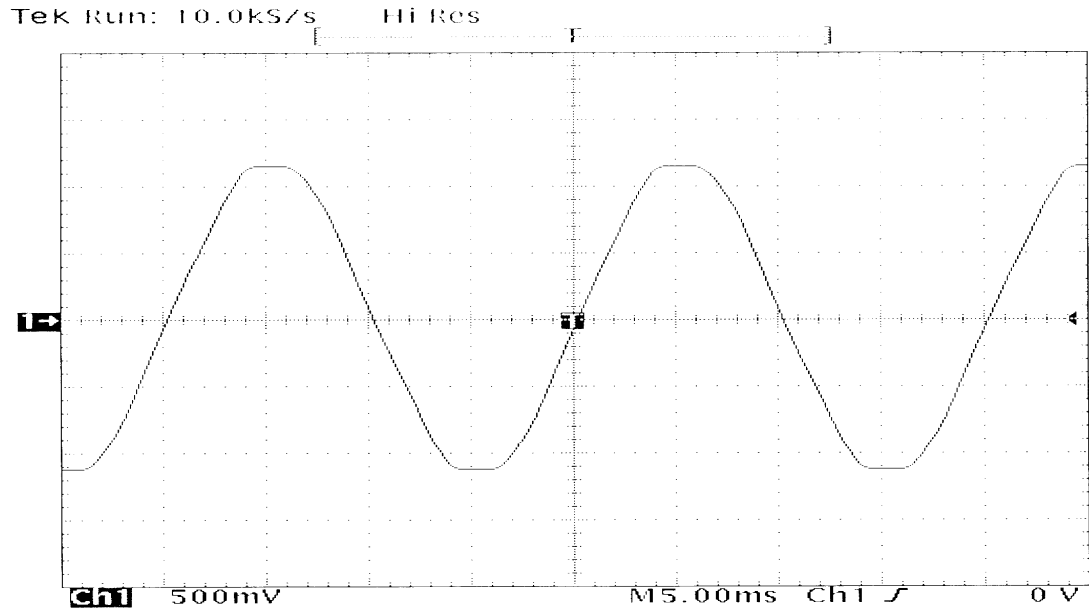
distortion standards the secondary voltage THD remains within the 5% limit over the range tested. In terms of individual harmonics the 5th harmonic exceeds the 3% limit after 210 mA is injected.

The increase in secondary current harmonics has led to a corresponding significant rise in the level of primary current harmonic distortion as is evident in Figure C.2. The 2nd, 3rd and 4th harmonics exhibit very similar trends which after about 120 mA increase linearly.

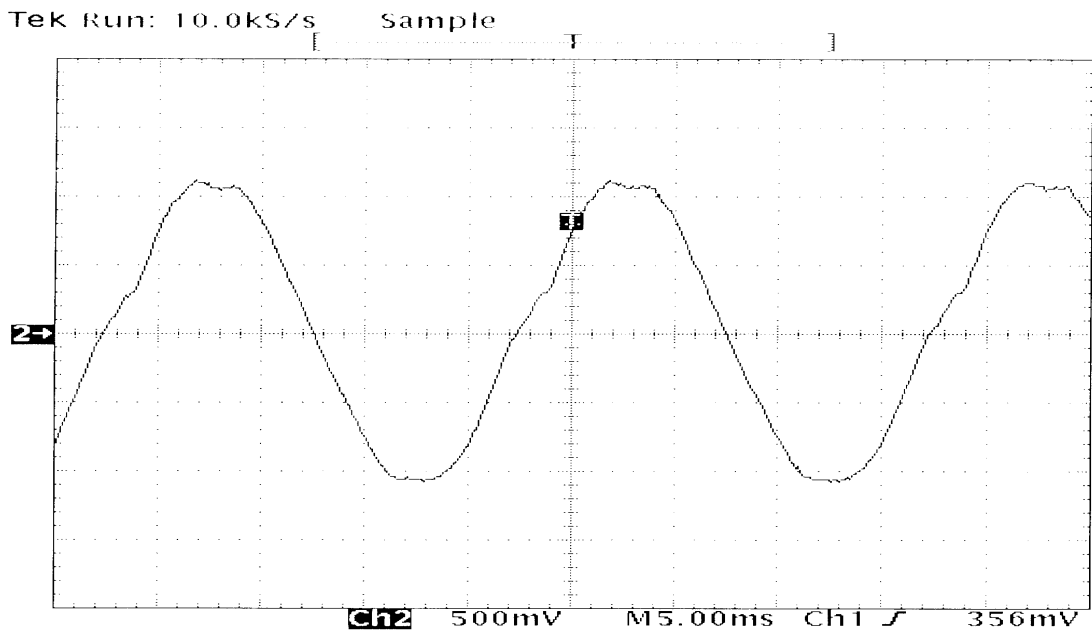
Minimal increase in the primary side voltage harmonic distortion is noted. This is indicative of a strong supply.

A visual of the effects of the DC induced secondary voltage harmonic distortion can be obtained through comparison of Figures 7.9 (a) and (b). Figure 7.9 (a) depicts the secondary voltage waveform for a zero secondary DC component. It is noticed that there is an existing flat top effect on both the positive and negative cycles. This is indicative of the supply provided in the Engineering Block at USQ. No investigation has been made into the cause of this.

Shown in Figure 7.9 (b) is a CRO screenshot of the secondary voltage waveform when a secondary DC component of 300 mA is injected. It is evident the voltage waveform is only affected on the positive cycle. This can be attributed to the fact that the half-wave rectifier only conducts during the positive half cycle. During the negative half cycle the secondary current should not contain a DC component.



(a)



(b)

Figure 7.9: (a) Secondary Voltage Waveform for Zero DC Secondary Component; (b) Secondary Voltage Waveform for 300 mA DC Secondary Component

Chapter 8

Flux and Magnetising Current Prediction

A transformer's operational capabilities are limited to a large extent by the characteristics of its core. A transformer cannot support an infinite level of flux and hence the relationship between magnetizing current and flux is a non-linear one. This chapter aims to analyse the relationship between flux and magnetizing current when a single phase transformer is exposed to biased load current operating conditions. An overview of relevant theory will be conducted. A number of experiments were conducted to determine the flux-magnetising current relationship of a 1.2kVA single phase transformer. The methodology employed as well as the results obtained will be investigated. A MATLAB program called *Magnetising_Current_Prediction.m* was created to predict a transformer's primary side magnetising current given a certain level of flux bias. An analysis of the process will be undertaken and limitations established. The results obtained will be compared with actual experimental data.

8.1 Theory Overview

Power transformers are characterised by a non-linear $i - \phi$ hysteresis characteristic. This trend is displayed in Figure 8.1. On analysis of the mid point locus of this trend a number of operating regions can be isolated. For small values of magnetising

current either side of the origin a fairly linear increase in flux is witnessed. Around the knee of the curve, which is designated by point ‘f’, a distinctly non-linear relationship exists between current and flux. This non-linear characteristic is maintained and the transformer can be seen to be entering the saturated region of operation in the vicinity of point ‘c’. When in the saturated region large increases in magnetising current are required to create noticeable increases in flux. The characteristic depicted below is very much dependent on the material utilised in the core.

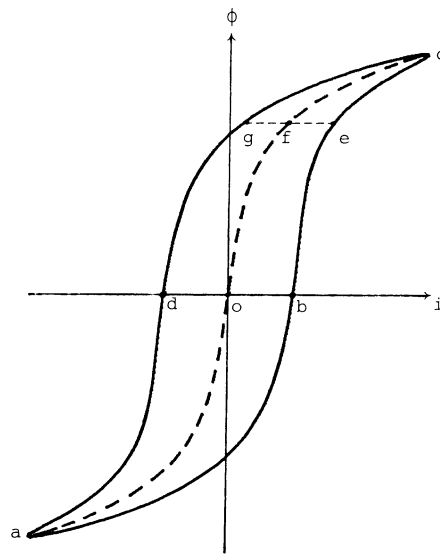


Figure8.1: Transformer Flux-Magnetising Current Hysteresis Characteristic
(Huang et al. 1989)

In general the magnetisation trend for a saturable inductor is given by the following:

$$v = Ri + L(i) \frac{di}{dt} \quad (8.1)$$

Through a process of integration the following can be obtained:

$$\int v \, dt = \int Ri \, dt + \int L(i) \, di = \int Ri \, dt + \int d\phi \quad (8.2)$$

Hence,

$$\Phi = \int v dt - \int Ri dt \quad (8.3)$$

Often the effect of the winding resistive voltage drop (represented by Ri) is neglected. This results in a certain amount of error. The magnitude of this error decreases for larger transformers due to the lower winding resistance. The magnetisation trend for a transformer must also take into account the effect of multiple turns in windings. As such the flux in a transformer can be determined as shown in Equation 8.4 (Calabro, Coppadoro & Crepaz 1986).

$$\Phi = \frac{1}{N} \int v dt \quad (8.4)$$

It should be noted that the relationship for flux given in Equation 8.4 cannot account for a unidirectional component of flux created by a secondary DC component when 'v' represents the primary side voltage. The DC component of flux can be derived as shown in Equation 8.5.

$$\Phi = \frac{MMF}{\mathfrak{R}} \quad (8.5)$$

In equation 8.5 ' MMF ' represents magnetomotive force whilst ' \mathfrak{R} ' indicates reluctance. The relationship for magnetomotive force and reluctance are provided in Equations 8.6 and 8.7 respectively.

$$MMF = NI, \text{ Ampere-turns} \quad (8.6)$$

$$\mathfrak{R} = \frac{l}{\mu A} \quad (8.7)$$

The terms specified in the reluctance equation can be defined as follows:

l	=	length of magnetic circuit
μ	=	core permeability
A	=	core cross-sectional area

Hence when a secondary DC current is present in a transformer's load current, a DC flux is created. This flux will induce a net flux bias within the transformer core. This is shown in Figure 3.3. The net flux in the core will be given by the following:

$$\Phi_{net} = \Phi_{ac} + \Phi_{dc} \quad (8.8)$$

One final point that can be mentioned in regards to the relationship between AC flux and magnetising current is that they are in phase. Equation 8.4 depicts the flux as being the integral of the sinusoidal supply voltage. This integral will equate out to a negative cosine function which lags the supply voltage by 90 degrees. Similarly the magnetising current is purely inductive as it can be attributed entirely to the magnetising reactance. This inductive current will also lag the supply voltage by 90 degrees and thus be in phase with the alternating component of core flux.

8.2 Practical Hysteresis Measurements

A transformer's hysteresis curve provides a graphical representation of the magnetisation characteristics of the unit. This section will present actual results of hysteresis tests undertaken on a 1.2 kVA single phase transformer. The methodology employed as well as the validity of results will be detailed.

8.2.1 Test Theory and Method

The circuit utilised in this experimental procedure relies on the fact that the flux is the integral of the applied voltage. The integration of the supply voltage is achieved through use of the series RC circuit as shown in Figure 8.2. The series RC circuit has

been arranged such that the capacitive reactance at 50 Hz is significantly less than the series resistor value, and as such a reasonably accurate integration will be obtained. Channel 2 of the Tektronix Cathode Ray Oscilloscope (CRO) has been placed across the capacitor. With the CRO set to the x-y plot mode, channel 2 will be the 'y' co-ordinate for the hysteresis plot. It should also be noted that the connection across the capacitor to channel 2 on the CRO was done via a high voltage probe interface. This was done as an equipment safety precaution.

As shown below in Figure 8.2 a current clamp has been placed across the neutral return of transformer 1 to serve as the channel 1 input to the CRO. With switch S1 open the current clamp measures the no-load current which is largely comprised of the magnetising current component. It should be noted that there is some error introduced due to the presence of a core loss current component.

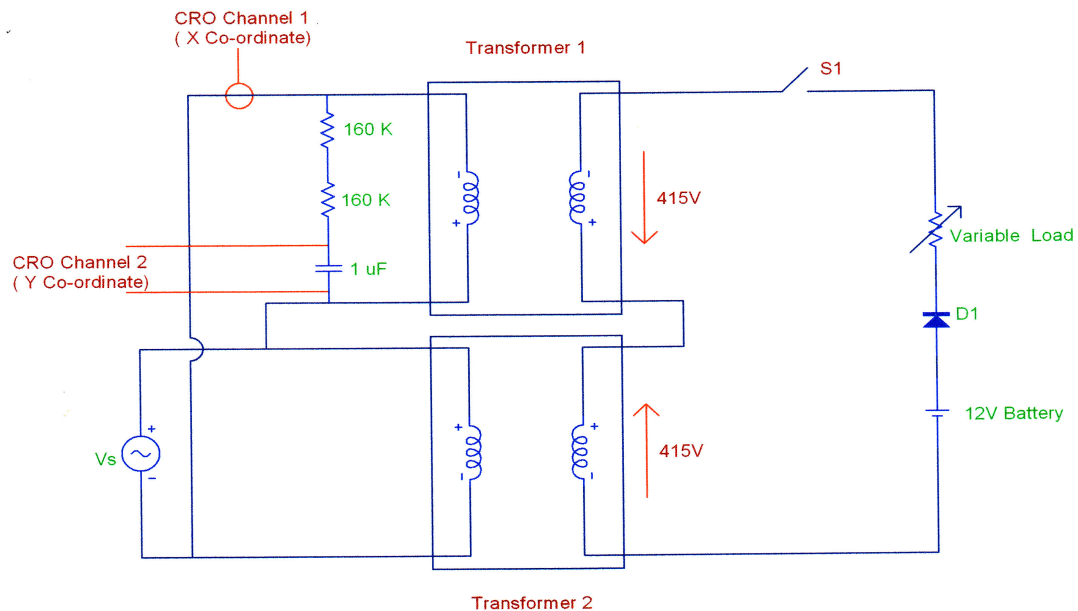


Figure 8.2: Circuit Utilised to Conduct Hysteresis Experiment

The dual transformer voltage cancellation technique as described in Chapter 6 is once again utilised in this test. This ensures that the secondary alternating current component is suppressed.

8.2.2 Test Results and Analysis

The first two experiments undertaken using the circuit depicted in Figure 8.2 entailed gaining a plot of the hysteresis characteristic (flux vs. magnetising current) at a supply voltage equivalent to 1 pu (240 V) then at 1.125 pu (270 V) with switch S1 open. The hysteresis characteristic at 240 V was necessary to provide an indication of the transformer performance when operating under normal conditions. Shown in Figure 8.3 is a plot of the resulting hysteresis characteristic. The vertical axis represents flux whilst the horizontal axis depicts magnetising current. The relationship between flux and magnetising current can be seen to be largely linear with a small amount of non-linearity near the peak of the flux waveform. The transformer has not entered saturation.

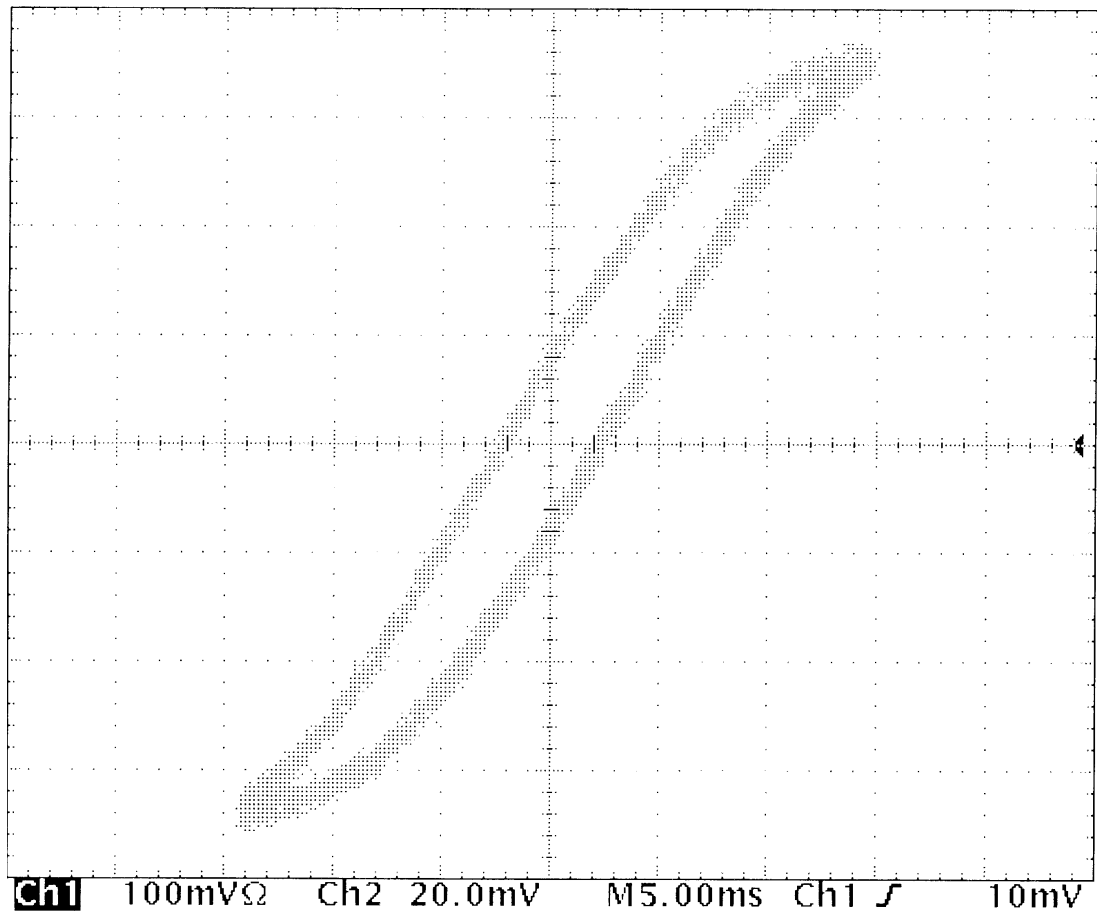


Figure 8.3: Hysteresis Characteristic with 240 V Supply and Open Circuit Secondary

Figure 8.4 depicts the hysteresis curve when the supply voltage has been elevated to 270 V with switch S1 still open. A considerably greater level of non-linearity can be seen in this plot as opposed to Figure 8.3. The peak magnitude of current has increased by approximately 30 % whilst the flux has only increased by about 10 %. The transformer is operating in the saturated region and this is indicated by the distinct flattening off effect that is evident at both the positive and negative peaks of the hysteresis loop.

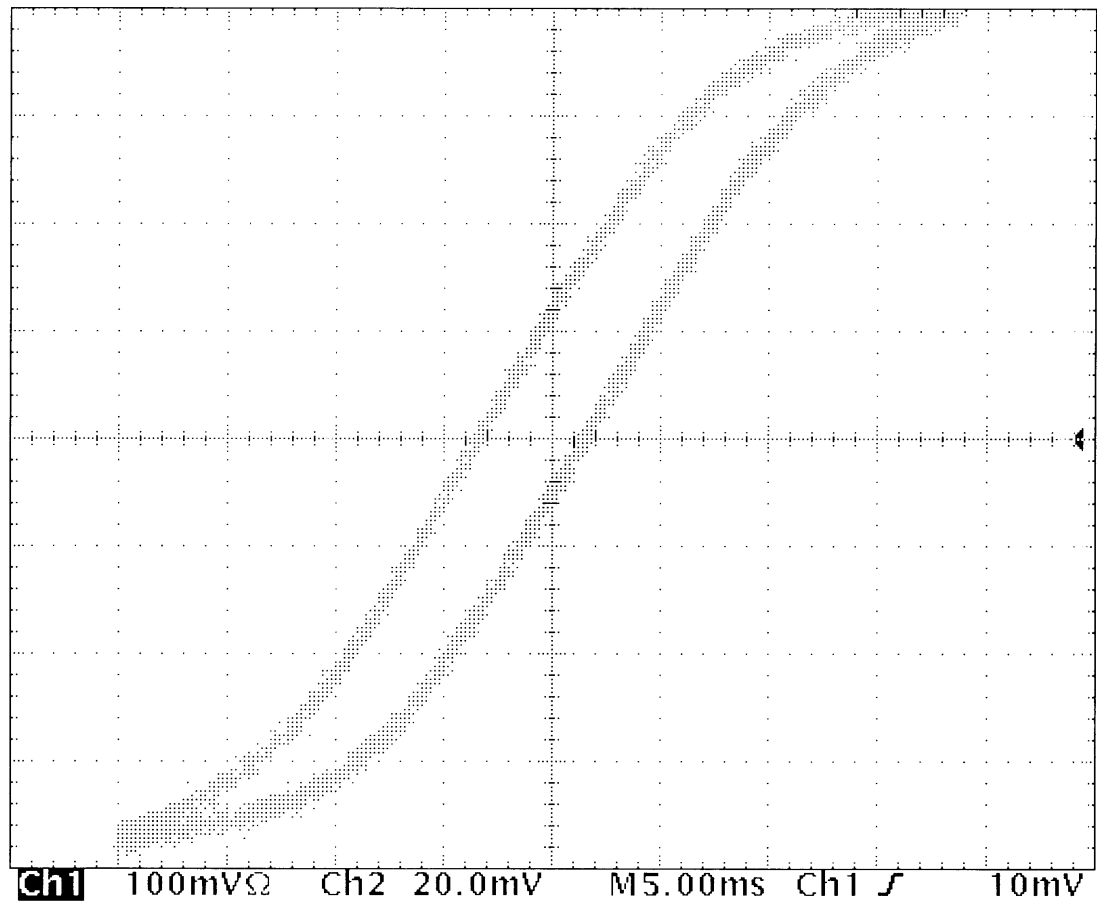


Figure 8.4: Hysteresis Characteristic with 270 V Supply and Open Circuit Secondary

A number of hysteresis measurement experiments were conducted for the case where a secondary DC component was injected. The hysteresis plots obtained from these tests are provided in Appendix D. It is noted however that these plots are not a true representation of the hysteresis characteristic exhibited by the core when DC is injected in the secondary. The series RC circuit depicted in Figure 8.2 provides a

means of measurement of the integral of the supply voltage. In turn it provides a means of measurement of the alternating component of flux. It cannot however provide a true representation of the flux in the core when this flux is biased.

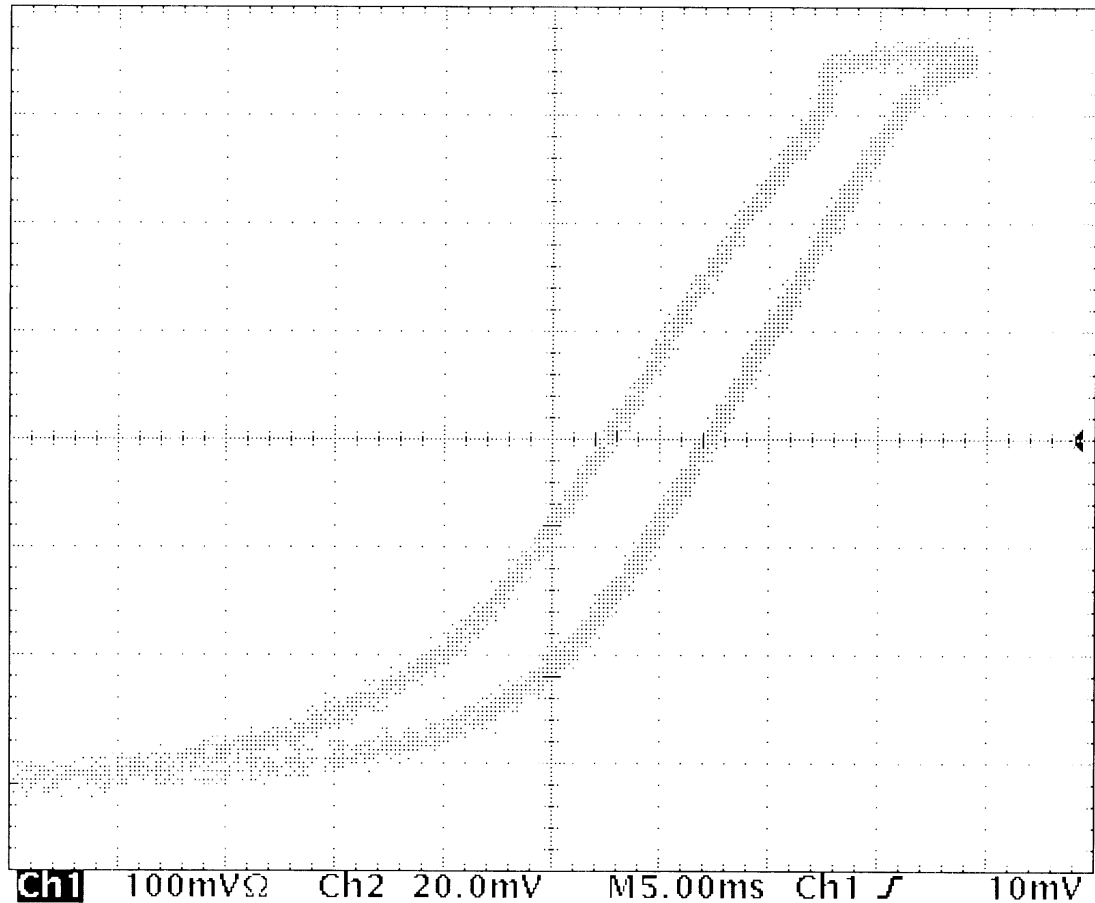


Figure 8.5: Hysteresis Characteristic with a 100 mA Secondary DC Component

An analysis of the hysteresis results obtained when DC is injected yields some interesting findings. Shown above in Figure 8.5 is a plot of the hysteresis characteristic when a 100 mA DC component is injected through the secondary. The secondary DC component creates a flux bias which is not depicted in this loop as a result of the flux measurement method.

What is witnessed though is the large increase in the peak value for the negative cycle of magnetising current. A similar trend is noticed in the no-load current plots provided in Appendix B. With an applied positive bias this large peak value of

negative magnetising current is necessary to maintain symmetry of the primary side current. Further analysis is necessary to explain the presence of the distortion which is evident at the positive peak of the hysteresis loop displayed in Figure 8.5. Also the apparent shift in the hysteresis loop requires further investigation.

8.3 Software Simulation of Magnetising Characteristics

Given established theory and the results of tests conducted in this project, an attempt was made at simulating magnetising trends for a DC biased single phase transformer in a consistent manner through creation of a software program. Given a transformer's core magnetising characteristic and assuming a certain level of bias the program returns a graphical approximation of the $i - \phi$ relationship and magnetising current waveform. MATLAB was chosen as the language for which the program would be created in. This was due to its powerful mathematical capabilities and ease of access.

This section investigates the program methodology employed, simplifying assumptions and related limitations. A discussion of the results obtained will also be conducted.

8.3.1 Program Methodology, Assumptions and Limitations

Due to time limitations a number of simplifying assumptions were made prior to undertaking the program development phase. Firstly the effects of hysteresis were neglected and as such it was assumed that the transformer core exhibited zero residual magnetisation. Next it was assumed that the supply was a perfect sinusoid, a condition that is never matched in practice. Finally the winding resistance effect depicted in Equation 8.3 is assumed to be negligible. Implementing these assumptions does to a certain extent limit the credibility of results obtained.

For the program concept to be feasible it is essential that the magnetising characteristics of the transformer core be known for the no-load operating condition. This is obtained through gaining a plot of the flux-magnetising current relationship as depicted in Figure 8.3. Once the plot is obtained a piecewise linear approximation for the mid point locus is made as shown below in Figure 8.6. In this particular instance the piecewise approximation consisted of four linear sections. Further improvements to the accuracy of this method could be made by simply increasing the number of sections used to approximate the mid point locus.

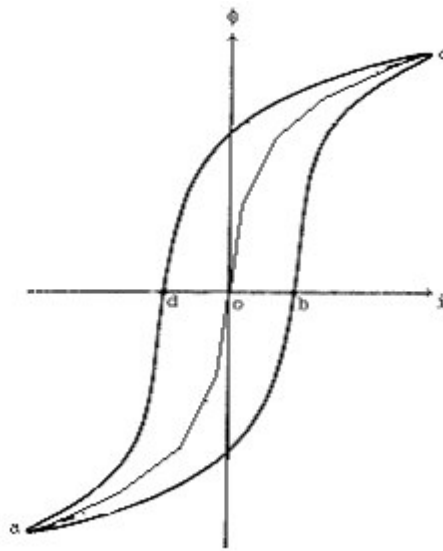


Figure 8.6: Hysteresis Plot with Piecewise Linearly Approximated Mid Point Locus

Once the piecewise approximation has been made the peak flux value and slope for each section must be determined and entered as data into the program. The user will then be prompted to enter the level of bias. This will come in the form of a core flux bias. The program currently is limited to the calculation using only positive bias. This however is not of serious concern as the case with negative bias is simply the reverse of the positive case.

With the bias determined the new flux-magnetising current relationship can be found. With a positive bias entered the extension into the negative cycle of flux must be reduced whilst the positive cycle is increased. This will lead to a corresponding

bias in the magnetising current. When the positive flux cycle is extended the flux-magnetising current relationship is extrapolated past its measured values on a slope equivalent to that of the last section.

This biased current can be plotted against time. When this is completed it is evident that there is asymmetry present between the positive and negative half cycles. The magnetising current that is present on the primary side of the transformer must not exhibit this trend as the waveform cannot contain a DC component. As such the primary side magnetising current will be the biased magnetising current with the DC component removed.

The complete code listing is provided in Appendix E for the program *Magnetising_Current_Prediction.m*. This code includes documentation to explain the processes used.

8.3.2 Discussion of Results

Due to the number of simplifying assumptions made it is expected that there may be some difficulty in making a valid comparison between the results achieved through theoretical means (using program) and those that were obtained through experimental work. Following is an analysis of the results achieved from *Magnetising_Current_Prediction.m*.

Shown in Figure 8.7 is a plot of the theoretical flux-magnetising current relationship with zero induced flux bias. Since the number of primary and secondary turns for the test transformer was unknown, an exact value for the peak value of the alternating flux component could only be estimated. The peak value of magnetising current was approximately 250 mA. Hence with zero flux bias a symmetrical trend noted for both flux and magnetising current. Thus the magnetising current that is read of this curve will be symmetrical about the horizontal axis as shown in Figure 8.8.

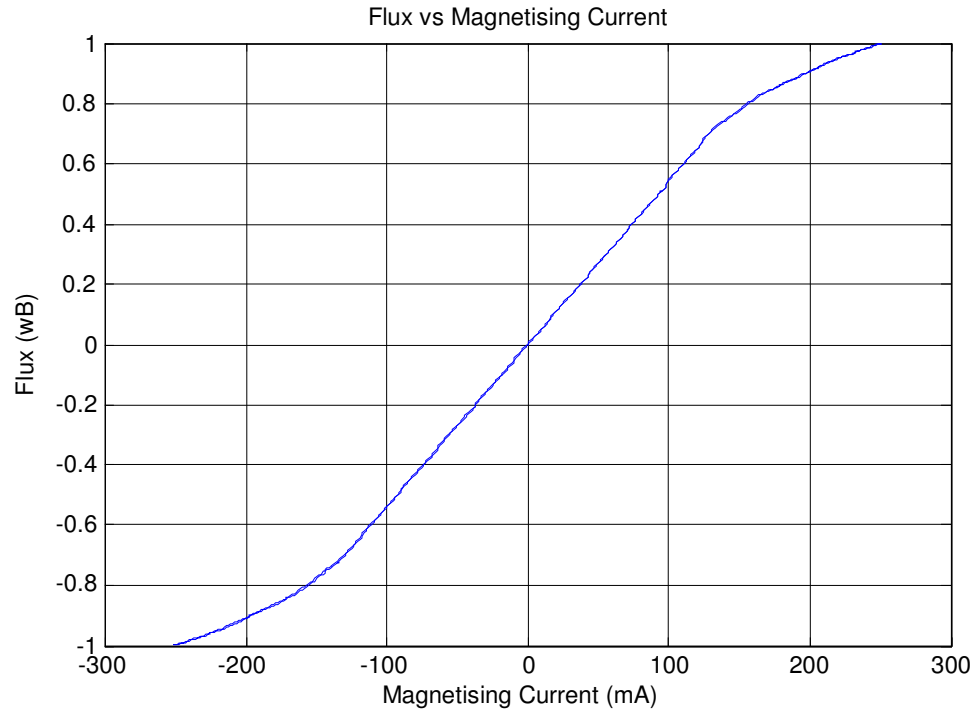


Figure 8.7: Plot of Flux-Magnetising Current Relationship with Zero Flux Bias

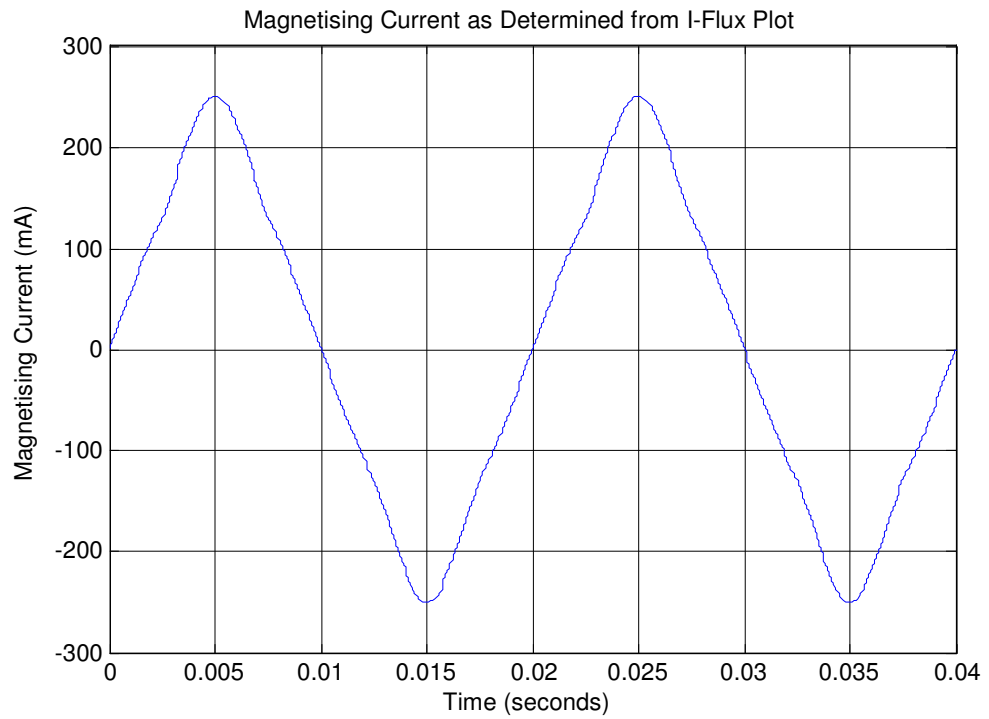


Figure 8.8: Plot of Biased Magnetising Current with Zero Flux Bias

With no asymmetry in the magnetising current shown in Figure 8.8 the primary side magnetising current will be an exact replica and this is shown in Figure 8.9. It should also be noted that the tendency for the magnetising current to replicate a triangular wave can be linked back to the non-linearity that is present in the flux-magnetising characteristic. The RMS value for the primary side magnetising current was calculated as 155.54 mA.

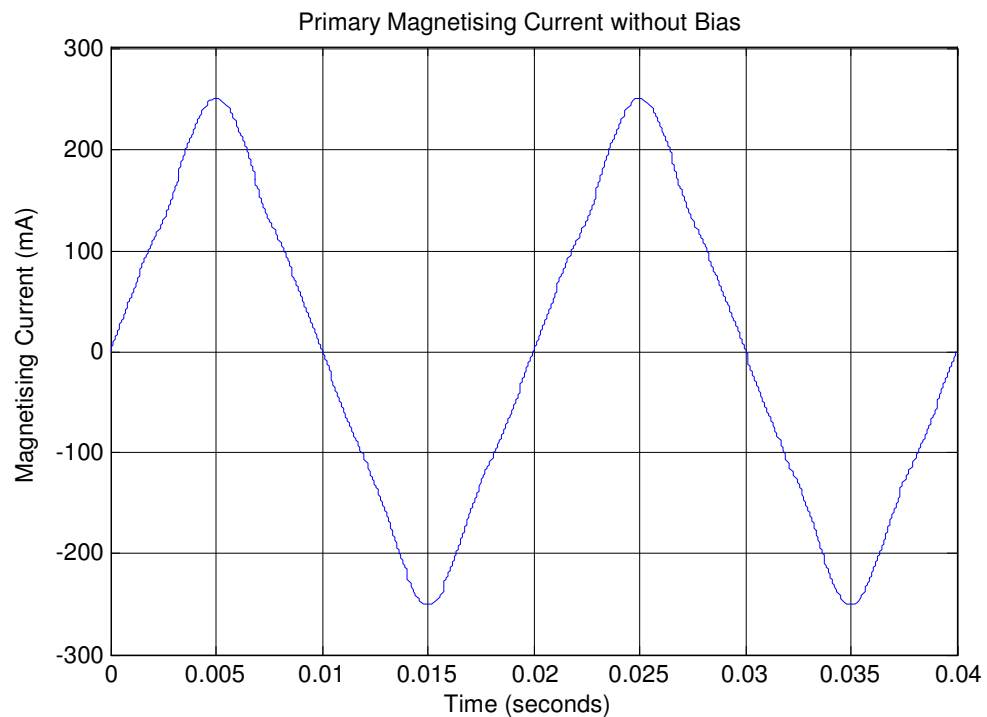


Figure 8.9: Plot of Primary Magnetising Current with Zero Flux Bias

The next results displayed here are for the case where a positive flux bias equivalent to 20% of the peak value of alternating flux is induced. As can be seen in Figure 8.10 this has as expected caused the peak value of positive flux to increase to 1.2 and the negative flux peak to increase to -0.8. This flux asymmetry has led to a corresponding asymmetry in the magnetising current and this is best displayed when the magnetising current is shown as a function of time as in Figure 8.11.

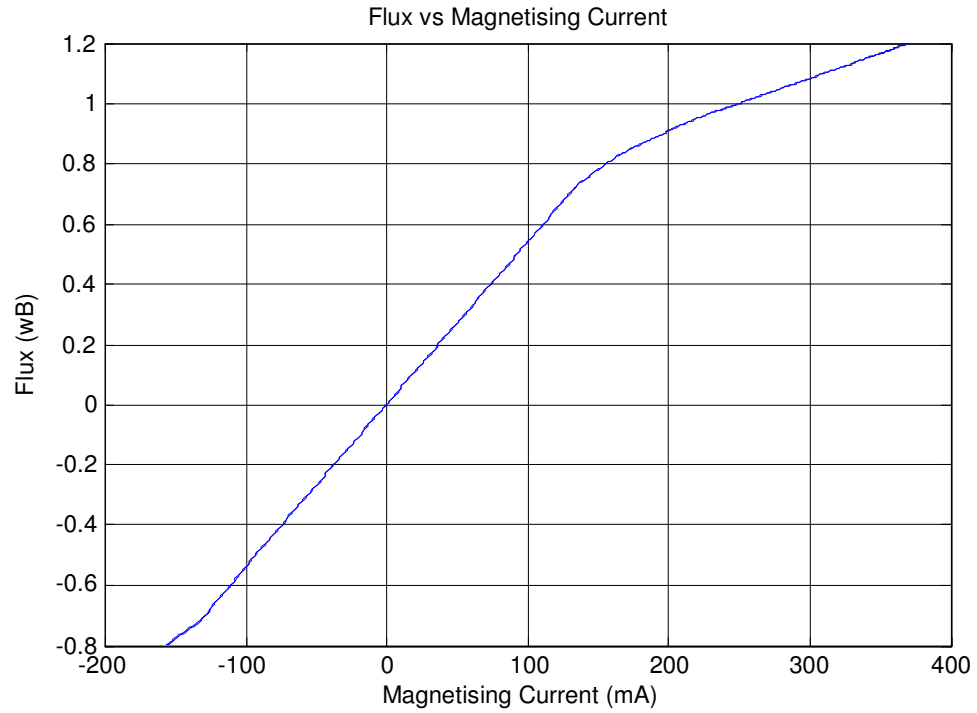


Figure 8.10: Plot of Flux-Magnetising Current Relationship with 20% Flux Bias

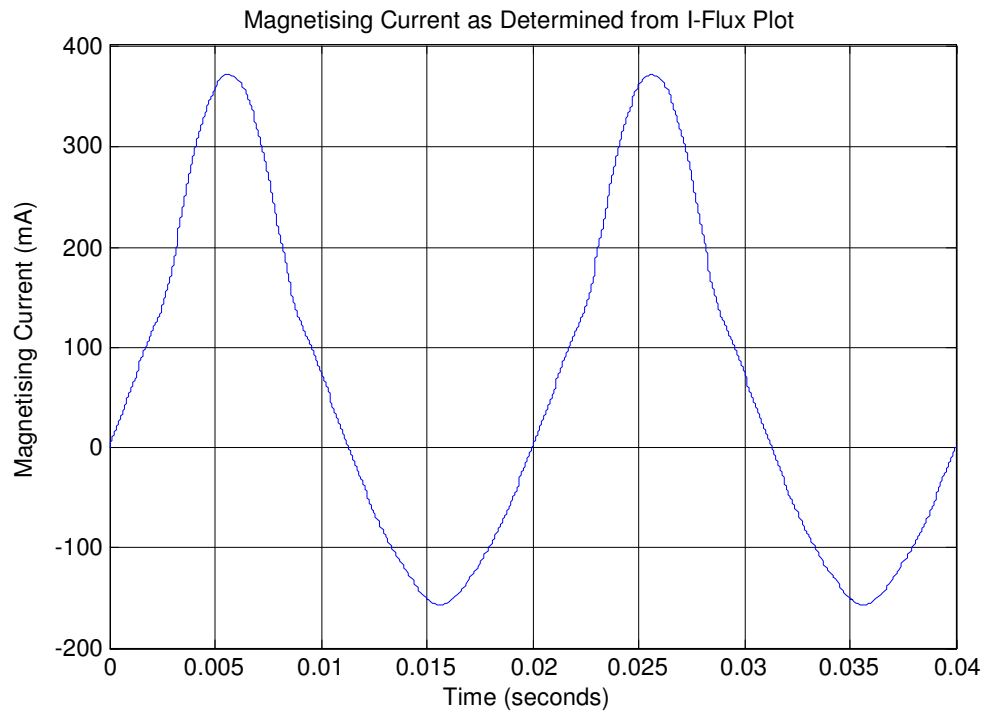


Figure 8.11: Plot of Biased Magnetising Current with 20% Flux Bias

The asymmetry that is evident in Figure 8.11 cannot manifest itself on the primary side since transformers do not reflect direct current. As a result the average value or DC component is removed from it to yield the primary side waveform as shown in Figure 8.12. The RMS value of this waveform is 171.29 mA.

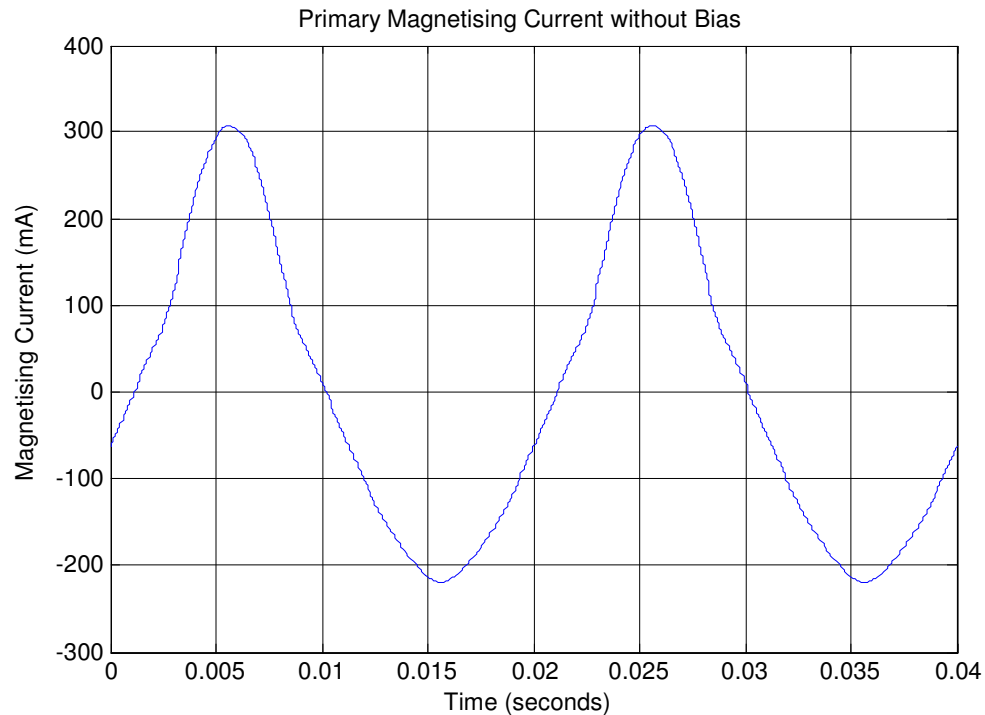


Figure 8.12: Plot of Primary Magnetising Current with 20% Flux Bias

A careful analysis of Figure 8.12 does yield some interesting observations. From this plot it appears that the duration of the negative cycle is increasing at the expense of the positive cycle. This is the opposite of what was expected and measured. The no-load current plots provided in Appendix B indicate that for an increasing positive DC bias the duration of the negative cycle should in fact decrease. This trend is expected since the flux waveform is spending a greater portion of time in the positive cycle. Due to time limitations further investigations into the variation between the theoretical and practical results could not be made.

Chapter 9

Three Phase Analysis

All prior analysis concerning the effect of DC current on power transformers has addressed the single phase case. This is a necessary stepping stone that should be completed before progressing to three phase arrangements. Three phase analysis has associated with it a number of complexities which are brought about by a range of factors. These factors include the interaction of multiple windings, different core arrangements (shell type, core type, three phase-three leg and three phase-five leg), numerous winding arrangements (Delta, Star, Zig-Zag, different vector groupings) and in larger power units the presence of a tank. Hence it is evident that an in depth study of the effect of DC on three phase power transformers would require an expansive research effort.

This chapter aims to present the findings of preliminary investigations that were conducted with a view to determining a three phase transformer's magnetising characteristics with DC bias. A number of tests were conducted on a 7.5 kVA three phase Delta/Star connected transformer with a Dyn11 vector group. The transformer was of core type construction with three limbs. The tests were arranged such that only a secondary DC current was present. This allowed any variations in the units magnetising characteristics to be attributed to the changes in the secondary DC component.

9.1 Magnetising Characteristics – Phase to Neutral DC Injection

This series of testing covered the case of phase to neutral DC injection. This form of DC bias is a potential problem for those three phase transformers that supply a large portion of single phase loads. An example could be an office building containing a large number of computers (which in Chapter 5 were established as a potential source of DC bias) which require a single phase supply. This section aims to pinpoint any defining trends.

9.1.1 Test Theory and Method

As previously mentioned this series of experiments aimed to analyse the magnetising current performance of the transformer under test when a phase to neutral DC component was induced. The test was conducted for each phase to neutral combination and it was expected that some differences may be noted due to the asymmetrical core construction. Figure 9.1 depicts a schematic of the circuit utilised. Once again the injection of DC was achieved through use of a half-wave rectifier topology. Also this particular vector grouping meant that primary 'A' phase was in phase with secondary 'A' phase; primary 'B' phase was in phase with secondary 'B' phase and primary 'C' phase was in phase with the secondary 'C' phase.

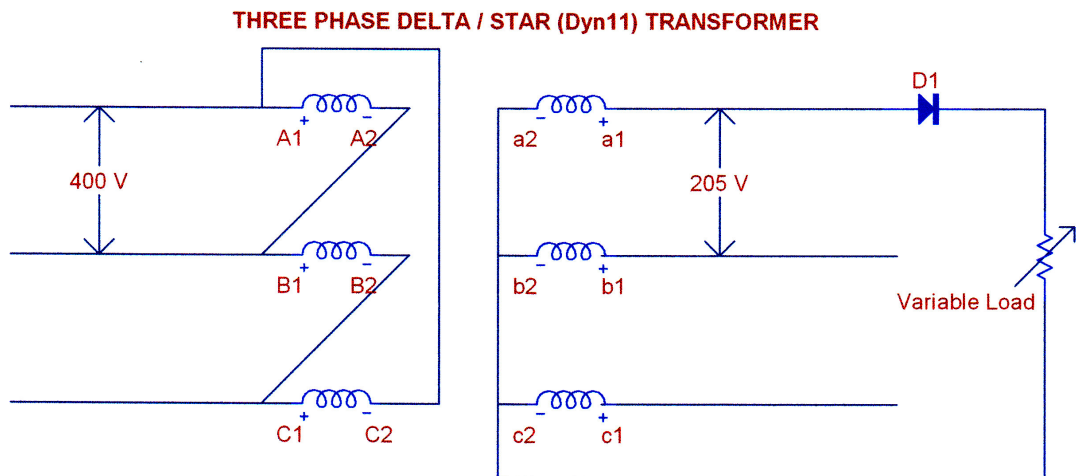


Figure 9.1: Secondary Phase to Neutral DC Injection

9.1.2 Test Results and Analysis

For each phase to neutral combination a range of results were collected and these are presented in Appendix F. On analysis of the results presented in Appendix F it is evident that the most noticeable primary side affect occurred for the phase for which the DC was being injected into. For instance Figure 9.2 depicts the case of primary phase current variations when a secondary DC component is induced through ‘A’ phase and neutral. A significant increase in the ‘A’ phase primary current is witnessed however there appears to be little increase in the other two phase currents.

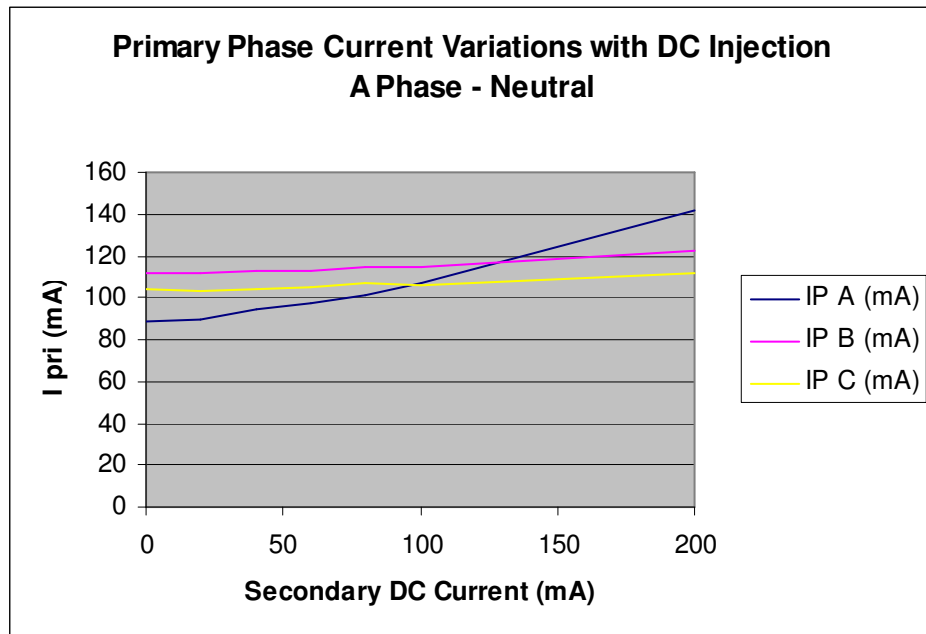


Figure 9.2: Plot of Primary Phase Currents with ‘A’ Phase to Neutral DC Injection

Through analysis of the displacement power factor figures provided in Appendix F it is evident that the magnetising current component forms a large portion of the primary phase current. Also VAR increases indicate that this magnetising current is increasing. Hence the increase in ‘A’ phase primary current which can in part be attributed to magnetising current increases is indicative of a transformer that is tending toward the saturated region of operation. Similar trends are exhibited in Figure 9.3 and Figure 9.4 for the other phase to neutral combinations. It appears that

when an individual phase contains a DC component the resulting magnetising current effect is largely limited to the corresponding primary phase.

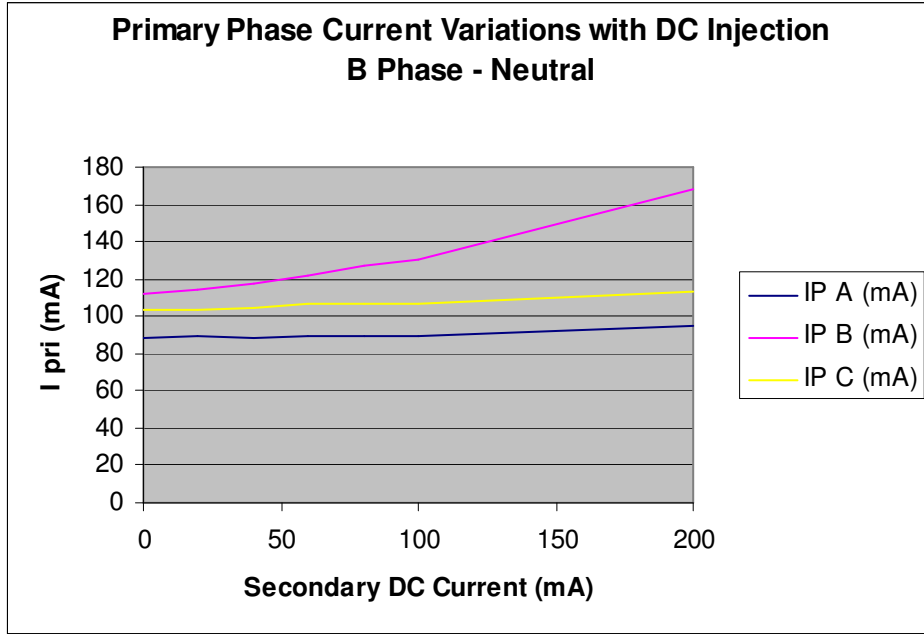


Figure 9.3: Plot of Primary Phase Currents with ‘B’ Phase to Neutral DC Injection

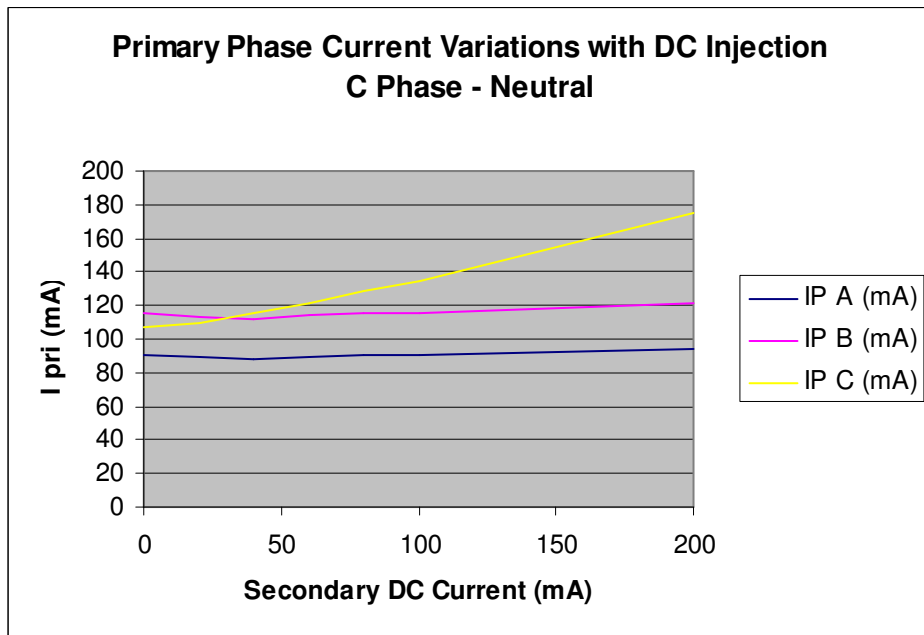


Figure 9.4: Plot of Primary Phase Currents with ‘C’ Phase to Neutral DC Injection

On inspection of the no-load current waveforms for the affected phase some similarities are noticed when compared with the single phase case. Figures 9.5 and 9.6 depict the 'A' phase no-load current waveforms for the secondary 'A' phase unbiased and biased conditions respectively. A reduction in the duration of the negative cycle of primary phase current is noted in Figure 9.6 when compared with Figure 9.5. This is indicative of a flux bias.

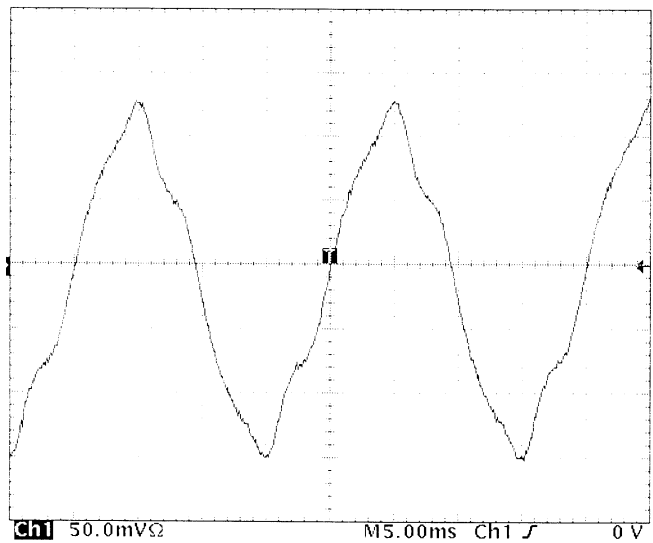


Figure 9.5: 'A' Phase Primary Current Waveform with Zero Secondary DC Injection

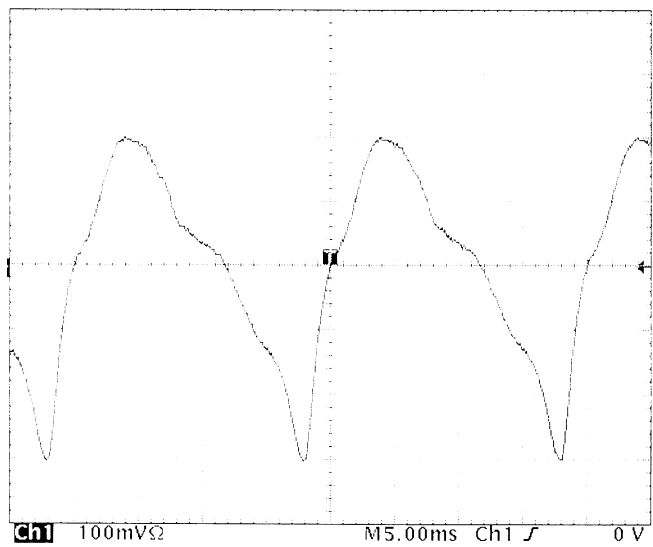


Figure 9.6: 'A' Phase Primary Current Waveform with 200 mA Secondary DC Injection

The peak negative current has extended considerably in magnitude (the vertical scale in Figure 9.6 is twice that of Figure 9.5) for the biased secondary case. This is also a trait that was witnessed for the single phase DC injection tests.

9.2 Magnetising Characteristics – Phase to Phase DC Injection

The next series of tests undertaken aimed to analyse the variation in magnetising characteristics with phase to phase DC injection. This form of bias is a potential problem in three phase equipment.

9.2.1 Test Theory and Method

The schematic for the circuit utilised to effect phase to phase secondary direct current injection is shown below in Figure 9.7. Once again the half-wave rectifier arrangement was employed. Each phase to phase combination was tested. When a phase to phase combination was tested the direction of injection was reversed (A-C, C-A) so as to ascertain whether the direction of injection created any major variations.

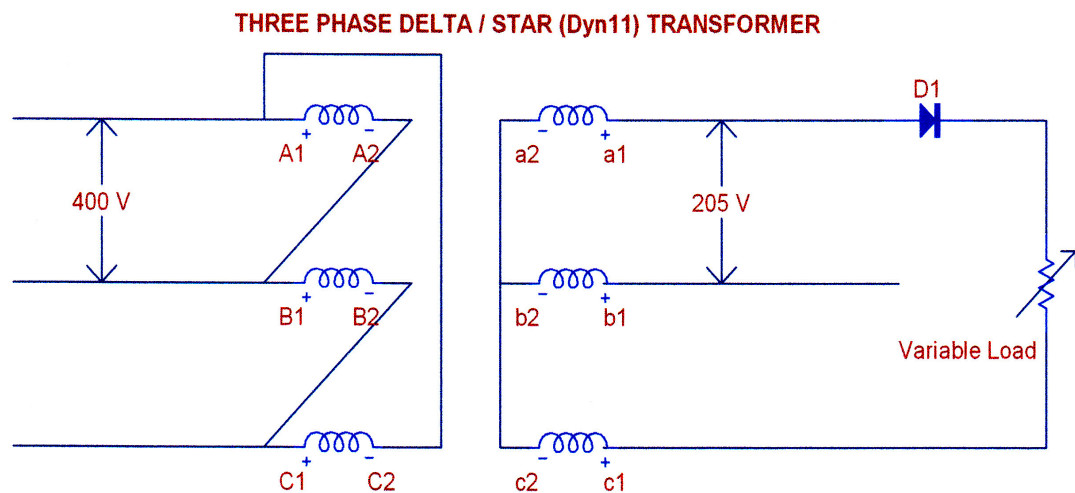


Figure 9.7: Secondary Phase to Phase DC Injection

9.2.2 Test Results and Analysis

The results of this series of testing are supplied in Appendix F. A similar method was employed to display the predominate effects. The primary phase current variations provide the best means of displaying results. It is again noticed that the bulk of the effect on the primary side occurs for those phases which are being injected upon on the secondary side. This effect is displayed in Figures 9.8, 9.9 and 9.10 which exhibit the primary phase current variations for each of the three phase combinations. It is interesting to note that reversing the direction of injection had little effect on the trends displayed in the following figures.

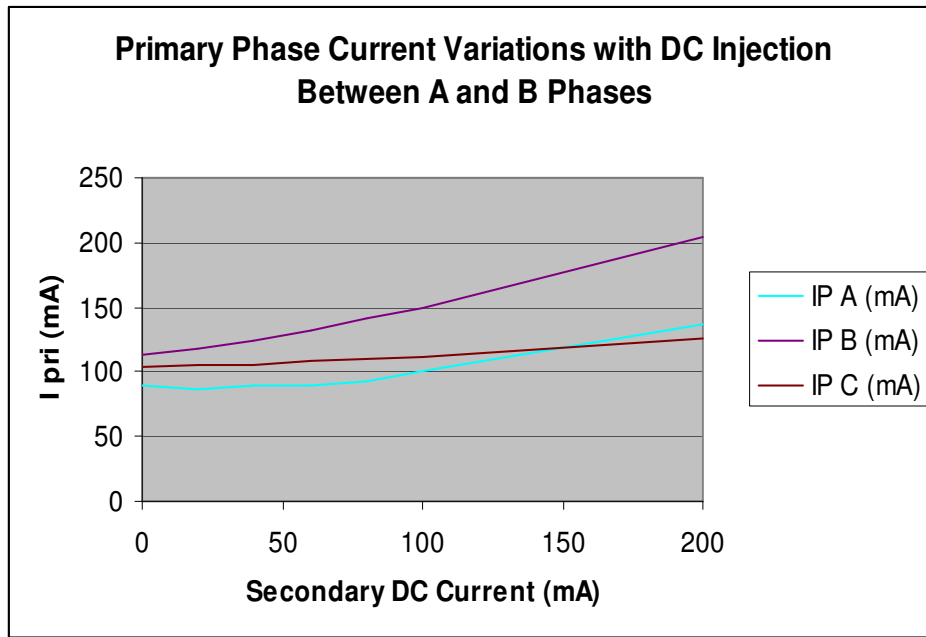


Figure 9.8: Plot of Primary Phase Currents with 'A' Phase to 'B' Phase DC Injection

It is observed that there is an increase in the phase current for the phase which is not directly effected by a secondary DC component. This can be attributed to mutual flux linkages. This increase is shown to be greatest for phase 'B' when a secondary DC injection occurs between 'A' and 'C' phases. Phase 'B' winding is physically situated between the other two phase windings. As such it is subject to mutual flux

linkages from both windings. In the other instances the majority of the mutual flux linkage comes from only one other winding.

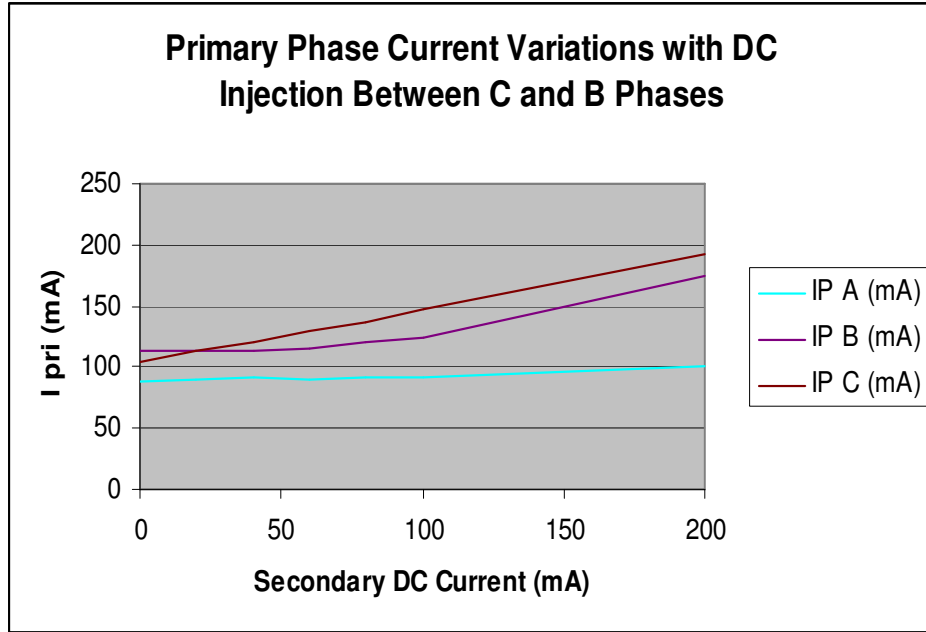


Figure 9.9: Plot of Primary Phase Currents with 'C' Phase to 'B' Phase DC Injection

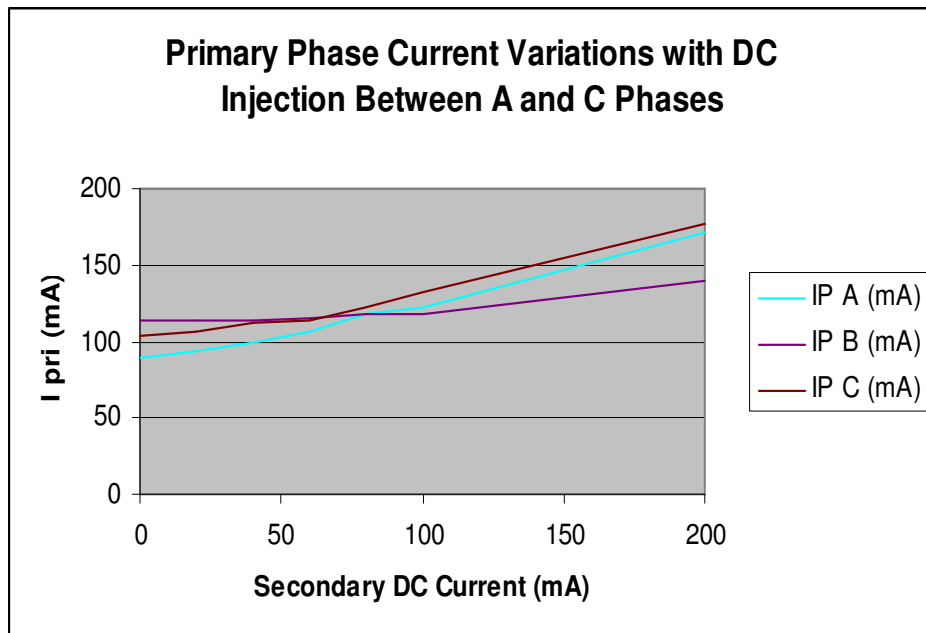


Figure 9.10: Plot of Primary Phase Currents with 'C' Phase to 'A' Phase DC Injection

Chapter 10

Conclusions and Recommendations for Future Work

10.1 Achievement of Objectives

This project has sought to investigate the affect that direct current has on power transformers. Initial analysis conducted has aimed at addressing this issue from a single phase perspective. Some preliminary three phase analyses were conducted.

Each of the objectives defined in Chapter 1 have been addressed. A comprehensive review of literature was conducted providing a summary of the affect that direct current has on power transformers. The saturation phenomenon has been fully explored and the theory behind its occurrence elaborated upon.

An analysis was conducted on computers and AC and DC drives in an attempt to establish whether or not they represent a significant source of bias. Results obtained indicated that both PC's and motor drives do represent a credible source. It was shown that the potential does exist for a cumulative effect to occur. This would magnify the affect of the bias source. It has also been established that tests need to be conducted with larger sample sizes before confident assertions can be made regarding the presence of a cumulative affect.

An in depth single phase analysis was conducted covering three major areas. These included magnetising characteristics, harmonic distortion behaviour and hysteresis characteristics. In terms of magnetising characteristics it was found that in the single phase case the presence of a secondary DC current did induce half cycle saturation. Saturation effects were accompanied by significant increases in magnetising current levels which in turn resulted in increased VAR absorption. The presence of a rated AC load on the secondary appeared to have little affect on magnetising characteristics.

A number of tests were conducted to determine the harmonic performance of a transformer operating under load conditions and exposed to a secondary direct current component. Tests showed increases in secondary voltage distortion beyond the 5 % THD limit and 3 % individual harmonic limit as defined by the IEEE519 standard. The level at which the standard was exceeded was in excess of 100 % of the transformer's magnetising current. Hence while potential exists for undesirable increases in secondary voltage distortion due to biased currents, the level of DC required to cause this is significant.

An analysis of single phase hysteresis characteristics was conducted in Chapter 8. A number of hysteresis measurements were conducted. The results obtained were acceptable for the case where there was zero secondary DC current present. However when a secondary bias was present the hysteresis measurement method utilised did not provide an accurate assessment of the core flux conditions.

Chapter 8 also provided the development and results of the program *Magnetising_Current_Prediction.m*. This program sought to predict the Flux-Magnetising Current characteristic and magnetising current waveform for a given value of flux bias. Due to time limitations a number of simplifying assumptions were made. The results for the prediction of the Flux-Magnetising Current relationship were as expected. The results for the magnetising current were not as expected and future work should focus on rectifying this.

Chapter 9 presented the results of preliminary three phase tests aimed at determining the magnetising characteristics for a 7.5 kVA Delta/Star three phase transformer. Results indicated that for single phase to neutral DC injection the affect on the primary side was limited to the phase for which the DC injection was conducted upon. A similar occurrence was noted for phase to phase secondary DC injection. For phase to neutral injected a reduction in the duration of the negative cycle of the affected phase current was witnessed. A similar affect was noted with the single phase results.

10.2 Future Work

This project has covered a very small portion of the potential research content pertaining to the effect of DC current on power transformers. This section aims to make recommendations regarding the potential avenues for future research. The three main areas for which further work should be conducted in are sources of DC, single phase analysis and three phase analysis.

10.2.1 Sources of DC

Chapter 5 provides the results of a series of brief investigations aimed at determining the DC bias contributions made by computers and AC and DC drives. The experimental data retrieved suggested that computers and AC and DC drives do represent a significant source of DC bias. To improve the credibility of these findings tests need to be conducted with much larger sample sizes.

Investigations into other potential sources of direct current should be conducted. This may include observing the contributions of grid interfaced renewable energy schemes such as photovoltaic systems. Where resources permit, further research should be performed into the phenomenon of Geomagnetically Induced Currents.

Finally an analysis of the mechanisms that create DC injection within equipment could be beneficial. It would allow development of methods to counteract the undesired occurrence of direct current injection.

10.2.2 Single Phase Analysis

A large portion of this project has concentrated on assessing the problem of direct current injection in single phase transformers. This was the primary basis for Chapters 6, 7 and 8. There is however still a number of areas that require further expansion.

Testing on different core arrangements should be looked at. The single phase transformer used in this project was of the core type. Tests should be undertaken on a similar sized shell type transformer to determine if there exists any significant variation in transformers performance with DC bias that can be traced back to core design.

Considerable modifications are required to the *Magnetising_Current_Prediction.m* program which was described in Chapter 8. Hysteresis should be factored into the model as well as the effect of winding resistive voltage drop. Investigations should be conducted into the variations which occur between the theoretical magnetising current waveform and the experimentally obtained magnetising current waveform.

A means of measuring the actual core flux waveform should be determined. This may require use of Hall Effect sensing technology placed in the core. From this it will become possible to attribute a given flux bias to a level of secondary direct current.

10.2.3 Three Phase Analysis

There exists considerable scope for further work to be conducted concerning the effect of direct current on three phase transformers. Much of that which was conducted for the single phase situation can be used to assist in interpretation of three phase cases.

The hysteresis model that was derived for the single phase situation should be extended to the three phase case. Modelling of core flux distribution needs to be conducted and this may require in depth mathematical analysis through use of finite element analysis.

Three phase transformers come in a variety of arrangements. In terms of core design future studies may compare the performance of core type and shell type constructions that are exposed to biased flux operating conditions. In industry the Delta/Star winding arrangement is commonly found. It is believed that an interesting comparison would be found between the performances of Delta/Star units that have four wire secondaries as opposed to those that have three wire secondaries.

The performance of other winding arrangements such as Star/Star and Star/Delta is of more importance to generation and transmission applications. If GIC's are regarded as a potential problem it may be prudent to assess the performance of these types of transformers when subject to a DC bias.

Three phase transformers are generally either three limb or five limb. It is expected that the potential exists for a variation in the performance of each construction type due to the differing flux distributions.

On-load tests should be conducted with varying degrees of secondary DC injection to determine the level of harmonic distortion that is created in the three phase situation. The secondary DC injected should simulate symmetrical bias conditions as

occurs with GIC's and asymmetrical bias conditions as is commonly created by single phase equipment.

References

- Al-Haj, AH & El-Amin, I 2000, '*Factors That Influence Transformer No-Load Current Harmonics*', IEEE Transactions on Power Delivery, vol. 15, January, no. 1, pp. 163-66.
- Baranowski, JF, Benna, SJ, Bishop, MT & Heath, D 1996, '*Evaluating Harmonic-Induced Transformer Heating*', IEEE Transactions on Power Delivery, vol. 11, January, no. 1, pp. 305-11.
- Bolduc, L, Dutil, A, Pham, VQ & Picher, P 1997, '*Study of the Acceptable DC Current Limit in Core-Form Power Transformers*', IEEE Transactions on Power Delivery, vol. 12, January, no. 1, pp. 257-65.
- Calabro, S, Coppadoro, F & Crepaz, S 1986, '*The Measurement of the Magnetization Characteristics of Large Power Transformers and Reactors through DC Excitation*', IEEE Transactions on Power Delivery, vol. PWRD-1, October, no. 4, pp. 224-34.
- Cardoso, JR, Delaiba, AC, Nabeta, SY & Oliveira, JC 1998, '*Behaviour of Three-Phase Transformers Supplying Non Linear Loads Using Time Domain Representation and Finite Element Analysis*', IEEE Transactions on Magnetics, vol. 34, September, no. 5, pp. 3174-77.

- Colosino, M, Hoevenaars, T & LeDoux, K 2003, '*Interpreting IEEE Std 519 and Meeting its Harmonic Limits in VFD Applications*', Copyright Material IEEE, Paper No. PCIC-2003-15, May, pp. 1-6.
- De La Ree, J, Liu, Y & Lu, S 1993, '*Harmonics Generated From a DC Biased Transformer*', IEEE Transactions on Power Delivery, vol. 8, April, no. 2, pp. 725-31.
- De Leon, F, Gladstone, B, Tatu, V & Van Der Veen, M 2000, '*Measuring Acoustic Noise Emitted by Power Transformers*', AES 109th Convention, Los Angeles, pp. 1-19.
- Dutil, A, Eitzmann, MA, Granger, M, Huynh, H, Khan, A, Sublich, M & Walling, RA 1992, '*Alternatives for Blocking Direct Current in AC System Neutrals at the Radisson/LG2 Complex*', IEEE Transactions on Power Delivery, vol. 7, July, no. 3, pp. 1328-37.
- Emanuel, AE & Orr, JA 2000, '*On the Need for Strict Second Harmonic Limits*', IEEE Transactions on Power Delivery, vol. 15, July, no. 3, pp. 967-71.
- Fuchs, EF, Roesler, DJ & You, Y 1999, '*Modeling and Simulation, and Their Validation of Three-Phase Transformers with Three Legs Under DC Bias*', IEEE Transactions on Power Delivery, vol. 14, April, no. 2, pp. 443-49.
- Fujiwara, Y, Miyawaki, F, Saito, S, Takasu, N & Tetsuo, O 1994, '*An Experimental Analysis of DC Excitation of Transformers by Geomagnetically Induced Currents*', IEEE Transactions on Power Delivery, vol. 9, April, no. 2, pp. 1173-82.
- Grainger, JJ & Stevenson, WD 1994, '*Power System Analysis*', McGraw-Hill, Singapore.

- Huang, CJ, Huang, CL, Lin, CE & Wei, JB 1989, '*A New Method for Representation of Hysteresis Loops*', IEEE Transactions on Power Delivery, vol. 4, January, no. 1, pp. 413-20.
- Jenneson, JR 1999, 'Electrical Principles for the Electrical Trades', McGraw-Hill, NSW, Australia.
- Jewell, WT & Warner, DE 1999, '*An Investigation of Zero Order Harmonics in Power Transformers*', IEEE Transactions on Power Delivery, vol. 14, July, no. 3, pp. 972-77.
- Khouzam, KY 1999, '*Technical and Economic Assessment of Utility Interactive PV Systems for Domestic Applications in South East Queensland*', IEEE Transactions on Energy Conversion, vol. 14, December, no. 4, pp. 1544-50.
- Kuphaldt, TR 2003, *Core Saturation*, All About Electronic Circuits, http://www.allaboutcircuits.com/vol_2/chpt_9/11.html
current October 2004.
- Ledwich, G & Masseur, K 1999, '*Grid Connection without Mains Frequency Transformers*', Journal of Electrical and Electronics Engineering, vol. 19, June, no.'s 1 & 2, pp. 31-36.
- Nave, R 2000, *Coercivity and Remanence in Permanent Magnets*, Georgia State University,
<http://hyperphysics.phy-astr.gsu.edu/hbase/solids/magperm.html#c1>
current October 2004.
- Price, PR 2002, '*Geomagnetically Induced Current Effects on Transformers*', IEEE Transactions on Power Delivery, vol. 17, October, no. 4, pp. 1002-08.

Sankaran, C 2000, *The Basics of Zigzag Transformers*, EC&M,
http://ecmweb.com/ar/electric_basics_zigzag_transformers
current October 2004.

Swamy, MM & Rossiter, SL 1998, '*Harmonic Interaction Between 1500-kVA Supply Transformer and VFD Load at an Industrial Plant*', IEEE Transactions on Industry Applications, vol. 34, September/October, no. 5, pp. 897-903.

Appendix A

Project Specification

University of Southern Queensland

FACULTY OF ENGINEERING AND SURVEYING

**ENG 4111/4112 Research Project
PROJECT SPECIFICATION**

FOR: **ASHLEY ZEIMER**

TOPIC: THE EFFECT OF DC CURRENT ON POWER TRANSFORMERS

SUPERVISOR: Ron Sharma

PROJECT AIM: This project aims to investigate the affect of the presence of DC current on the operational characteristics of power transformers.

PROGRAMME: Issue A, 10th March 2004

1. Research existing theory pertaining to the affect of DC current on power transformers as well as review transformer theory.
2. Investigate saturation with respect to transformers and detail how DC injection induces this phenomenon
3. Explore potential sources of DC biasing and look into the severity of these sources.
4. Examine factors that exacerbate and potentially accelerate the adverse affects of DC injection.
5. Investigate the variation in affect due to DC biasing across the variety of transformer construction styles that exist and conduct tests to simulate this.
6. Examine variation in affects for DC injection common across all three phases and localized to one or two of the three phases.
7. Research methods for the alleviation or elimination of the adverse effects of DC biasing.

As time permits:

8. Investigate the creation of software that could model this phenomenon.

AGREED: _____ (Student) _____ (Supervisor)

__ / __ / __

__ / __ / __

Appendix B

Single Phase Analysis – Magnetising Characteristic Results

DC Inj.(mA) (Measured)	W (Measured)	VA (Measured)	VAR (Measured)	PF (Measured)	DPF (Measured)
0	11	45	43	0.25	0.27
10	11	45	43	0.25	0.27
20	11	46	45	0.25	0.27
30	11	47	46	0.24	0.27
40	12	50	49	0.23	0.24
50	12	52	50	0.23	0.24
60	12	59	58	0.21	0.23
70	13	62	61	0.2	0.23
80	13	71	69	0.18	0.23
90	13	76	75	0.18	0.22
100	14	83	82	0.16	0.22
200	15	166	165	0.12	0.15
300	18	257	256	0.07	0.12
400	20	337	337	0.06	0.11

DC Inj.(mA) (Measured)	I _{rms} (Measured)	I _{lrms} (Measured)	I _{core} (mA) (Calculated)	I _{mag} (mA) (Calculated)	I _{thd} (Measured)
0	183	182	46	177	10.2
10	183	182	46	177	10.1
20	189	187	46	183	13.3
30	195	192	46	190	17.2
40	202	198	50	196	19.7
50	224	215	50	218	27.3
60	242	228	50	237	33.2
70	263	243	54	257	38.3
80	292	262	54	287	43.6
90	324	283	53	320	48.8
100	349	299	57	344	51.4
200	688	505	59	685	67.9
300	1048	730	67	1046	71.8
400	1383	947	69	1381	72.9

<p>Calculation Procedures</p> <p>Core Loss Current = $(W - I_{rms}^2 \times R) / V$</p> <p>where R = Primary Winding Resistance = 1.81Ω</p> <p>and V = Primary Supply Voltage = 240 V</p> <p>Magnetising Current = Square Root($I_{rms}^2 - I_{core}^2$)</p>

Table B.1: Results of Zero AC Load DC Injection Tests

DC Inj.(mA) (Measured)	Pri. Volts (Measured)	Vthd (Measured)	Ithd (Measured)	W (Measured)	VA (Measured)	VAR (Measured)
0	240.7	2.9	7.9	36	49	33
10	241.9	2.9	9.7	34	47	33
20	242.7	2.7	13.1	36	50	34
30	240.8	2.6	16.9	36	50	34
40	240.1	2.5	21.0	36	53	39
50	240.9	2.8	26.0	36	54	40
60	242.4	2.7	31.6	37	60	47
70	240.8	2.7	39.8	36	53	53
80	239.9	2.6	44.4	37	70	60
90	242.6	2.9	50.3	37	73	61
100	241.8	3.0	53.4	39	86	76
200	241.5	2.8	71.7	39	166	161
300	241.5	2.9	76.7	41	253	250
400	239.4	2.9	79.0	37	366	363
DC Inj.(mA) (Measured)	Irms (mA) (Measured)	I1rms (mA) (Measured)	Icore (mA) (Calculated)	Imag (mA) (Calculated)	PF (Measured)	DPF (Measured)
0	196	194	140	137	0.74	0.72
10	197	197	142	137	0.74	0.72
20	204	203	146	143	0.71	0.72
30	209	206	146	149	0.72	0.71
40	216	210	145	160	0.68	0.69
50	229	220	145	177	0.68	0.66
60	246	233	147	197	0.62	0.63
70	271	250	155	223	0.59	0.62
80	293	261	154	249	0.52	0.59
90	329	284	159	287	0.52	0.56
100	349	294	156	312	0.45	0.53
200	687	480	163	667	0.22	0.34
300	1054	677	176	1039	0.16	0.26
400	1471	901	189	1459	0.12	0.21
Calculation Procedures						
Core Loss Current = I1rms × DPF						
Magnetising Current = Square Root(Irms² - Icore²)						

Table B.2: Results of Rated AC Load DC Injection Tests

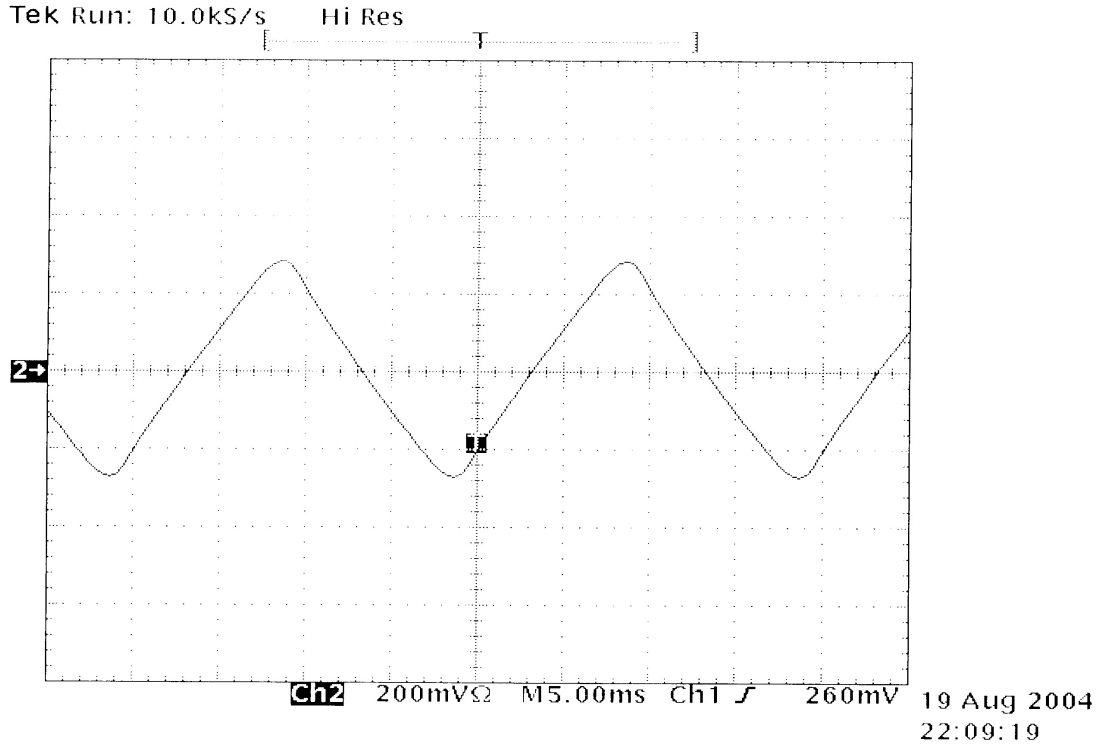


Figure B.1: Primary Current Waveform with Zero AC Load and Zero Secondary DC Current

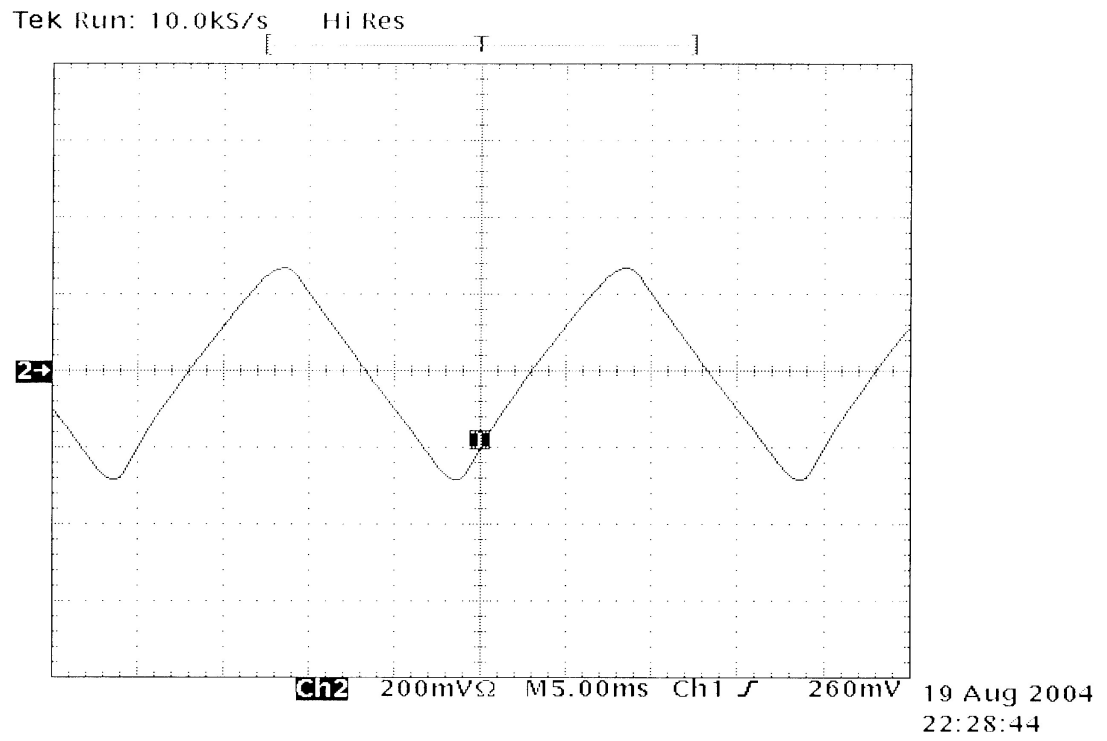


Figure B.2: Primary Current Waveform with Zero AC Load and 10 mA Secondary DC Current

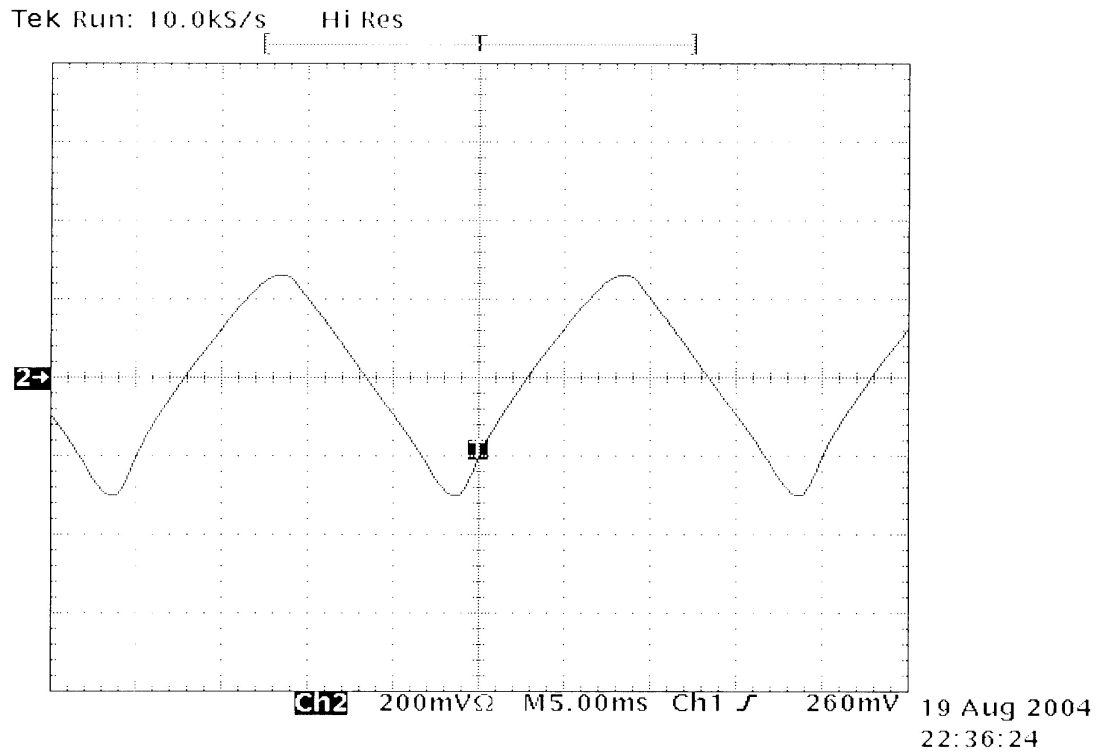


Figure B.3: Primary Current Waveform with Zero AC Load and 20 mA Secondary DC Current

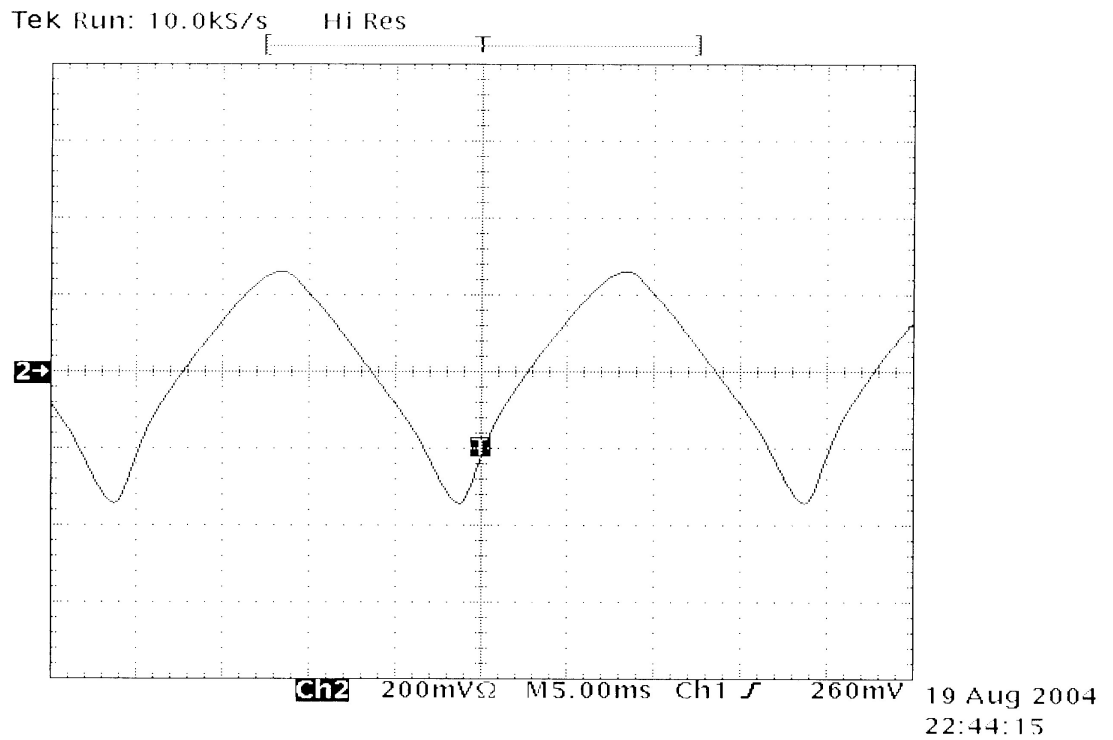


Figure B.4: Primary Current Waveform with Zero AC Load and 30 mA Secondary DC Current

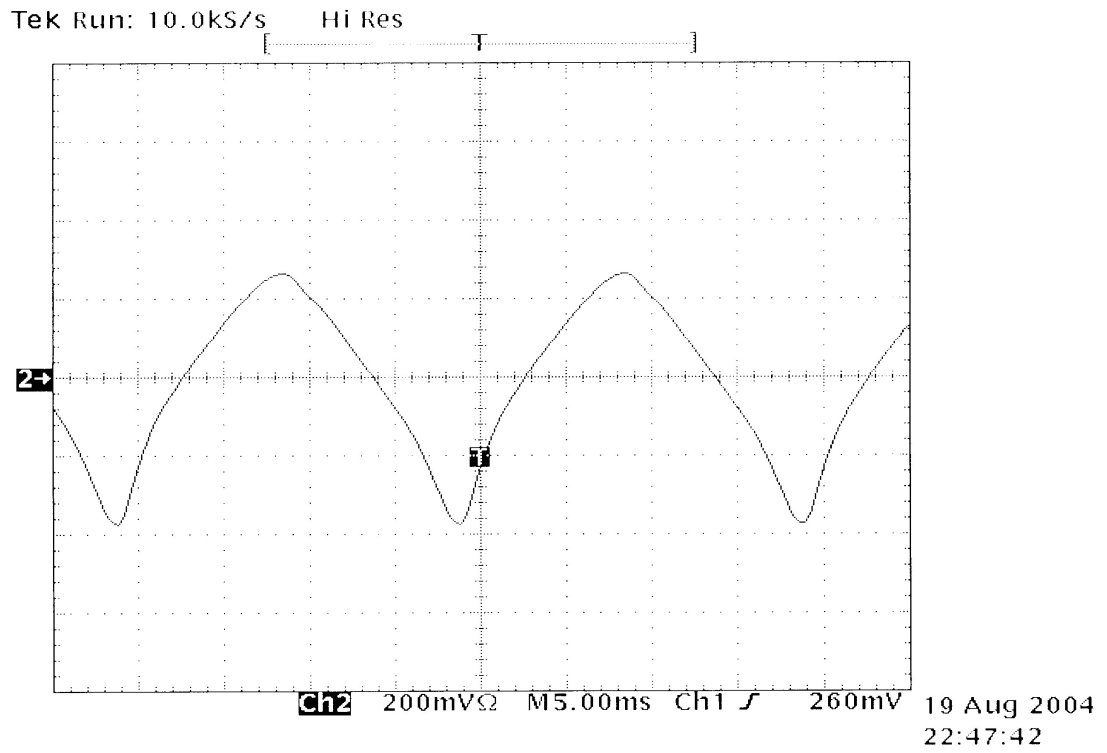


Figure B.5: Primary Current Waveform with Zero AC Load and 40 mA Secondary DC Current

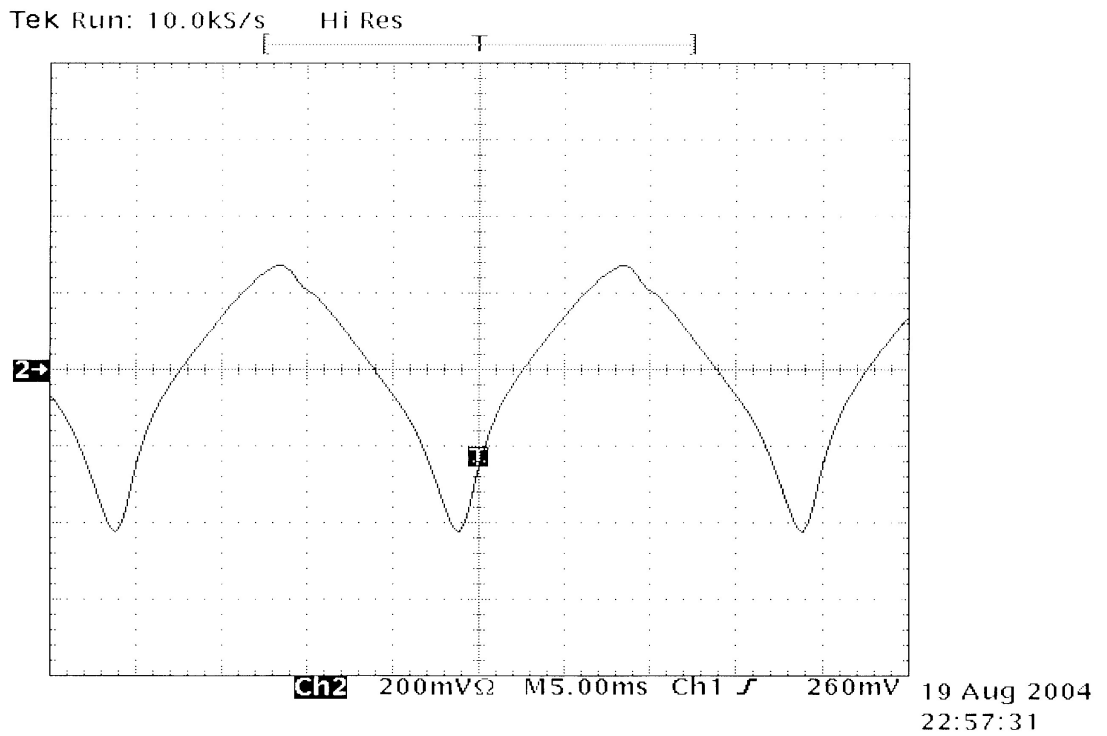


Figure B.6: Primary Current Waveform with Zero AC Load and 50 mA Secondary DC Current

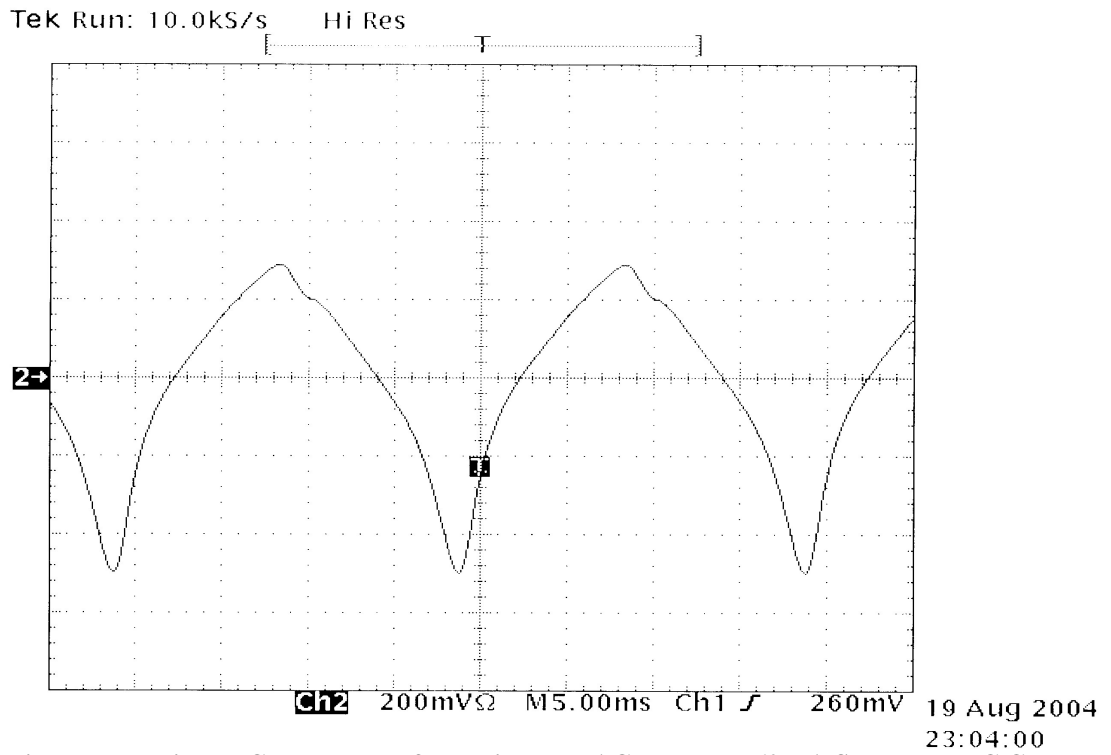


Figure B.7: Primary Current Waveform with Zero AC Load and 60 mA Secondary DC Current

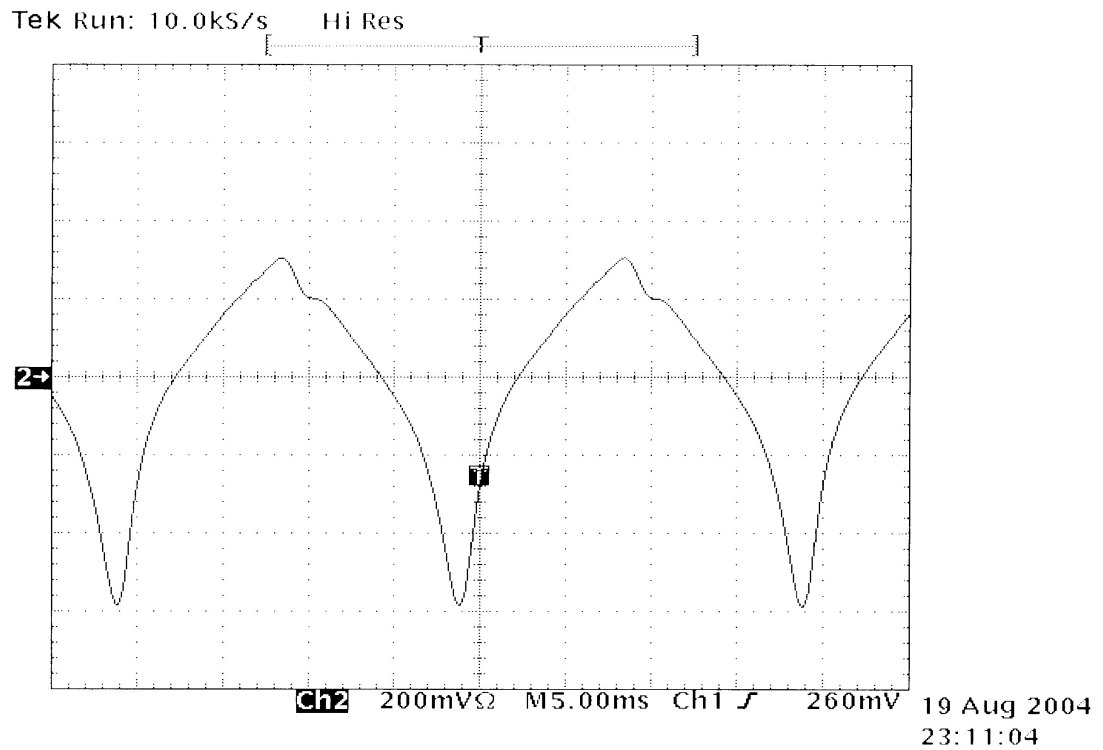


Figure B.8: Primary Current Waveform with Zero AC Load and 70 mA Secondary DC Current

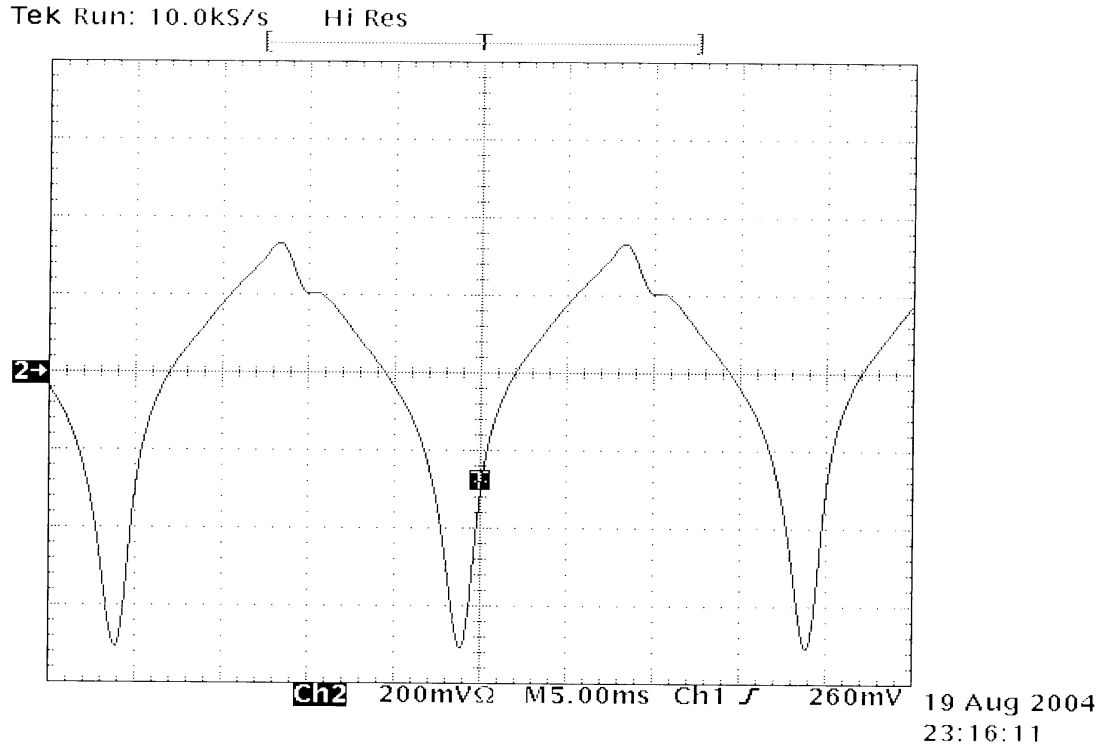


Figure B.9: Primary Current Waveform with Zero AC Load and 80 mA Secondary DC Current

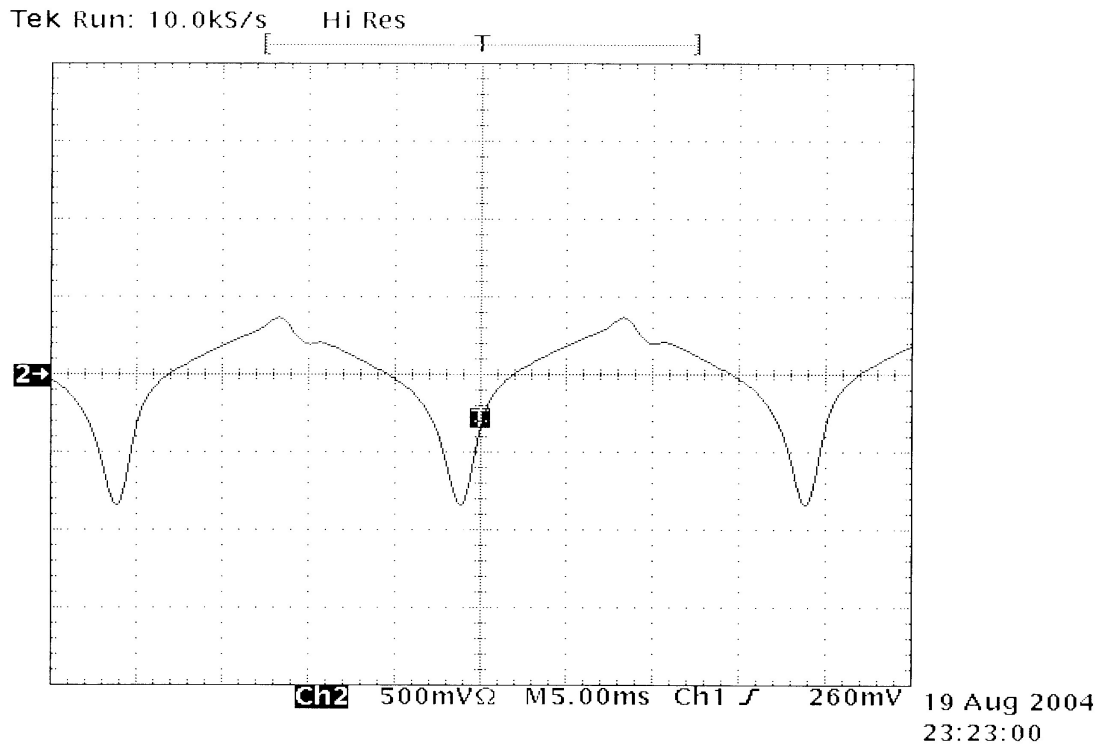


Figure B.10: Primary Current Waveform with Zero AC Load and 90 mA Secondary DC Current

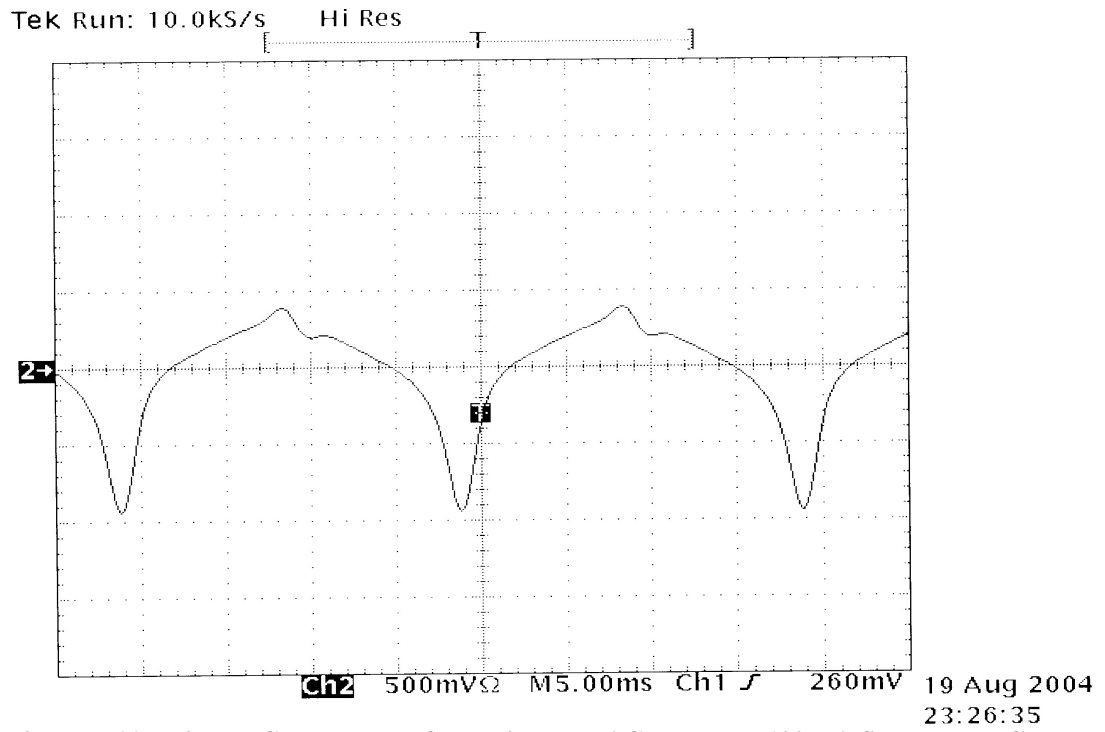


Figure B.11: Primary Current Waveform with Zero AC Load and 100 mA Secondary DC Current

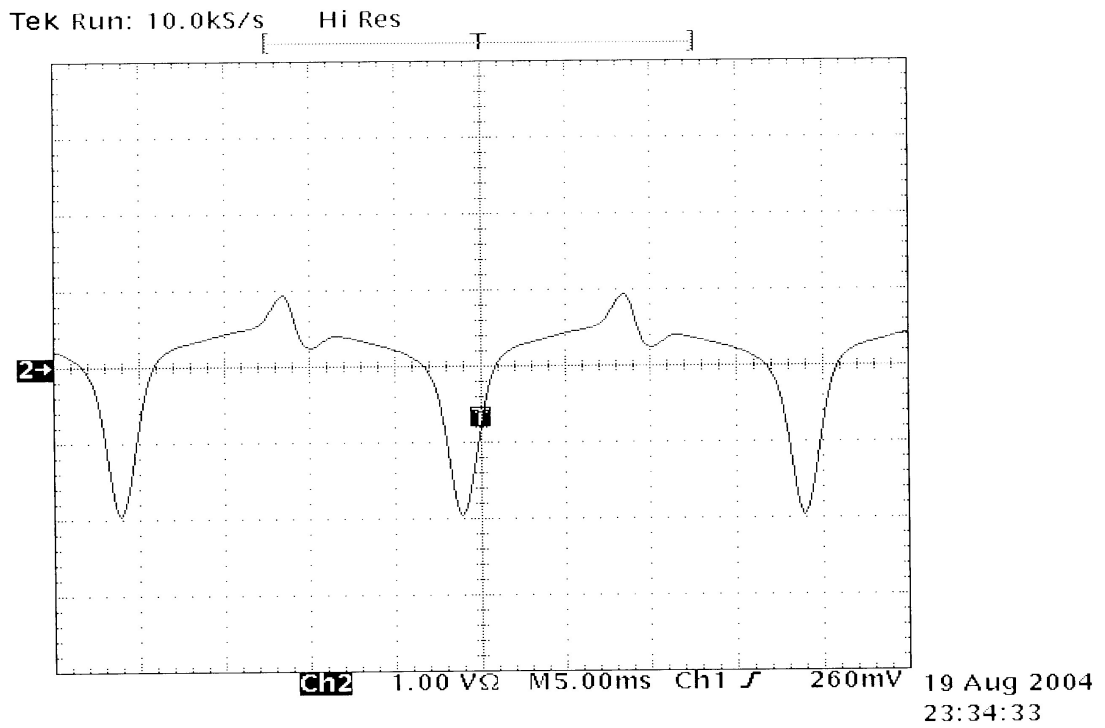


Figure B.12: Primary Current Waveform with Zero AC Load and 200 mA Secondary DC Current

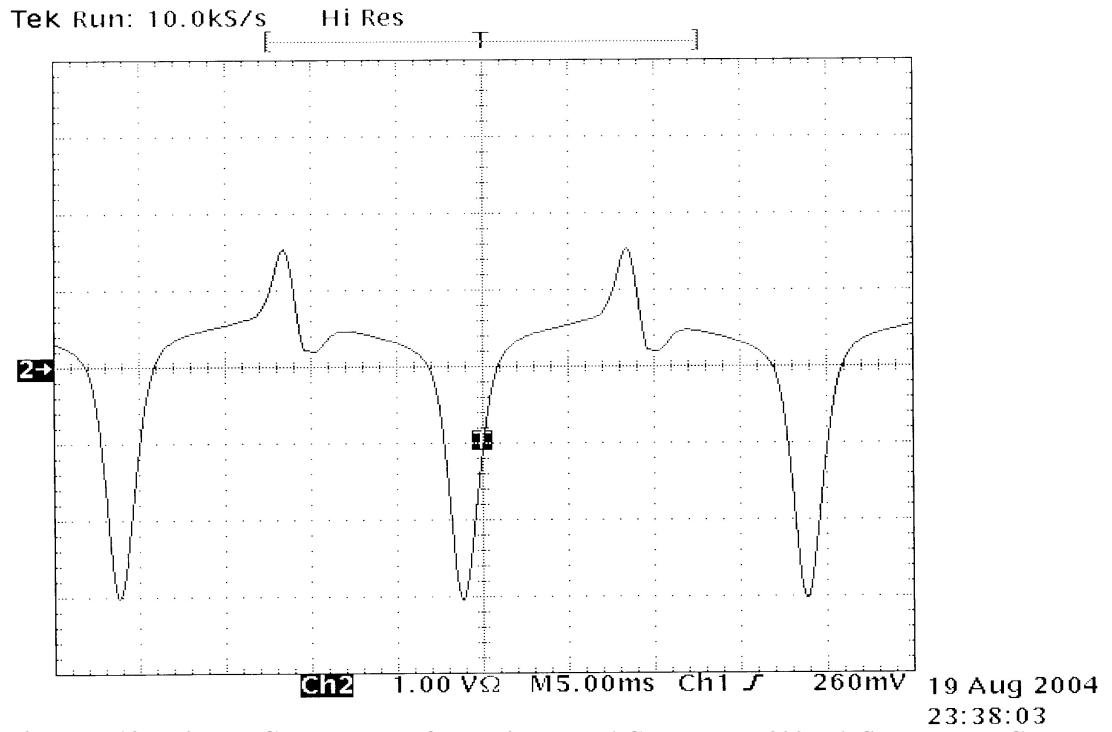


Figure B.13: Primary Current Waveform with Zero AC Load and 300 mA Secondary DC Current

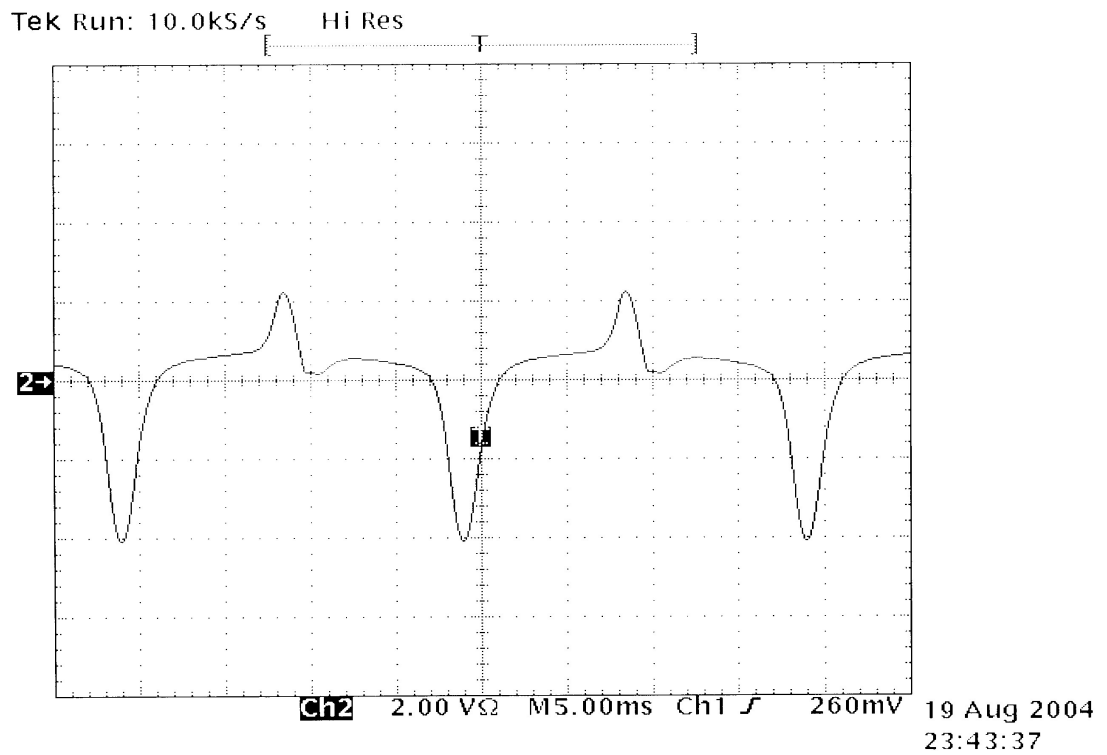


Figure B.14: Primary Current Waveform with Zero AC Load and 400 mA Secondary DC Current

Appendix C

Single Phase Analysis – Harmonic Effects Results

Primary Side Harmonic Effects with Half-Wave Rectified Secondary DC Component									
Primary Voltage Harmonic Components									
DC Injected (mA)	2nd	3rd	4th	5th	6th	7th	8th	9th	THD
0	0.1	0.7	0.0	2.1	0.0	0.9	0.0	0.1	2.3
30	0.1	0.7	0.0	2.1	0.0	0.8	0.0	0.1	2.3
60	0.2	0.7	0.1	2.0	0.0	0.9	0.0	0.1	2.4
90	0.3	0.8	0.2	2.1	0.1	0.8	0.0	0.1	2.4
120	0.5	0.9	0.3	2.3	0.1	0.7	0.1	0.1	2.7
150	0.6	1.1	0.5	2.4	0.3	0.6	0.2	0.1	2.9
180	0.9	1.2	0.6	2.5	0.3	0.6	0.2	0.2	3.0
210	1.0	1.3	0.8	2.7	0.5	0.6	0.2	0.2	3.2
240	1.3	1.3	0.9	2.7	0.6	0.4	0.2	0.3	3.5
270	1.5	1.6	1.1	2.9	0.6	0.5	0.3	0.3	4.0
300	1.7	1.7	1.2	3.1	0.8	0.3	0.3	0.4	4.2
Primary Current Harmonic Components									
DC Injected (mA)	2nd	3rd	4th	5th	6th	7th	8th	9th	THD
0	0.1	0.1	0.0	1.7	0.0	0.7	0.0	0.1	1.9
30	0.6	0.0	0.1	1.7	0.0	0.7	0.0	0.1	1.9
60	1.2	0.0	0.3	1.7	0.0	0.7	0.0	0.2	2.3
90	2.6	0.3	0.8	1.8	0.3	0.7	0.1	0.1	3.2
120	3.5	0.9	1.4	1.9	0.3	0.6	0.2	0.3	4.4
150	5.1	1.9	2.2	2.2	0.8	0.7	0.3	0.3	6.3
180	6.2	2.5	2.8	2.3	1.1	0.8	0.4	0.3	7.8
210	7.6	3.1	3.3	2.5	1.3	1.0	0.5	0.2	9.5
240	9.2	4.2	4.2	3.1	1.7	1.1	0.6	0.4	11.5
270	10.2	4.8	4.8	3.3	2.0	1.3	0.7	0.4	12.9
300	11.4	5.6	5.3	3.4	2.2	1.3	0.8	0.4	14.2

Table C.1: Primary Side Harmonic Effects with Half-Wave Rectified Secondary DC Component

Secondary Side Harmonic Effects with Half-Wave Rectified Secondary DC Component									
Secondary Voltage Harmonic Components									
DC Injected (mA)	2nd	3rd	4th	5th	6th	7th	8th	9th	THD
0	0.0	0.7	0.0	2.1	0.0	0.7	0.0	0.2	2.3
30	0.1	0.7	0.0	2.1	0.0	0.6	0.0	0.1	2.3
60	0.3	0.8	0.1	2.2	0.0	0.6	0.0	0.1	2.4
90	0.5	0.9	0.3	2.4	0.2	0.5	0.1	0.1	2.6
120	0.7	1.1	0.5	2.5	0.3	0.3	0.2	0.2	2.8
150	0.9	1.2	0.7	2.9	0.5	0.4	0.2	0.2	3.3
180	1.3	1.4	1.1	2.9	0.6	0.3	0.3	0.3	3.8
210	1.6	1.7	1.2	3.0	0.7	0.2	0.4	0.4	4.1
240	1.8	1.9	1.5	3.2	0.9	0.1	0.5	0.3	4.6
270	2.1	2.1	1.7	3.4	1.1	0.2	0.5	0.4	5.0
300	2.5	2.3	1.9	3.6	1.2	0.1	0.6	0.5	5.5
Secondary Current Harmonic Components									
DC Injected (mA)	2nd	3rd	4th	5th	6th	7th	8th	9th	THD
0	0.5	0.3	0.1	2.0	0.2	0.5	0.1	0.2	2.1
30	0.5	0.4	0.1	2.0	0.2	0.5	0.1	0.2	2.1
60	0.2	0.6	0.1	1.9	0.1	0.4	0.1	0.1	2.2
90	0.4	0.6	0.1	2.0	0.1	0.4	0.1	0.3	2.4
120	1.2	0.9	0.3	2.1	0.3	0.2	0.1	0.1	2.7
150	1.3	1.2	0.4	2.6	0.2	0.4	0.1	0.1	3.0
180	1.9	1.4	0.7	2.4	0.4	0.1	0.1	0.1	3.4
210	2.2	1.3	0.9	2.8	0.4	0.1	0.1	0.2	3.9
240	2.5	1.6	1.0	3.1	0.6	0.1	0.1	0.1	4.5
270	2.9	1.8	1.3	3.2	0.8	0.1	0.3	0.3	5.0
300	3.2	2.1	1.5	3.4	0.8	0.1	0.3	0.4	5.5

Table C.2: Secondary Side Harmonic Effects with Half-Wave Rectified Secondary DC Component

Primary Side Harmonic Effects with a Smoothed Half-Wave Rectified Secondary DC Component									
Primary Voltage Harmonic Components									
DC Injected (mA)	2nd	3rd	4th	5th	6th	7th	8th	9th	THD
0	0.1	0.7	0.0	2.5	0.0	0.9	0.0	0.1	2.9
30	0.1	0.8	0.0	2.4	0.0	0.9	0.0	0.1	2.8
60	0.1	0.8	0.0	2.3	0.0	0.8	0.1	0.1	2.7
90	0.1	0.9	0.1	2.2	0.1	0.8	0.1	0.0	2.6
120	0.2	1.1	0.2	2.3	0.1	0.9	0.1	0.3	2.7
150	0.3	1.1	0.2	2.1	0.1	1.0	0.1	0.2	2.8
180	0.3	1.1	0.3	2.2	0.2	1.1	0.1	0.4	2.8
210	0.4	1.2	0.3	2.3	0.2	1.1	0.1	0.3	2.9
240	0.4	1.3	0.4	2.4	0.2	1.1	0.0	0.3	3.1
270	0.4	1.3	0.5	2.5	0.2	1.1	0.0	0.3	3.1
300	0.5	1.4	0.4	2.5	0.2	1.1	0.0	0.2	3.3
Primary Current Harmonic Components									
DC Injected (mA)	2nd	3rd	4th	5th	6th	7th	8th	9th	THD
0	0.1	0.2	0.0	2.3	0.0	0.8	0.0	0.1	2.5
30	1.4	1.3	1.0	2.6	1.0	1.8	0.9	0.9	5.1
60	2.9	2.5	2.0	3.1	1.7	2.7	1.6	1.5	7.0
90	4.5	3.9	3.1	4.3	2.3	3.2	2.2	2.1	9.6
120	6.3	5.5	4.7	5.6	2.5	3.4	2.5	2.4	12.3
150	7.3	6.8	5.8	5.7	2.6	3.1	2.5	2.5	14.4
180	8.5	7.8	6.6	6.0	3.0	2.7	2.2	1.9	15.6
210	9.5	8.7	7.4	6.3	3.2	1.6	1.4	1.1	16.8
240	10.7	9.6	8.1	6.6	3.5	0.6	0.4	0.2	18.4
270	11.6	10.5	8.8	6.8	3.9	0.5	0.5	0.4	19.8
300	12.8	11.3	9.6	7.2	4.2	1.4	1.1	1.2	21.4

Table C.3: Primary Side Harmonic Effects with Smoothed Half-Wave Rectified Secondary DC Component

Secondary Side Harmonic Effects with a Smoothed Half-Wave Rectified Secondary DC Component									
Secondary Voltage Harmonic Components									
DC Injected (mA)	2nd	3rd	4th	5th	6th	7th	8th	9th	THD
0	0.0	0.7	0.0	2.5	0.0	1.0	0.0	0.1	2.7
30	0.1	0.8	0.1	2.2	0.1	0.9	0.2	0.1	2.7
60	0.2	1.0	0.2	1.9	0.3	0.8	0.4	0.2	2.6
90	0.4	1.2	0.4	2.0	0.4	0.9	0.6	0.4	2.9
120	0.6	1.5	0.7	2.1	0.6	1.3	0.7	0.6	3.3
150	0.7	1.6	0.8	2.4	0.5	1.5	0.7	0.9	3.9
180	0.8	1.8	1.0	2.9	0.6	1.5	0.7	0.9	4.2
210	0.9	1.9	1.1	3.0	0.7	1.5	0.5	0.8	4.5
240	1.0	2.1	1.3	3.3	0.8	1.3	0.1	0.4	4.7
270	1.2	2.2	1.5	3.5	0.8	1.1	0.0	0.2	4.8
300	1.3	2.3	1.6	3.8	1.0	0.7	0.3	0.1	5.0
Secondary Current Harmonic Components									
DC Injected (mA)	2nd	3rd	4th	5th	6th	7th	8th	9th	THD
0	0.1	0.8	0.1	2.1	0.2	0.8	0.1	0.2	2.5
30	0.9	1.2	1.1	2.8	0.9	1.8	0.8	0.8	4.3
60	1.9	1.7	2.0	3.6	1.7	2.7	1.5	1.3	6.5
90	2.9	2.2	3.1	4.9	2.6	3.1	1.9	1.9	8.5
120	4.4	2.8	3.5	6.0	3.3	3.8	2.4	2.2	10.5
150	5.0	3.1	3.9	6.5	3.9	3.7	2.5	1.9	11.6
180	5.6	3.6	4.3	6.5	4.2	3.5	2.5	2.1	12.1
210	6.4	3.9	4.2	6.1	4.2	3.0	1.8	0.7	11.6
240	6.8	3.9	4.0	5.8	3.9	2.3	1.7	0.8	12.1
270	7.3	3.9	3.7	5.4	3.6	1.6	1.1	1.0	11.5
300	7.8	3.9	3.8	4.9	3.3	1.1	1.0	1.5	11.6

Table C.4: Secondary Side Harmonic Effects with Smoothed Half-Wave Rectified Secondary DC Component

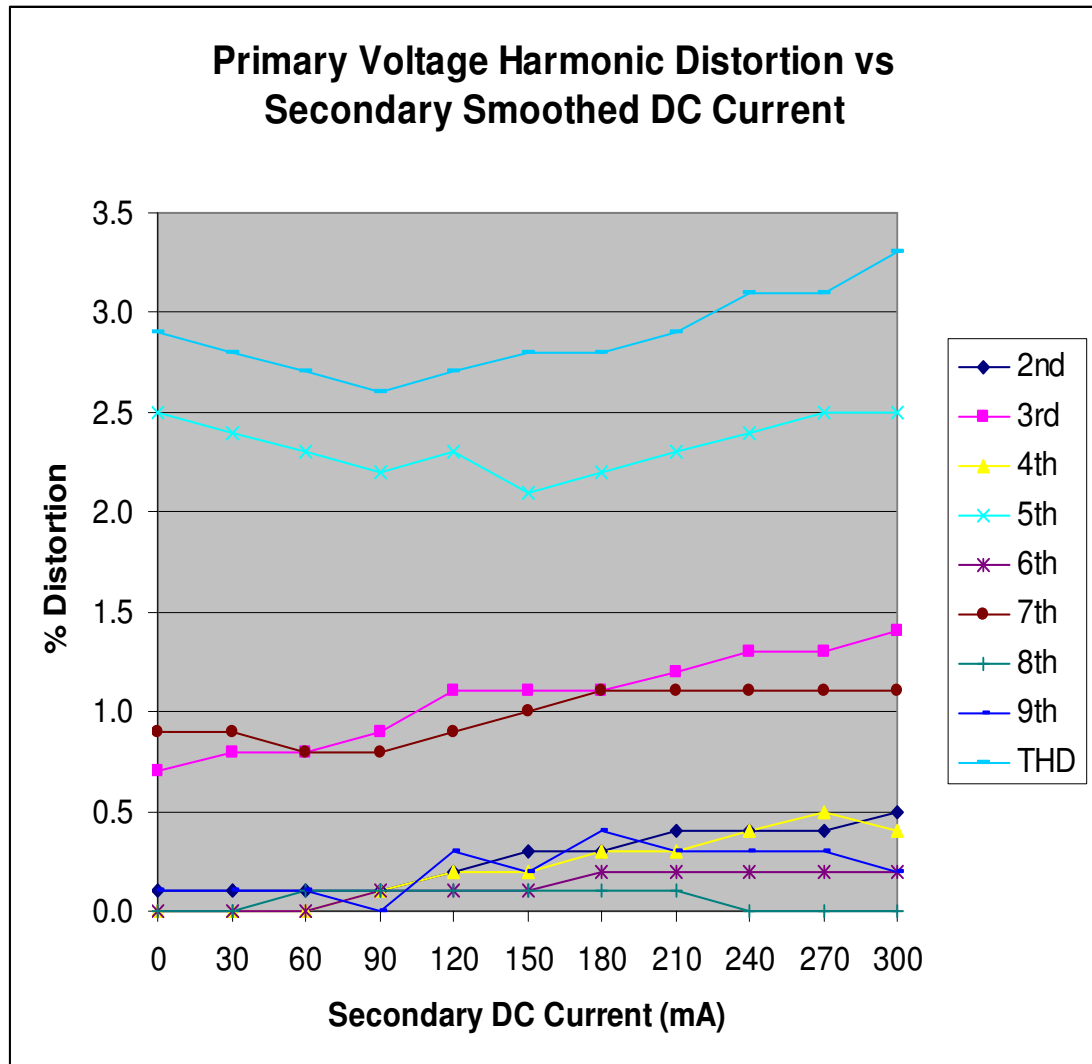


Figure C.1: Variation in Primary Voltage Harmonic Distortion for Secondary Smoothed Half-Wave Rectified Current

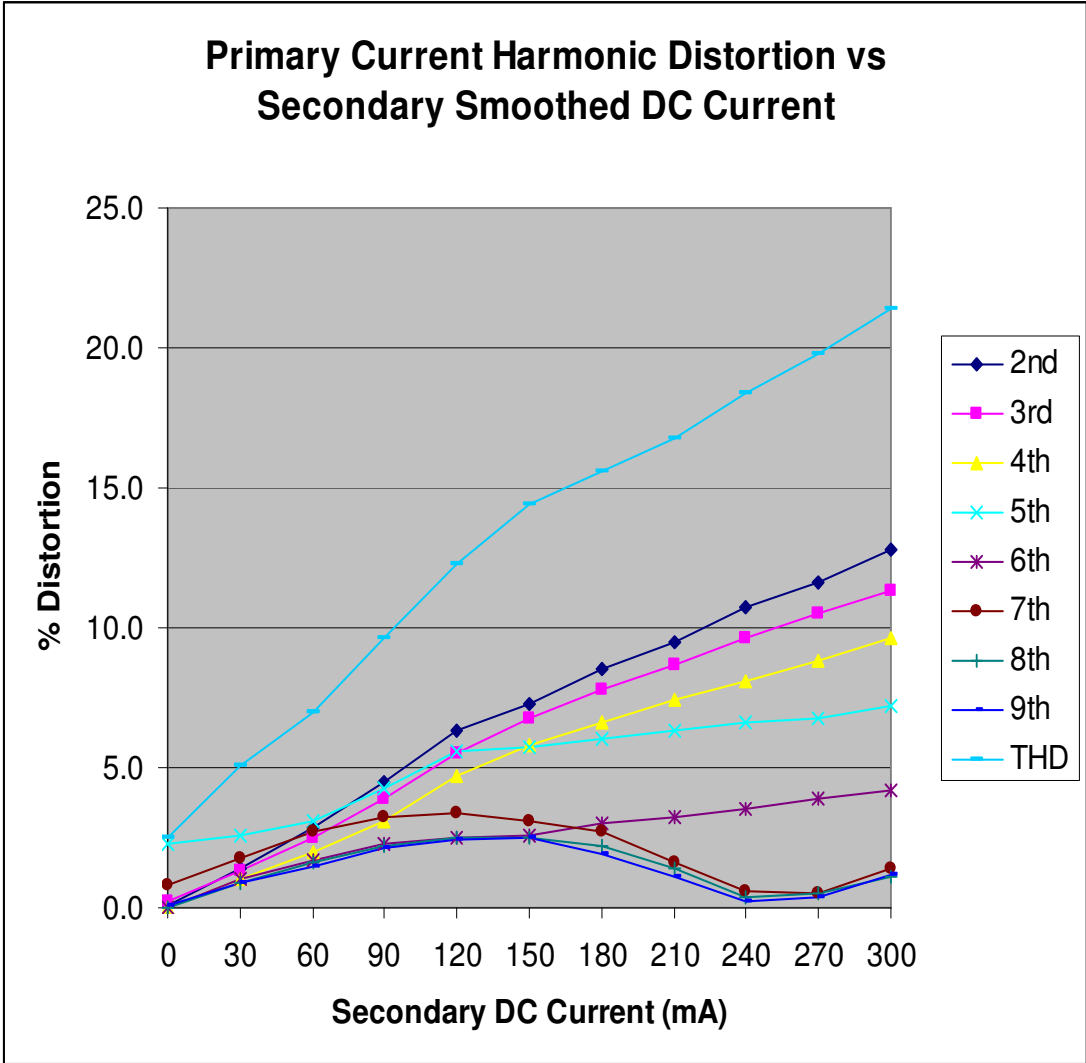


Figure C.2: Variation in Primary Current Harmonic Distortion for Secondary Smoothed Half-Wave Rectified Current

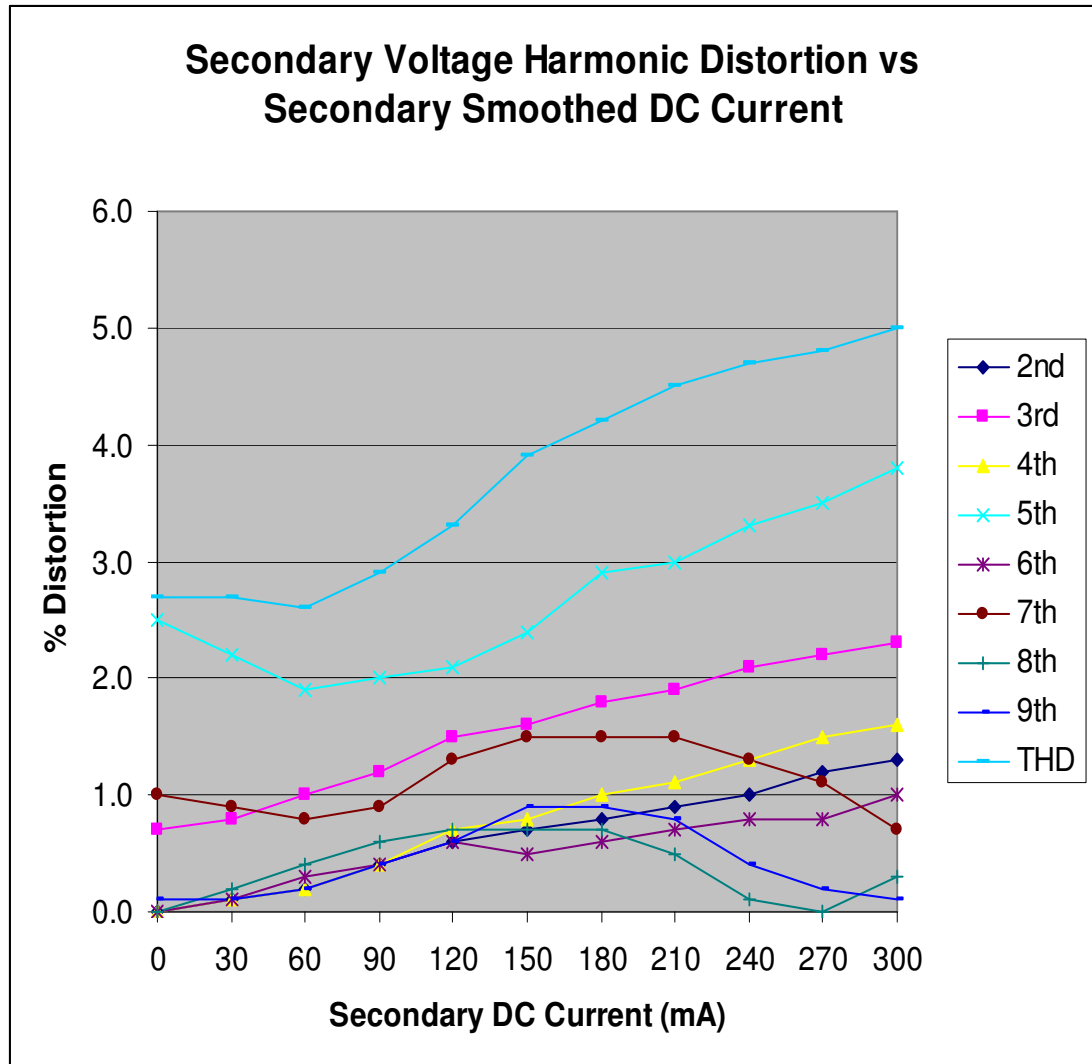


Figure C.3: Variation in Secondary Voltage Harmonic Distortion for Secondary Smoothed Half-Wave Rectified Current

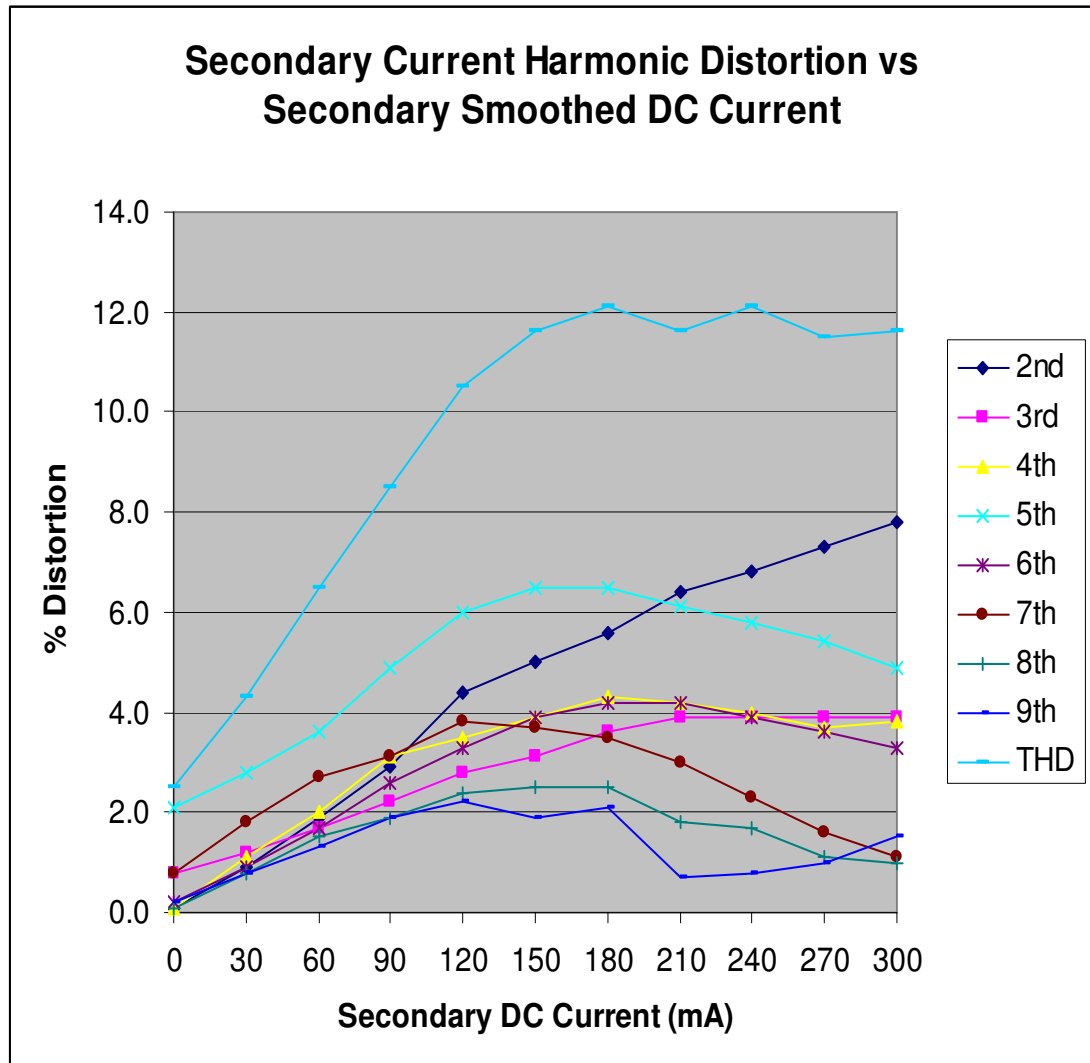


Figure C.4: Variation in Secondary Current Harmonic Distortion for Secondary Smoothed Half-Wave Rectified Current

Appendix D

Experimental Hysteresis Results

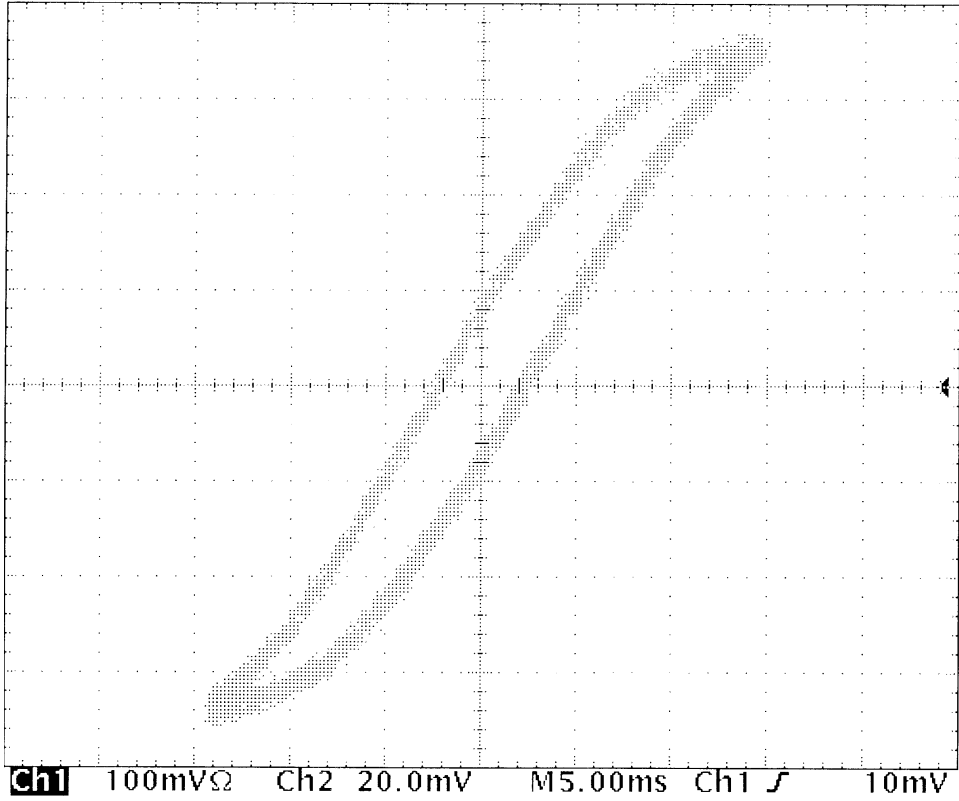


Figure D.1: Hysteresis Characteristic with 240 V Supply and Open Circuit Secondary

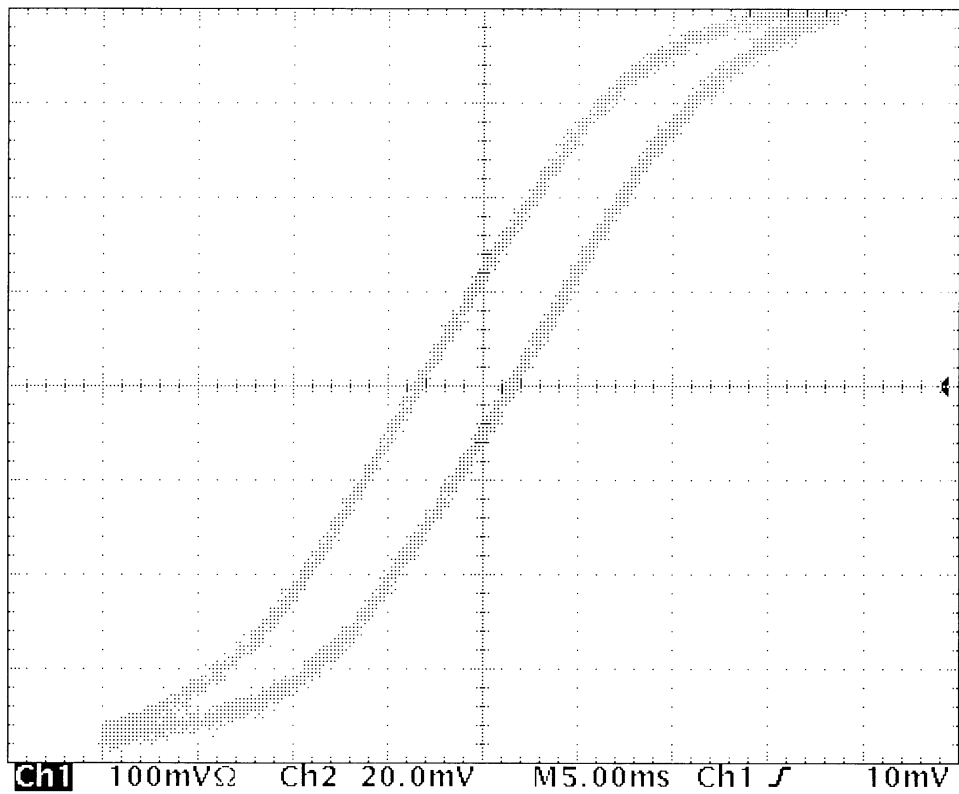


Figure D.2: Hysteresis Characteristic with 270 V Supply and Open Circuit Secondary

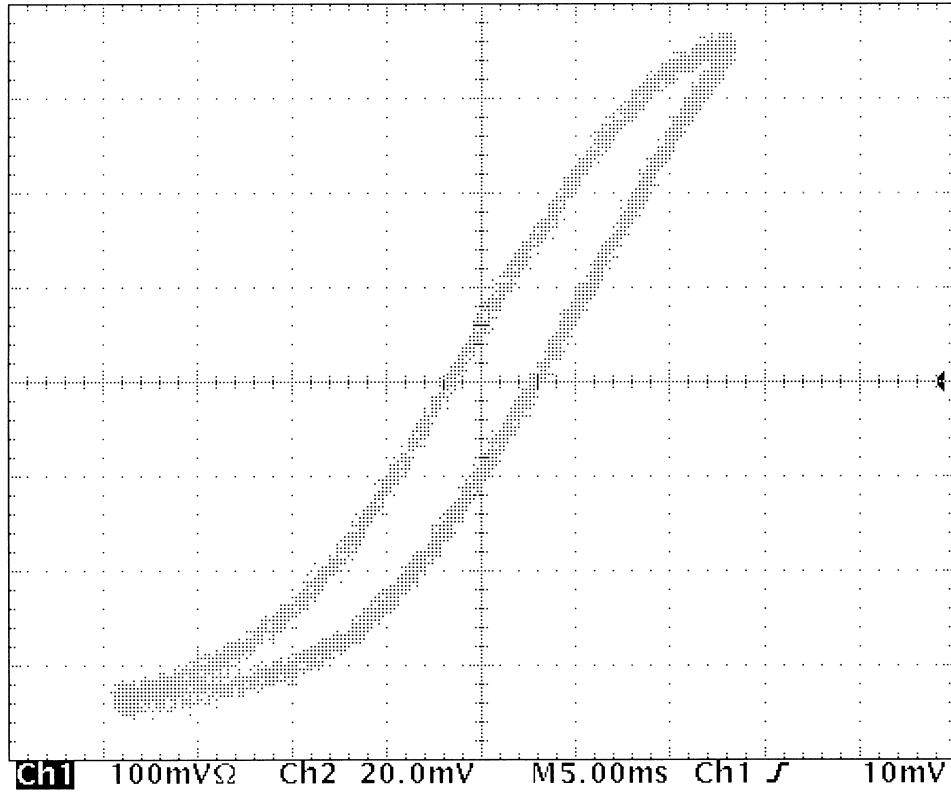


Figure D.3: Hysteresis Characteristic with 240 V Supply and 25 mA Secondary DC Component

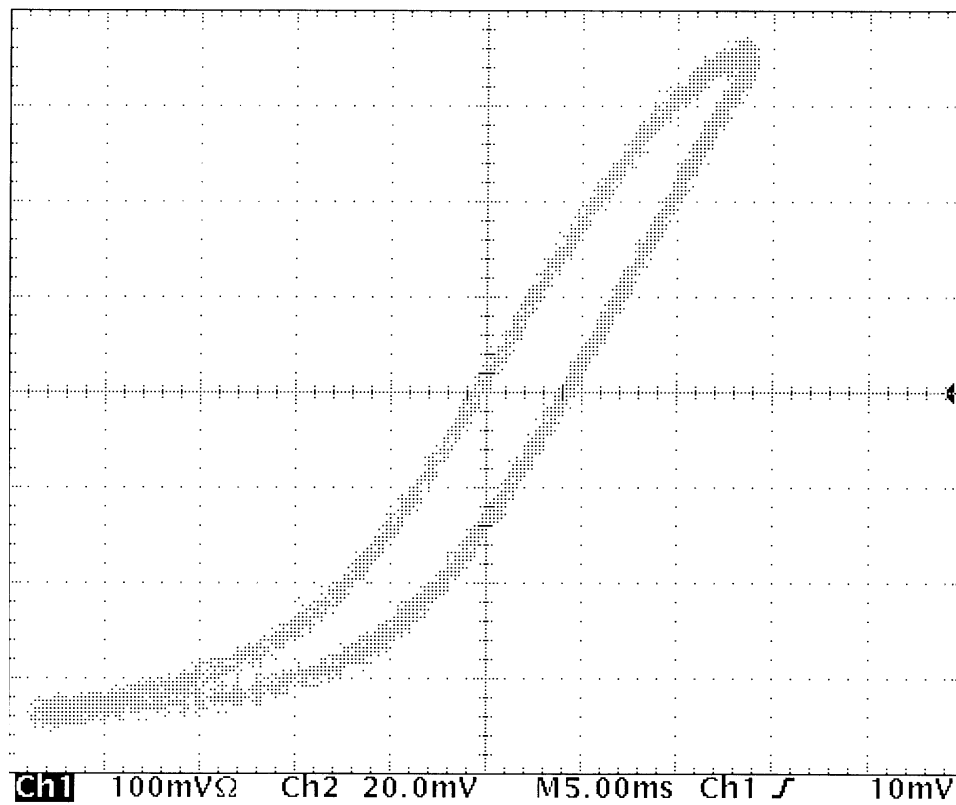


Figure D.4: Hysteresis Characteristic with 240 V Supply and 50 mA Secondary DC Component

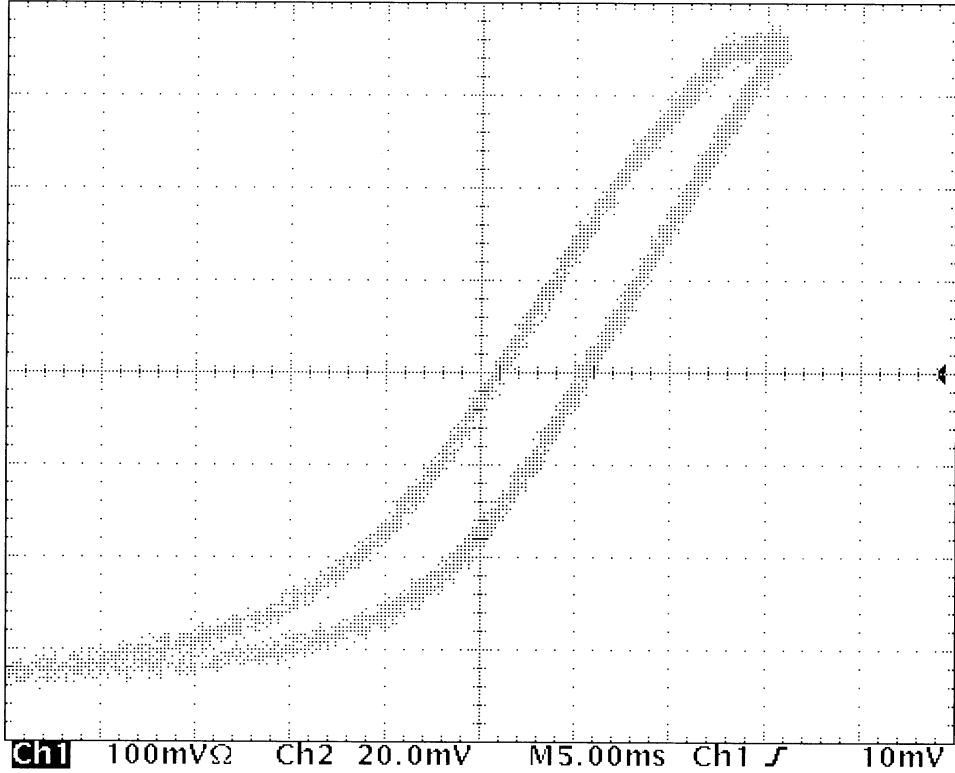


Figure D.5: Hysteresis Characteristic with 240 V Supply and 75 mA Secondary DC Component

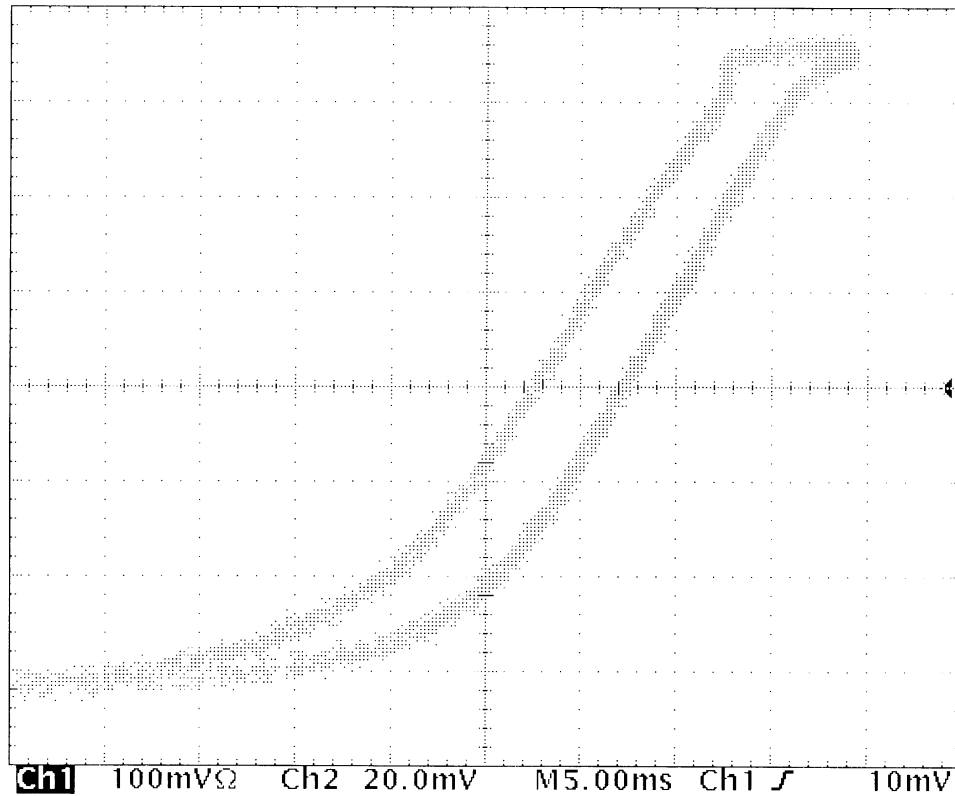


Figure D.6: Hysteresis Characteristic with 240 V Supply and 100 mA Secondary DC Component

Appendix E

MATLAB CODE –

Magnetising_Current_Prediction.m

```
-----%  
% Script: Magnetising_Current_Prediction.m  
%  
% Purpose: The purpose of this program is to determine the Flux-I  
%          characteristic and primary magnetising current for a given level  
%          of flux bias. The inputs to the program can be taken off actual  
%          hysteresis curve measurements. The model used in this program  
%          neglects the affect of hysteresis and uses a mid point locus  
%          piecewise linear approximation.  
%  
% Author: Ashley Zeimer, 20/10/04  
-----%  
  
% Define piecewise linear parameters for flux and gradient from  
% Flux-Magnetising Current plot for an unloaded transformer  
fluxvalue=[0.7222 0.8333 0.9444 1 0 -0.7222 -0.8333 -0.9444 -1];  
slope=[0.005417 0.003333 0.002222 0.001667];  
  
-----%  
  
% Request user for input to determine level of DC Bias  
% The DC bias will be simulated in the form of a flux bias  
bias=input('Please input level of positive core flux bias (max. AC flux is 1): ');  
% Determine new maximum flux value  
fluxvalue(4)=fluxvalue(4)+bias;  
% Set maximum value of AC flux  
flux_max=1;  
% Determine radian frequency  
w=2*pi*50;  
  
-----%  
  
% Set up cycle times  
cycle_time=[0:0.00001:0.02]; % Define 50 Hz cycle period  
% Determine flux array with bias  
xx=bias+flux_max*sin(w.*cycle_time);  
% Determine time indices positive flux values which are less than the bias  
time_indices=find(xx<bias&xx>=0);  
% Calculate time shift to allow display of unbroken positive cycle  
time_shift=length(time_indices)/length(cycle_time)*0.01;  
pos=find(xx>=0);  
neg=find(xx<0);  
% Determine duration of positive current values  
pos_duration=length(pos)/length(cycle_time)*0.02;  
% Determine duration of negative current values  
neg_duration=length(neg)/length(cycle_time)*0.02;  
% Define time shifted start time assuming Flux-I loop starts at axis origin  
start_time=-1*time_shift;  
% Determine finish time of first quarter of Flux-I loop  
fqt=pos_duration/2-time_shift;  
% Determine finish time of first half of Flux-I loop  
sqt=pos_duration-time_shift;  
% Determine finish time of third quarter of Flux-I loop  
tqt=pos_duration+(neg_duration/2)-time_shift;  
  
-----%  
%-----Calculation Procedure for First Half of Flux-I Loop-----%  
-----%
```

```
-----%  
n=1; % Initialise increment variable  
flux_previous=0;  
Imag_previous=0;  
for t=start_time:0.00001:fqt % Define loop duration  
    flux=bias+flux_max*sin(w*t); % Calculate flux according to variable 't'  
    if (flux<=fluxvalue(1))  
        % Calculate current in first positive piecewise linear section  
        Imag(n)=Imag_previous+(flux-flux_previous)/slope(1);  
    end  
    if (flux>fluxvalue(1))&(flux<=fluxvalue(2))  
        % Calculate current in second positive piecewise linear section  
        Imag(n)=Imag_previous+(flux-flux_previous)/slope(2);  
    end  
    if (flux>fluxvalue(2))&(flux<=fluxvalue(3))  
        % Calculate current in third positive piecewise linear section  
        Imag(n)=Imag_previous+(flux-flux_previous)/slope(3);  
    end  
    if (flux>fluxvalue(3))&(flux<=(fluxvalue(4)))  
        % Calculate current in fourth positive piecewise linear section  
        Imag(n)=Imag_previous+(flux-flux_previous)/slope(4);  
    end  
    flux_previous=flux;  
    Imag_previous=Imag(n);  
    n=n+1; % Increment  
end  
Imag1=Imag;  
% Create array to represent second quarter of Flux-I loop  
Imag2=flipdim(Imag1,2);  
% Create array to represent first half of Flux-I loop  
Imag=[Imag1,Imag2];  
  
-----%  
%-----Calculation Procedure for Second Half of Flux-I Loop-----%  
-----%  
  
Imag=[]; % Reinitialise Imag array  
n=1; % Reinitialise increment variable  
Imag(n)=0;  
flux_previous=0;  
Imag_previous=0;  
for t=sqt:0.00001:tqt % Define loop duration  
    flux=bias+flux_max*sin(w*t);  
    if (flux>fluxvalue(6))&(flux<=fluxvalue(5))  
        % Calculate current in first negative piecewise linear section  
        Imag(n)=Imag_previous+(flux-flux_previous)/slope(1);  
    end  
    if (flux>fluxvalue(7))&(flux<=fluxvalue(6))  
        % Calculate current in second negative piecewise linear section  
        Imag(n)=Imag_previous+(flux-flux_previous)/slope(2);  
    end  
    if (flux>fluxvalue(8))&(flux<=fluxvalue(7))  
        % Calculate current in third negative piecewise linear section  
        Imag(n)=Imag_previous+(flux-flux_previous)/slope(3);  
    end  
    if (flux>fluxvalue(9))&(flux<=fluxvalue(8))
```

```
        % Calculate current in fourth negative piecewise linear section
        Imag(n)=Imag_previous+(flux-flux_previous)/slope(4);
    end
    flux_previous=flux;
    Imag_previous=Imag(n);
    n=n+1;
end
Imag3=Imag;
% Create array to represent fourth quarter of Flux-I loop
Imag4=flipdim(Imag3,2);
% Create array to represent total Flux-I loop
Imag=[Imag1,Imag2,Imag3,Imag4];

%-----%

x=linspace(0-time_shift,0.02-time_shift,length(Imag));
x1=bias+flux_max*sin(w.*x);
% Plot of Flux-Magnetising Current relationship
plot(Imag,x1)
title('Flux vs Magnetising Current')
xlabel('Magnetising Current (mA)')
ylabel('Flux (wB)')
grid on
pause
% Plot of magnetising current over two cycles with bias
Imag1=[Imag,Imag];
t=linspace(0,0.04,length(Imag1));
plot(t,Imag1)
title('Magnetising Current as Determined from I-Flux Plot')
xlabel('Time (seconds)')
ylabel('Magnetising Current (mA)')
grid on
pause

%-----%
%-----Removal of DC Bias-----%
%-----%

DCImag=Imag;
Idc=mean(DCImag); % Detemine level of current bias
ACImag=DCImag-Idc; % Remove bias
ACImag=[ACImag, ACImag]; % Create array to represent current over 2 cycles
% Plot primary side magnetising current without bias
plot(t,ACImag)
title('Primary Magnetising Current without Bias');
xlabel('Time (seconds)')
ylabel('Magnetising Current (mA)')
grid on

%-----%

%Calculate RMS Value of primary side magnetising current
RMS=norm(ACImag)/sqrt(length(ACImag));
disp('The RMS value of the primary side magnetising current is (in mA): ')
RMS
%-----%

clear all
```

Appendix F

Three Phase Analysis Results

A Phase to Neutral DC Injection						
DC Level (mA)	IL A (mA)	IL B (mA)	IL C (mA)	IP A (mA)	IP B (mA)	IP C (mA)
0	188	171	152	89	112	104
20	187	175	151	90	112	103
40	190	183	153	94	113	104
60	192	188	154	97	113	105
80	194	195	153	101	115	107
100	199	204	154	107	115	106
200	231	251	157	142	122	112
	W (A)	VA (A)	VAR (A)	W (B)	VA (B)	VAR (B)
0	10	33	31	15	42	39
20	12	33	31	14	40	37
40	15	35	32	16	43	40
60	16	34	30	15	41	38
80	18	38	33	14	40	38
100	21	39	33	15	41	38
200	32	52	41	15	44	41
	W (C)	VA (C)	VAR (C)	lthd % (A)	lthd % (B)	lthd % (C)
0	30	39	24	7.7	9.3	7.4
20	29	37	22	10.8	9.1	7
40	30	39	24	15.3	10.5	6.4
60	29	37	23	17.3	11.5	8.7
80	30	38	23	19.6	11.4	8.5
100	30	40	24	24.9	12.1	8.7
200	32	40	24	39.8	17.8	15.3
	PF (A)	PF (B)	PF (C)	DPF (A)	DPF (B)	DPF (C)
0	0.29	0.37	0.78	0.31	0.38	0.81
20	0.36	0.37	0.8	0.36	0.36	0.81
40	0.41	0.38	0.79	0.43	0.38	0.8
60	0.48	0.38	0.78	0.49	0.38	0.8
80	0.49	0.35	0.8	0.53	0.36	0.8
100	0.54	0.37	0.79	0.57	0.35	0.81
200	0.62	0.35	0.81	0.69	0.35	0.83

Table F.1: Results of 'A' Phase to Neutral DC Injection

B Phase to Neutral DC Injection						
DC Level (mA)	IL A (mA)	IL B (mA)	IL C (mA)	IP A (mA)	IP B (mA)	IP C (mA)
0	187	171	152	88	112	103
20	190	170	160	89	114	104
40	189	170	165	88	118	105
60	192	172	174	90	122	107
80	192	174	182	90	127	107
100	194	176	189	89	130	107
200	199	201	235	95	168	113
	W (A)	VA (A)	VAR (A)	W (B)	VA (B)	VAR (B)
0	10	32	31	16	42	39
20	8	33	32	18	43	39
40	10	32	30	19	42	37
60	4	31	30	22	43	37
80	10	33	31	24	47	41
100	9	33	31	30	53	43
200	10	34	33	39	61	47
	W (C)	VA (C)	VAR (C)	lthd % (A)	lthd % (B)	lthd % (C)
0	30	39	25	8.1	9.2	7
20	29	36	22	7.8	8.6	7.3
40	30	40	27	9.7	9.9	7.6
60	30	38	23	10.4	11.7	9.5
80	30	38	23	11.8	14.4	10.5
100	30	39	24	14.9	16.1	12.7
200	32	41	27	23.3	27.1	18.4
	PF (A)	PF (B)	PF (C)	DPF (A)	DPF (B)	DPF (C)
0	0.3	0.38	0.77	0.34	0.39	0.8
20	0.29	0.43	0.8	0.3	0.44	0.83
40	0.3	0.46	0.75	0.3	0.47	0.79
60	0.27	0.5	0.79	0.3	0.53	0.8
80	0.3	0.52	0.79	0.3	0.54	0.8
100	0.29	0.57	0.78	0.28	0.58	0.79
200	0.3	0.64	0.77	0.31	0.67	0.79

Table F.2: Results of 'B' Phase to Neutral DC Injection

C Phase to Neutral DC Injection						
DC Level (mA)	IL A (mA)	IL B (mA)	IL C (mA)	IP A (mA)	IP B (mA)	IP C (mA)
0	193	175	157	91	116	107
20	195	171	154	89	113	109
40	195	168	153	88	112	115
60	207	171	158	89	114	121
80	216	173	161	91	116	128
100	220	170	166	90	115	135
200	266	174	203	94	122	175
	W (A)	VA (A)	VAR (A)	W (B)	VA (B)	VAR (B)
0	3	32	31	15	41	38
20	10	33	31	17	43	39
40	8	33	31	15	41	38
60	4	32	31	17	44	41
80	8	32	31	15	40	37
100	5	33	31	16	43	40
200	6	35	35	21	48	44
	W (C)	VA (C)	VAR (C)	lthd % (A)	lthd % (B)	lthd % (C)
0	30	37	23	9.6	8.9	6.4
20	32	40	23	7.4	8.5	7.5
40	35	43	24	7.4	9.6	10.1
60	37	45	26	9	10.6	12.6
80	39	45	24	10.2	12.2	15.1
100	41	50	27	10.8	12.6	19.1
200	53	63	33	18.3	21.6	30.4
	PF (A)	PF (B)	PF (C)	DPF (A)	DPF (B)	DPF (C)
0	0.28	0.37	0.8	0.27	0.38	0.81
20	0.3	0.4	0.81	0.31	0.39	0.83
40	0.27	0.37	0.83	0.3	0.38	0.85
60	0.29	0.39	0.82	0.28	0.39	0.85
80	0.27	0.38	0.85	0.3	0.39	0.87
100	0.26	0.37	0.84	0.3	0.36	0.87
200	0.22	0.44	0.85	0.2	0.46	0.9

Table F.3: Results of 'C' Phase to Neutral DC Injection

DC Injection Between A and B Phases						
DC Level (mA)	IL A (mA)	IL B (mA)	IL C (mA)	IP A (mA)	IP B (mA)	IP C (mA)
0	189	171	153	89	113	104
20	187	178	160	87	118	105
40	188	188	169	90	125	105
60	189	198	176	90	132	108
80	190	211	184	93	141	110
100	196	226	192	100	150	111
200	235	321	243	137	205	126
	W (A)	VA (A)	VAR (A)	W (B)	VA (B)	VAR (B)
0	10	32	31	11	41	38
20	12	32	30	14	47	44
40	14	33	30	21	46	42
60	17	36	32	21	48	43
80	18	34	29	22	54	49
100	20	36	30	26	57	50
200	33	51	39	32	75	68
	W (C)	VA (C)	VAR (C)	lthd % (A)	lthd % (B)	lthd % (C)
0	32	41	25	8.8	9.7	7
20	31	39	23	10.9	8.8	7.5
40	30	39	24	15.4	10.9	8.8
60	31	39	24	24.4	13.5	11.2
80	30	40	26	30.3	15.9	13.3
100	31	39	24	36.6	18.8	18.1
200	32	42	28	55.8	29.4	28.6
	PF (A)	PF (B)	PF (C)	DPF (A)	DPF (B)	DPF (C)
0	0.31	0.38	0.79	0.31	0.38	0.81
20	0.37	0.37	0.8	0.38	0.39	0.81
40	0.43	0.44	0.79	0.44	0.44	0.8
60	0.46	0.44	0.79	0.49	0.47	0.8
80	0.53	0.42	0.77	0.57	0.46	0.8
100	0.56	0.47	0.79	0.61	0.47	0.81
200	0.65	0.43	0.76	0.78	0.46	0.81

Table F.4: Results of DC Injection between 'A' and 'B' Phases

DC Injection Between C and B Phases						
DC Level (mA)	IL A (mA)	IL B (mA)	IL C (mA)	IP A (mA)	IP B (mA)	IP C (mA)
0	189	171	153	89	113	104
20	196	170	163	90	114	113
40	207	167	175	91	113	121
60	214	164	187	90	116	129
80	224	161	203	91	120	137
100	235	163	221	92	124	148
200	290	190	316	100	175	193
	W (A)	VA (A)	VAR (A)	W (B)	VA (B)	VAR (B)
0	10	32	31	11	41	38
20	9	32	31	17	41	37
40	4	33	32	19	41	36
60	6	33	32	21	43	38
80	8	34	33	23	46	39
100	9	34	33	25	41	33
200	6	38	37	42	57	39
	W (C)	VA (C)	VAR (C)	lthd % (A)	lthd % (B)	lthd % (C)
0	32	41	25	8.8	9.7	7
20	33	41	25	8.6	10.3	8
40	35	45	28	10.2	13.3	11.7
60	37	47	29	13.3	16.2	15.6
80	39	50	32	15.5	20.5	18.1
100	41	54	35	18.3	24.8	21.7
200	52	73	51	33.2	39.1	32.5
	PF (A)	PF (B)	PF (C)	DPF (A)	DPF (B)	DPF (C)
0	0.31	0.38	0.79	0.31	0.38	0.81
20	0.27	0.42	0.8	0.3	0.44	0.8
40	0.27	0.46	0.79	0.3	0.49	0.81
60	0.27	0.49	0.79	0.3	0.54	0.8
80	0.24	0.52	0.77	0.27	0.58	0.8
100	0.27	0.61	0.76	0.27	0.64	0.79
200	0.16	0.74	0.71	0.18	0.78	0.76

Table F.5: Results of DC Injection between 'C' and 'B' Phases

DC Injection Between A and C Phases						
DC Level (mA)	IL A (mA)	IL B (mA)	IL C (mA)	IP A (mA)	IP B (mA)	IP C (mA)
0	189	171	153	89	113	104
20	195	178	151	93	114	107
40	206	186	150	99	114	112
60	219	195	151	107	115	114
80	234	206	154	118	118	122
100	247	214	158	122	118	132
200	342	276	196	171	139	177
	W (A)	VA (A)	VAR (A)	W (B)	VA (B)	VAR (B)
0	10	32	31	11	41	38
20	11	33	31	15	41	39
40	12	35	33	15	42	39
60	15	38	35	17	45	42
80	19	42	38	13	44	41
100	21	46	41	15	41	38
200	32	65	57	47	50	46
	W (C)	VA (C)	VAR (C)	lthd % (A)	lthd % (B)	lthd % (C)
0	32	41	25	8.8	9.7	7
20	33	41	24	10.6	9.3	8.1
40	33	39	21	11.3	11.3	11.5
60	36	45	26	17.8	12.8	14.6
80	39	45	21	20.4	16.7	18.3
100	43	48	22	22.1	19.6	22.4
200	57	65	32	33.7	36.5	36.5
	PF (A)	PF (B)	PF (C)	DPF (A)	DPF (B)	DPF (C)
0	0.31	0.38	0.79	0.31	0.38	0.81
20	0.34	0.35	0.81	0.36	0.38	0.83
40	0.34	0.35	0.85	0.38	0.36	0.87
60	0.4	0.37	0.82	0.42	0.39	0.87
80	0.44	0.37	0.88	0.46	0.38	0.91
100	0.46	0.36	0.89	0.47	0.36	0.92
200	0.49	0.34	0.87	0.47	0.39	0.94

Table F.6: Results of DC Injection between ‘A’ and ‘C’ Phases